

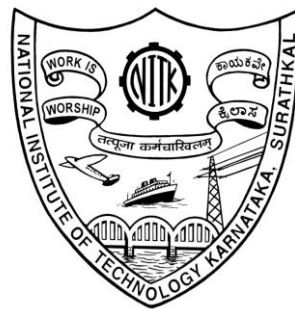
**MODELING AND PERFORMANCE
ANALYSIS OF MICROGRID WITH WIND
AND PHOTOVOLTAIC BASED DISTRIBUTED
GENERATION SYSTEMS**

Thesis

Submitted in partial fulfillment of the requirement for the award of degree of
DOCTOR OF PHILOSOPHY

By

JAYALAKSHMI N. S.



DEPARTMENT OF ELECTRICAL AND ELECTRONICS ENGINEERING
NATIONAL INSTITUTE OF TECHNOLOGY KARNATAKA
SURATHKAL, MANGALORE-575025

December, 2015

DECLARATION

By the Ph. D. Research Scholar

I hereby declare that the Research Thesis entitled “**Modeling and Performance Analysis of Microgrid with Wind and Photovoltaic Based Distributed Generation Systems**” which is being submitted to the *National Institute of Technology Karnataka, Surathkal* in partial fulfillment of the requirements for the award of the Degree of *Doctor of Philosophy* in **Electrical and Electronics Engineering Department** is a *bonafide report of the research work carried out by me*. The material contained in this Research Thesis has not been submitted to any other University or Institution for the award of any degree.

JAYALAKSHMI N. S.

(100528EE10P01)

Department of Electrical and Electronics Engineering

Place: NITK - Surathkal

Date: 11/12/2015

CERTIFICATE

This is to certify that the Research Thesis entitled “**Modeling and Performance Analysis of Microgrid with Wind and Photovoltaic Based Distributed Generation Systems**” submitted by **Mrs. Jayalakshmi N. S.** (Register Number: 100528EE10P01) as the record of the research work carried out by her, is accepted as the *Research Thesis submission* in partial fulfillment of the requirements for the award of degree of **Doctor of Philosophy**.

Research Guide

(Name and Signature with Date and Seal)

Chairman – DRPC

(Signature with Date and Seal)

ABSTRACT

The advancement in technology, environmental concerns, emerging power markets and deregulation of electric power utilities are leading to increased interconnection of distributed generators (DGs) to the utility system. The different types of DGs, such as microturbines and fuel cells in addition to the traditional solar and wind power are creating significant new opportunities. The benefits of interconnection of these generators are improved reliability, power quality, efficiency, alleviation of system constraints along with the environmental benefits. Due to the growing momentum towards sustainable energy developments and considering these benefits it is expected that a large number of DG systems will be interconnected to the power system in the coming years. Interconnecting large number of small DG systems with diverse characteristics to low voltage network causes many problems. The microgrid is a section of network operating in a systematic way, comprising sufficient generating resources in the autonomous or grid connected mode in an efficient and controlled way. The microgrid has more control flexibilities and larger power capacity to fulfil power quality requirements and system reliability. Along with generation sources microgrid also consists of storage devices such as flywheels, batteries and super capacitors. The wind and photovoltaic (PV) power generation are two of the most promising renewable energy technologies. Hybridizing wind and solar power sources together with storage batteries to cover the periods of time without sun or wind provides a realistic form of power generation. Currently variable speed drives (VSD), lighting, batteries and electronics constitute major part of the load. The DC power can be supplied to these loads from microgrid system with usage of minimum converters with decreased losses.

In this research work, a microgrid with wind and PV as the energy resources with single 3 phase inverter considering both DC and AC loads, which can reduce the multiple conversion stages has been implemented. Both wind generator and PV panels are controlled to operate at their maximum power point. The wind power system presented in this work uses the permanent magnet synchronous generator (PMSG), because of its property of self excitation, which allows operation at a high power factor and high efficiency. It also results in smaller size, minimum weight and higher

torque to size ratio. This work mainly focuses on mathematical modeling, control schemes for operation of microgrid with energy storage devices for both isolated and grid connected mode under various generation and load conditions. Based on the dynamic component models, a simulation model for the microgrid system has been implemented in the Matlab/Simulink environment.

In this work, the load following performance of microgrid system is studied in an isolated mode of operation. The microgrid model with integration of wind and PV energy system with battery energy storage devices has been implemented. The battery is thus controlled to provide the deficit power when the combined wind and PV energy sources cannot meet the net power demand. All three energy systems are connected in parallel to a common DC bus line through three different DC/DC converters. The performance study is analyzed with consideration of DC loads, non-linear and induction motor loads for variable nature of the individual DG source.

In this thesis the simulation results for evaluation of the performance of the microgrid system in grid interconnected mode of operation using case studies are also presented. For grid integrated microgrid system, grid behaves as backup energy source. The overall power management strategy for coordinating the power flows among the different energy sources is presented in the thesis. The results show that the overall power management strategy is effective and the power flows among the different energy sources and the load demand is balanced successfully. Also the performance of the microgrid system is studied under grid perturbations conditions. The common grid perturbations considered in this study are balanced voltage dip, voltage unbalance and harmonic distortions. The simulation result reported in this work also shows that, the performance of the model presented is not affected by the grid disturbances considered.

The last part of the dissertation focuses on power smoothing of the grid integrated microgrid system using ultracapacitors, also with combination of battery and ultracapacitors. The battery performance can be improved in terms of the power density by combining ultracapacitors with batteries which are typically low power devices. The power obtained from wind and PV system varies with the changes in weather conditions. Especially in weak power systems with large penetration of intermittent renewable energy (RE) generation sources into the utility grid, may

introduce adverse effects on the utility grid. To compensate or absorb the difference between the generated power and the required grid power, energy storage systems are used. Most of the technical literatures discuss the control performance of battery storage devices used for power smoothing of renewable power sources such as wind or PV power system. However in this research, the control schemes have been developed for power smoothing of the grid integrated microgrid system using ultracapacitors and combination of battery and ultracapacitors. In order to observe the real-time performance of energy storage system in smoothing the output power fluctuations, the practical site data for wind speed and solar irradiation are considered. The final result of proposed control strategy is a smooth and ramp controlled power output that can be injected to the grid.

Keywords: Distributed generation, wind power generation, photovoltaic system, PMSG, maximum power extraction, microgrid, PWM voltage source inverter, grid integration, Active and reactive power (PQ) control, isolated operation, Voltage and frequency (VF) control, battery storage, DC load, power smoothing, ultracapacitors.

ACKNOWLEDGMENTS

I would like to express sincere gratitude to my guide Dr. Dattatraya N. Gaonkar, Assistant Professor, Department of Electrical and Electronics Engineering, for giving me an opportunity to work under his guidance which is invaluable. He has been a constant source of inspiration and support in all possible ways for successful completion of my research work.

I am extremely grateful to Dr. Swapan Bhattacharya, Director, NITK, Surathkal and Prof. Vinatha U, HOD, Department of Electrical and Electronics Engineering, NITK, Surathkal for their encouragement and support.

I would like to express my deepest gratitude to research progress assessment committee members, Dr. Ashvini Chaturvedi and Dr. Nagaraja H. S, NITK, for their valuable suggestions and support throughout my research work.

I am thankful to Dr. Udaya Kumar R.Y. and Dr. Debashish Jena, Dept. of Electrical and Electronics Engineering, NITK, Surathkal for their encouragement, support and help during the research work. I appreciate the support which I received from Sanjeev K. Nayak and Santhosh Kumar A.

I am extremely grateful to Dr. G. K. Prabhu, Director, MIT, Manipal for providing research facilities. I would like to extend my sincere thanks to Prof. V. Nagaraj, Dr. B. K. Singh, Dr. R. Shivarudraswamy and Rohith Kumar, Department of E and E Engg., MIT, Manipal for their assistance, support and encouragement. I specially thank Dr. B. H. V. Pai and Prof. K. Phaniraj, Department of Civil Engg., MIT, Manipal for proof reading of thesis with valuable suggestions and corrections.

I feel very lucky to have a family that shares my enthusiasm for academic pursuits. I want to extend my deepest thanks and appreciation to my dear husband Dr. Narayana Sabhahit and children, Gautham N. S. and Madhura N. S. for their understanding, never ending support, encouragement and putting up with all the irregularities in our life during the time of my research. Furthermore, I greatly appreciate the moral support which I received from my parents and brother Ganesh Adiga.

Jayalakshmi N. S.

CONTENTS

ABSTRACT.....	i
ACKNOWLEDGMENTS	iv
CONTENTS.....	v
LIST OF FIGURES	ix
LIST OF TABLES	xiv
NOMENCLATURE	xv
LIST OF ABBREVIATIONS.....	xvii
CHAPTER 1.....	1
INTRODUCTION	1
1.1 OVERVIEW	1
1.2 ADVANTAGES OF DG SYSTEMS	3
1.3 DG TECHNOLOGIES	4
1.3.1 Wind Energy Conversion System.....	5
1.3.1.1 Topologies.....	5
1.3.1.2 Application of PMSG.....	7
1.3.2 PV Generator and Configurations of PV systems.....	7
1.3.3 Small Hydro Power Plant.....	10
1.3.4 Wave Energy Conversion	11
1.3.5 Geothermal.....	12
1.3.6 Fuel Cells	13
1.3.7 Microturbines.....	14
1.3.8 Internal Combustion Engine	15
1.4 ENERGY STORAGE DEVICES	16
1.4.1 Battery.....	16
1.4.2 Ultracapacitors	17
1.4.3 Other Storage Devices	17
1.5 MICROGRID SYSTEMS.....	18
1.5.1 Benefits and its Control.....	19
1.5.2 Topologies for Interfacing DG Systems	20
1.5.3 Advantages of Combined wind/PV Power System.....	22
1.6 LITERATURE REVIEW	23
1.7 MOTIVATION	34

1.8 AUTHOR CONTRIBUTIONS.....	35
1.9 ORGANIZATION OF THE THESIS.....	36
CHAPTER 2.....	38
MODELING OF WIND AND PV BASED MICROGRID SYSTEM.....	38
2.1 INTRODUCTION.....	38
2.2 MODELING OF MICROGRID WITH WIND AND PV SYSTEM.....	39
2.2.1 Wind Power Generation System.....	41
2.2.1.1 Wind Turbine.....	41
2.2.1.2 Permanent Magnet Synchronous Generator.....	43
2.2.2 PV Arrays.....	44
2.3 MAXIMUM POWER POINT CONTROLLERS.....	47
2.3.1 Wind Power System.....	48
2.3.2 PV System.....	51
2.4 ENERGY STORAGE DEVICES.....	52
2.4.1 Battery.....	52
2.4.2 Control Strategy of DC/DC Bi-directional Converter for Battery.....	53
2.4.3 Ultracapacitors.....	54
2.5 CONTROL SCHEMES FOR INVERTER.....	57
2.5.1 Active and reactive power control.....	57
2.5.2 Voltage and frequency control.....	59
2.5.3 DC link and Filter.....	61
2.6 MICROGRID SYSTEM MODEL IMPLEMENTED IN MATLAB/SIMULINK....	62
2.7 CONCLUSIONS.....	63
CHAPTER 3.....	64
PERFORMANCE ANALYSIS OF MICROGRID IN ISOLATED MODE OF OPERATION	
.....	64
3.1 INTRODUCTION.....	64
3.2 MICROGRID STUDY SYSTEM.....	66
3.3 PERFORMANCE STUDY AND DISCUSSION.....	67
3.3.1 Performance Characteristics of Wind and PV Systems.....	67
3.3.2 Power Sharing.....	69
3.3.3 Case Study with DC Load.....	74
3.3.4 Case Study with Nonlinear and Unbalanced Loads.....	75
3.3.5 Case Study with Wind or PV Generation Alone.....	79

3.4 MICROGRID PERFORMANCE WITH INDUCTION MOTOR	81
3.5 CONCLUSIONS.....	82
CHAPTER 4.....	84
PERFORMANCE ANALYSIS OF MICROGRID IN GRID CONNECTED MODE OF OPERATION.....	84
4.1 INTRODUCTION	84
4.2 GRID INTEGRATION OF MICROGRID.....	86
4.3 RESULTS AND DISCUSSION	87
4.3.1 Load Sharing.....	87
4.3.2 Case Study with Induction Motor Load.....	91
4.3.3 Case Study with Nonlinear Loads.....	94
4.3.4 Intentional Islanding Operation	95
4.4 PERFORMANCE OF MICRGRID SYSTEM WITH GRID PERTURBATIONS... 98	
4.4.1 Balanced Voltage Dip	98
4.4.2 Polluted Grid Voltages.....	99
4.4.3 Unbalanced Grid Voltages.....	101
4.5 CONCLUSIONS.....	103
CHAPTER 5.....	104
POWER SMOOTHING OF GRID INTEGRATED MICROGRID SYSTEM.....	104
5.1 INTRODUCTION	104
5.2 SYSTEM CONFIGURATION.....	106
5.3 CONTROL STRATEGIES FOR POWER SMOOTHING	107
5.3.1 Ultracapacitors	108
5.3.2 Combination of Battery and Ultracapacitors	109
5.4 RESULT ANALYSIS AND DISCUSSION.....	111
5.4.1 Case Study with Ultracapacitors	111
5.4.1.1 Microgrid without Local Loads	112
5.4.1.2 Microgrid Supplying Local Load.....	115
5.4.2 Case Study with Battery and Ultracapacitors Combination.....	116
5.5 CONCLUSIONS.....	122
CHAPTER 6.....	123
CONCLUSIONS AND SCOPE FOR FUTURE WORK.....	123
6.1 CONCLUSIONS.....	123
6.2 SCOPE FOR FUTURE WORK.....	125

APPENDIX A.....	126
APPENDIX B.....	128
REFERENCES.....	129
LIST OF PUBLICATIONS:	146

LIST OF FIGURES

Figure 1.1: Wind generation topologies a) with induction generator b) doubly-fed induction generator (c) permanent magnet synchronous generator.....	6
Figure 1.2: Configurations of PV systems (a) Centralized scheme (b) String technology	9
Figure 1.3: (a) Integrated PE interface (b) Single stage inverter for multiple modules.	9
Figure 1.4: (a) Common dual stage inverter	10
Figure 1.4: (b) Strings with individual DC/DC converter and a common inverter	10
Figure 1.5: Schematic diagram of geothermal power plant.....	12
Figure 1.6: Fuel cell systems with (a) DC/DC and DC/AC conversion (b) DC/AC and AC/AC conversion	14
Figure 1.7: Schematic of (a) Single shaft MTG system (b) Split shaft MTG system..	15
Figure 1.8: DC coupling configuration.....	21
Figure 1.9: AC coupling configuration.....	21
Figure 1.10: Schematic diagram of WECS with MPPT controller.....	24
Figure 1.11: Schematic block diagram for interconnection of PV arrays.....	25
Figure 1.12: (a) Microgrid architecture [Piagi and Lasseter (2006)].....	27
Figure 1.12: (b) General microgrid configuration with energy manager [Vechiu et al. (2009)]	27
Figure 1.13: DC coupled configuration [Cramer et al. (2003)]	28
Figure 1.14: A modular AC coupled configuration [Meinhardt et al. (2004)]	28
Figure 1.15: AC and DC coupled configuration [Moutawakkil and Elster (2006)]	29
Figure 1.16: CERTS microgrid test bed [Joseph et al. (2008)]	29
Figure 1.17: Standalone wind/PV hybrid generation system [Chunhua Liu et al. (2010)]	31
Figure 1.18: Grid connected wind/solar hybrid system [Seul Ki Kim et al. (2006)]...32	
Figure 2.1: Schematic block diagram of the microgrid system	40
Figure 2.2: Wind turbine model	43
Figure 2.3: d and q -axis equivalent circuit model of the PMSG	44
Figure 2.4: Simplified PV cell circuit model	45
Figure 2.5: Equivalent circuit of a PV array	45

Figure 2.6: Matlab/Simulink model of PV array	47
Figure 2.7: Flowchart for maximum power point tracking algorithm	50
Figure 2.8: Schematic diagram of WECS with PMSG and MPPT controller	50
Figure 2.9: P-V Curve of 40 kW solar system.....	51
Figure 2.10: Schematic block diagram for interconnection of PV arrays with MPPT controller.....	52
Figure 2.11: (a) Thevenin Battery Model [Appelbaum and Weiss (1982)].....	53
Figure 2.11: (b) Equivalent electrical circuit of battery.....	53
Figure 2.12: Control scheme of Buck-Boost Converter of the Battery	54
Figure 2.13: (a) Maxwell Boostcap ultracapacitors	55
Figure 2.13: (b) Classical equivalent circuit model of ultracapacitor.....	55
Figure 2.14: (a) Equivalent circuit of UC unit.....	56
Figure 2.14: (b) Arrangement of capacitors in a UC bank [Uzunoglu and Alam (2006)]	57
Figure 2.15: Grid side inverter.....	58
Figure 2.16: Active and reactive power controller	59
Figure 2.17: Voltage and frequency controller	60
Figure 2.18: Series RL filter	62
Figure 2.19: Model of microgrid system in Matlab/Simulink with MPPT controllers	63
Figure 3.1: Schematic of microgrid system for isolated operation	66
Figure 3.2: (a) C_p vs. λ (TSR) for various pitch angles	67
Figure 3.2 (b): Power vs. rotor speed at various wind speed.....	68
Figure 3.3 (a): I-V characteristics of the PV model under different irradiances	68
Figure 3.3 (b): P-V characteristics of the PV model under different irradiances	69
Figure 3.4 (a): I-V characteristics of the PV model under different temperatures	69
Figure 3.4 (b): P-V characteristics of the PV model under different temperatures	69
Figure 3.5: Solar irradiation, dI_{pv}/dV_{pv} and $-I_{pv}/V_{pv}$ curves for PV System	70
Figure 3.6: Active power of wind, PV system, battery and power supplied to load ...	71
Figure 3.7 (a): State of Charge (%) of battery	71
Figure 3.7 (b): Power coefficient C_p of wind turbine	71
Figure 3.8: Active power of wind, PV system, battery and power supplied to load ...	72

Figure 3.9 (a): State of Charge (%) of battery	72
Figure 3.9 (b): System frequency.....	73
Figure 3.10: DC link voltage	73
Figure 3.11 (a): Load voltage.....	73
Figure 3.11 (b): Load current.....	73
Figure 3.12: Active power of microgrid and load, d and q-axis components of voltage,load voltage, State of Charge (%) of battery and system frequency.....	75
Figure 3.13: Active power of wind, PV system, battery, power consumed by DC load and total unbalanced power supplied to load.....	76
Figure 3.14: Unbalanced load currents, load voltage, system frequency and THD (%) variation in inverter output voltage	76
Figure 3.15 (a): The load current	77
Figure 3.15 (b): State of Charge (%) of battery	77
Figure 3.16 (a): Load voltage.....	77
Figure 3.16 (b): System frequency.....	78
Figure 3.17: THD (%) in voltage and current on load side	78
Figure 3.18: Total power consumed by loads and battery power	78
Figure 3.19: The waveforms for load currents.....	79
Figure 3.20: THD (%) in load voltage and current.....	79
Figure 3.21: Active power with wind power generation alone.....	80
Figure 3.22: Active power with PV power generation alone.....	80
Figure 3.23: State of Charge (%) of battery.....	80
Figure 3.24 (a): Active and reactive power of load	81
Figure 3.24 (b): Induction motor torques.....	82
Figure 3.25: Waveforms for stator current, rotor speed, THD (%) variation in load voltage and system frequency.....	82
Figure 4.1: Schematic diagram of grid connected microgrid system	87
Figure 4.2: Active power of microgrid and load.....	88
Figure 4.3 (a): q -axis currents	89
Figure 4.3 (b): Reactive power	89
Figure 4.4 (a): DC link voltage	89

Figure 4.4 (b): THD (%) of inverter output current.....	89
Figure 4.5 (a): Active power of microgrid and load with variable irradiation	90
Figure 4.5 (b): Reactive power	91
Figure 4.6 (a): Active power of microgrid and load with variable wind speed	91
Figure 4.6 (b): Power coefficient C_P of wind turbine	91
Figure 4.7: Solar irradiation, dI_{pv}/dV_{pv} and $-I_{pv}/V_{pv}$ curves for PV System	92
Figure 4.8: Active power of microgrid system, load and power supplied by grid	92
Figure 4.9 (a): Active power of microgrid and load	93
Figure 4.9 (b): Reactive power	93
Figure 4.10: Load current	94
Figure 4.11: Induction motor torques	94
Figure 4.12: Rotor speed and stator current for step change in torque T_m	94
Figure 4.13: Active power of microgrid system, load and power supplied by grid	95
Figure 4.14: Waveforms for currents injected to grid.....	95
Figure 4.15: THD (%) of currents injected to grid	95
Figure 4.16: Active power of microgrid, power supplied by grid and load power.....	96
Figure 4.17: Reactive power of microgrid	97
Figure 4.18: State of Charge (%) of battery.....	97
Figure 4.19: Inverter output voltage	97
Figure 4.20: Frequency variation.....	98
Figure 4.21 (a): Balanced voltage dip in grid voltages	99
Figure 4.21 (b): DC link voltage.....	99
Figure 4.21 (c): Active and reactive power injected to the grid	99
Figure 4.22 (a): THD (%) in polluted grid voltages	100
Figure 4.22 (b): Polluted three phase grid voltages	100
Figure 4.22 (c): d and q -axis components of current injected to the grid.....	101
Figure 4.23: Active and reactive power injected to the grid.....	101
Figure 4.24: THD (%) for injected grid currents	101
Figure 4.25 (a): Grid unbalanced three phase voltages.....	102
Figure 4.25 (b): d and q -axis components of current injected to the grid.....	102

Figure 4.25 (c): Active and reactive power injected to the grid	102
Figure 5.1: Schematic diagram of grid integrated wind/PV microgrid system with storage devices.....	107
Figure 5.2 (a): SOC vs. multiplying factor in boost mode.....	108
Figure 5.2 (b): SOC vs. multiplying factor in buck mode	109
Figure 5.3: Control strategy for reference grid power generation	109
Figure 5.4: Control strategy for battery and ultracapacitors	110
Figure 5.5: The Bode diagram for DC/DC converter of battery bank	111
Figure 5.6: The Bode diagram for DC/DC converter ultracapacitor bank	111
Figure 5.7: Solar irradiation profile	112
Figure 5.8: Wind speed profile	112
Figure 5.9: Wind and solar power output corresponding to wind speed data and solar irradiation.....	113
Figure 5.10: Total power generated from microgrid and grid power reference of the system	113
Figure 5.11: Total power generated from microgrid and power output of ultracapacitors.....	113
Figure 5.12: Grid power reference and microgrid power supplied to the grid	114
Figure 5.13: DC link voltage	114
Figure 5.14: State of Charge (%) of ultracapacitors	114
Figure 5.15: q -axis component of current supplied to the grid.....	115
Figure 5.16: Active power of microgrid, load and utility grid.....	116
Figure 5.17: Reactive power of microgrid, load and utility grid	116
Figure 5.18 DC link voltage.....	116
Figure 5.19 (a): Wind speed profile for one day.....	117
Figure 5.19 (b): Solar irradiation profile for one day	117
Figure 5.20: Total wind and solar power generation	118
Figure 5.21 (a): Battery power.....	118
Figure 5.21 (b): State of charge (%) of battery	119
Figure 5.22: Voltage of battery	119
Figure 5.23 (a): Ultracapacitor power.....	119

Figure 5.23 (b): State of charge (%) of Ultracapacitor	120
Figure 5.24: Voltage of Ultracapacitor	120
Figure 5.25: Total wind/PV power generations and smoothed power injected to the grid.....	121
Figure 5.26 (a): DC link voltage	121
Figure 5.26 (b): Reactive power injected by the microgrid system to the grid	121

LIST OF TABLES

Table 1.1: Installed wind power capacity in India.....	5
Table 1.2: Installed solar PV power capacity in India.....	8
Table 1.3: Comparisons between DC and AC integration schemes.....	21

NOMENCLATURE

Symbols	Description	Units
A	Rotor swept area	(m ²)
a	Diode quality factor	
C_{DC}	DC link capacitor	(F)
C_p	Coefficient of performance	
E_{batt}	No load voltage of battery	(V)
E_0	Battery constant voltage	(V)
E_g	Band gap energy of the semiconductor cell	(eV)
E_{inst}	Instantaneous stored energy of UC	(V)
E_{max}	Maximum stored energy of UC	(V)
G	Actual solar radiation	(W/m ²)
G_{ref}	Solar radiation at standard test conditions	(W/m ²)
T_e	Electromagnetic (EM) torque	(N-m)
I_{ac}	Maximum possible RMS value of the AC load current	(A)
I_a, I_b, I_c	Three phase load currents	(A)
I_{batt}	Battery charging and discharging current	(A)
$I_{Ch,max}$	Maximum charging current of UC	(A)
$I_{Dis,max}$	Maximum discharging current of UC	(A)
i_d and i_q	d and q -axis currents of PMSG	(A)
I_{ph}	Photocurrent of the PV cell	(A)
I_{phref}	Photocurrent at standard test conditions	(A)
i_f	Filter current	(A)
I_s	Diode saturation current	(A)
I_{sref}	Diode saturation current at standard test conditions	(A)
k	Boltzmann's constant	
K	Polarization voltage	(V)
K_o	Temperature coefficient of current	A/kelvin
L_f	Inductance of RL filter	(H)

m_a	Modulation Index of the Inverter	
L_d, L_q	d and q -axis inductances	(H)
m	Mass of air	(kg)
p	Number of pole pairs	
P_{DC}	Average DC link power	(W)
P_{dc}	DC load power	(W)
$P_{battery}$	Battery power	(W)
P_{load}	Active power supplied to load	(W)
Q_{load}	Reactive power supplied to load	(Var)
P_{pv}	PV power output	(W)
P_{wind}	Wind power output	(W)
P_m	Mechanical power available from a wind turbine	(watts)
Q_b	Battery capacity	(Ah)
q	Electron charge	(C)
R	Blade radius	(m)
R_{batt}	Internal resistance of the battery	(ohm)
R_{epr}	Equivalent parallel resistance	(ohm)
R_{esr}	Equivalent series resistance	(ohm)
R_f	Resistance of RL filter	(ohm)
R_s	Stator resistance	(ohm)
R_{se}	Equivalent series resistance	(ohm)
R_{sh}	Equivalent parallel resistance	(ohm)
T	Cell temperature	(kelvin)
T_{ref}	Cell temperature at standard test conditions	(kelvin)
V	Voltage	(V)
V_{acLL}	Line to Line RMS voltage on inverter side	(V)
V_{batt}	Terminal voltage of the battery	(V)
V_{dc}	DC link voltage	(V)
V_{dcref}	Reference value of DC link voltage	(V)
v_d and v_q	d and q -axis voltage of PMSG	(V)
V_g	Grid voltage	(V)

V_{gd} and V_{gq}	d and q -axis components of V_g	(V)
V_{in}	Voltage at the terminal of the converter	(V)
V_{max}	Maximum working voltage of UC	(V)
V_{min}	Minimum working voltage of UC	(V)
V_w	Wind speed	(m/sec)
T_e	Electrical torque	(N-m)
T_m	Mechanical torque	(N-m)
ω_m	Rotor speed	(rad/sec)
ω_{ref}	Reference turbine speed	(rad/sec)
λ	Tip speed ratio (TSR)	
ρ	Air density	kg/m ²
β	blade pitch angle	(degrees)
ϕ_m	flux linkages	(wb/m)
ω	Electrical angular frequency	(rad/sec)

LIST OF ABBREVIATIONS

AC:	Alternating Current
BESS	Battery Energy Storage System
CHP:	Combined Heat and Power
DC:	Direct Current
DER:	Distributed Energy Resource
DG:	Distributed Generation
EDLC:	Electrochemical Double Layer Capacitor
EMS:	Energy Management System
ECS:	Energy Capacitor System
ESS:	Energy Storage System
FC:	Fuel cell
IEEE:	International Electrical and Electronics Engineering
IGBT:	Insulated Gate Bipolar Transistor
kV:	Kilo Volt
kVA:	Kilo Volt Ampere

kVAR:	Kilo Volt Ampere Reactive
kW:	Kilo Watt
MCC:	Microgrid Central Controller
MPPT:	Maximum Power Point Tracking
MTG:	Microturbine Generation
PE:	Power Electronic
PCC:	Point of Common Coupling
PCS:	Power Conditioning System
PLL	Phase Locked Loop
PMSG:	Permanent Magnet Synchronous Generator
PQ:	Active and Reactive power
PV:	Photovoltaic
PWM:	Pulse Width Modulated
RE:	Renewable Energy
RES:	Renewable Energy Sources
SOC:	State Of Charge
SPV:	Solar Photovoltaic
THD:	Total Harmonic Distortion
TSR:	Tip Speed Ratio
UC:	Ultracapacitor
UCSS:	Ultra Capacitor Storage System
VF	Voltage and Frequency
WECS:	Wind Energy Conversion System
WT:	Wind Turbine

CHAPTER 1

INTRODUCTION

1.1 OVERVIEW

Unlike centralized power plants, the DG units are directly connected to the distribution system and most often at the consumer end. The rating of the DG systems can vary between a few kW to as high as 100 MW. Interconnection of these generators to distribution network will offer a number of benefits such as improved reliability, power quality, efficiency and alleviation of system constraints along with the environmental benefits [Barker and de Mello (2000)]. With these benefits and due to the growing momentum towards sustainable energy developments, it is expected that a large number of DG systems will be interconnected to the distribution network in the coming years. Thus there is a rising interest in utilizing alternative energy resources known as distributed generation systems to produce clean and sustainable electrical energy. The renewable resource includes wind, solar, tidal and geothermal and the non-renewable technology comprises internal combustion engine, microturbine and fuel cell based power generation. In recent years, the production of electricity from wind and photovoltaic energy sources have increased significantly due to environmental problems and the shortage of traditional energy sources.

Most of the renewable energy sources are pollution free and abundant. Unfortunately, they are not very reliable. For example, the PV source is not available during the night time or during cloudy conditions. Wind energy may or may not be available at all times. The wind and PV power generation are two of the most promising renewable power generation technologies. Renewable energy sources have unpredictable random behaviors and also solar radiation and wind speed have complementary profiles [Fernando Valencaga et al. (2003)]. Generally sunny days have very low wind while cloudy days and night times are more likely to have strong wind. Therefore, hybrid wind/PV systems have higher availability and reliability than systems based on individual wind or PV sources [Kim et al. (2008); Kellogg et al.

(1996)]. In [Seul Ki Kim et al. (2006)], fully controlled DC/AC converter is employed for interfacing wind generator of the grid connected wind/PV hybrid generation system.

The small scale power grids that have sources in remote areas and can supply power for particular consumers are called microgrids [Hatziaargyriou et al. (2007)]. The microgrid is divided into DC microgrid and AC microgrid. This classification is based on whether the distributed energy resources (DERs) and loads are connected to DC or AC main bus. AC microgrid has a benefit of utilizing present AC grid technologies, protections and standards, but synchronization, stability, requirement for reactive power are its inherent demerits [Kakigano et al. (2007)]. On the other hand, DC microgrid has no such demerits of AC microgrid and satisfies today's demand because most of environment friendly distributed generation (DG) sources such as photovoltaic, fuel cells and variable speed wind power generate DC power. Also most of digital loads, electric vehicle and electronic devices etc. can be directly supplied by low voltage DC power system. Adopting DC microgrid can also reduce the number of conversion stages, thereby decreasing the system losses [Ahmad M. Eid, (2013)] and thus has advantages in terms of efficiency, cost and system size. Most of the research conducted so far is concentrated on AC microgrids e.g. islanding detection and autonomous operation of AC microgrids [Katiraei et al. (2005)] and power sharing of parallel connected multiple AC inverters [Chung et al. (2010)]. The microgrid with renewable energy based DGs, the energy storage devices are installed necessarily to compensate and smooth variation of both supplied power and load.

In many countries, there are remote communities where connection with the power grid is too expensive or impractical. Under such circumstances, a locally placed small scale standalone distributed generation system can supply power to the customers [Cetin (2010)]. Autonomous wind and PV power systems are among the most interesting and environment friendly technological solutions for the electrification of remote consumers. Compared with an individual generation system (wind power or PV power), the wind/PV hybrid generation system can harness more energy from nature. Also the wind power and PV power can compensate each other to some extent during the day and night; the development of the wind/PV hybrid power generation is very attractive [Chunhua Liu et al. (2010)]. In this context, the

investigation on the utility interconnection aspects such as, development of dynamic interface model, their operation and control, planning and design of microgrid DG system becomes significant. Thus, the modeling and performance study of microgrid system with wind and PV based DG system with necessary control schemes is presented in this thesis. Also the output power obtained from wind/solar power system fluctuates with changes in weather conditions. The voltage, frequency and transient stability of the utility grid are adversely affected due to these power fluctuations. Hence, it is essential to smoothen the power fluctuations before delivering to the utility grid. The control schemes are developed for power smoothing of grid integrated wind/PV microgrid system using ultracapacitors alone and combination of battery and ultracapacitors.

1.2 ADVANTAGES OF DG SYSTEMS

The DG produces electricity at a small scale at or close to the load site. Due to the ever increasing power demand, depletion of fossil fuel and the growing awareness for ecological protection the DG systems have attracted increased interest. The advantages of the system with the introduction of DGs on the distribution network are given below [Balamurugan et al. (2012)]:

- Most of the DG systems are environmental friendly and are abundant. They are physically small and produce less noise. From these systems, there is zero or low emission of pollutant and hence there is no environmental cleanup or waste disposal cost associated with them.
- The DG systems normally have modular structure and can be installed close to load centers. Therefore, no high voltage transmission lines are needed for them to supply electricity.
- As the demand for better quality electric power increases, DG can provide alternatives for reliable, cost effective, premium power for homes and business. DG can provide customers with continuity and reliability of supply, by restoring power in a short time when a power outage occurs.
- The distributed resources can be placed strategically to defer or eliminate the need for transmission and distribution (T&D) infrastructures to serve new loads. Deferring or eliminating T&D infrastructure can provide substantial

value to utilities and their customers. On site production minimizes the T&D losses as well as the T&D costs.

- Certain DG technologies placed on customer's sites can be operated in a cogeneration mode. Cogeneration can result in lower overall energy bills for the customer as well as provide some of the broader benefits. Also, distributed resources, by their nature, create investments in the local community. Such investments provide enhanced local economic benefits when compared to investments made in larger remote generation resources.
- DG can also encourage competition in supply, adjusting price via market forces. A DG operator can respond to price incentives reflecting fuel and electricity prices. In a free market environment DG operator can buy or sell power to the utility grid exporting only at peak demand and purchasing power at off-peak prices. DG can act as a physical advantage against volatile electricity prices.

In order to achieve these benefits with large penetration of DG source in the existing utility network several technical issues are to be faced such as voltage regulation, power quality problems, islanding of DG, degradation of system reliability, protection and stability of the network. These issues need to be resolved, to cover the way for a sustainable energy based DG system in future and hence a lot of research effort is required.

1.3 DG TECHNOLOGIES

The distributed generation includes a wide range of prime mover technologies. These technologies can be categorized as renewable and non-renewable. Renewable technologies include wind, photovoltaic, small hydro power plant, wave energy conversion and geothermal etc. Non-renewable technologies include fuel cells, microturbines and internal combustion engines. Knowledge of the characteristics of each of these DG units is very important as that defines how they have to be interconnected and their interaction with the grid. The challenges, potential, typical sizes, grid integration topologies and ability to control power output of these DG systems are described briefly in the following sections.

1.3.1 Wind Energy Conversion System

Wind is an abundant and free source of energy and hence, is attractive in terms of the energy security and price. Because of its cost effectiveness with respect to other types of energy sources used for power generation, wind energy has received considerable attention for producing electricity [Abedini and Nikkhajoei (2011)]. Wind energy is one of the world's fastest growing electricity generating technologies both in the industrialized and the developing world. Wind is a highly variable resource that cannot be stored and wind energy conversion systems must be operated accordingly. The energy present in the blowing wind is transformed to electrical energy using wind energy conversion systems (WECS). By using a wind turbine (that has one or several blades) wind energy is transformed into mechanical energy. The turbine is coupled to the electric generator by means of a mechanical drive train, which usually includes a gearbox. The development of wind power in India began in the year 1990 and has significantly increased in the last few years. In the year 2015, the target set for wind power generation capacity is 60,000 MW by the year 2022. The installed wind power capacity in India for the past 5 years is given in Table 1.1.

Table 1.1: Installed wind power capacity in India

Year	Installed wind power capacity (Cumulative capacity in MW)
2010	16,024
2011	18,421
2012	20,149
2013	21,264
2014	23,444

1.3.1.1 Topologies

The wind turbines (WT) can be of variable speed or fixed speed type. The generator is directly connected to the main supply grid in case of fixed speed machines. Basically there are three categories of wind turbine technology. They are namely, the systems without power electronics, the systems with partially rated power

electronics and the systems with full scale power electronic interfacing wind turbines which are shown in Figure 1.1 (a), (b) and (c) respectively [Frede Blaabjerg et al. (2004)]. The compensating unit may include active or passive power factor correction devices and filters. For the last 25 years the development in wind turbine systems has been steady and four to five generations of wind turbines exist. Wind power generators can be interconnected to low voltage (up to 11 kV), medium voltage (11 kV to 66 kV) and high voltage (110 kV and above) utility networks either individually or as group to form what is known as wind farm.

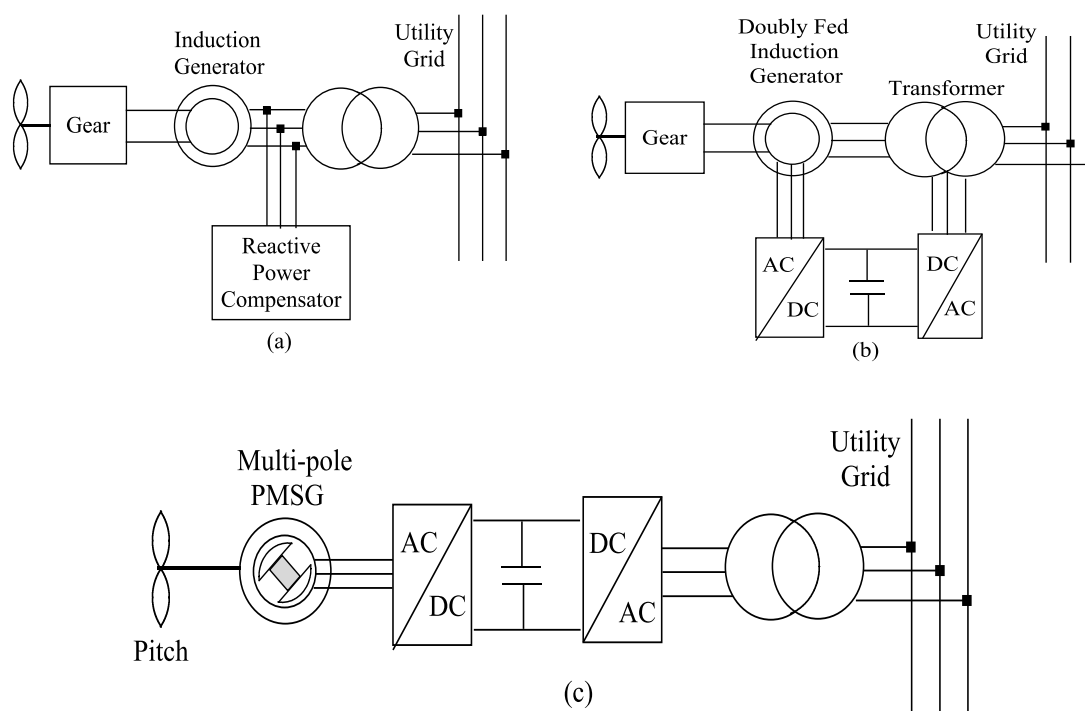


Figure 1.1: Wind generation topologies a) with induction generator b) doubly-fed induction generator (c) permanent magnet synchronous generator

The wind turbine systems using induction generators without power electronics, which are independent of torque variation, keep an almost constant speed. A soft-starter is normally used in order to reduce the inrush current during start-up. Also a reactive power compensator is needed to reduce the reactive power demand from the turbine generators and is usually done by activating continuously the capacitor banks following load variation. These solutions are very attractive due to low cost and high reliability. The wind turbines with a power converter between the generator and grid which gives extra losses in the power conversion but it will gain the technical

performance. Furthermore, the required rating of the power converter can be higher, depending on the designed fault handling capability as well as the ability of controlling reactive power, which give a better grid performance. The solution is naturally a little bit more expensive compared to the classical solutions, however it is possible to save on the safety margin of gear, having reactive power compensation/production and more energy captured from the wind.

1.3.1.2 Application of PMSG

The use of the variable speed PMSG in wind turbine application can increase the energy capture from wind, resolve other problems like noise, power losses and improve efficiency. For example, in a wind turbine system if a gearbox is used, noise, power losses, additional cost and potential of mechanical failure can cause problems. The use of a variable speed PMSG could solve these problems [Higuchi et al. (2000)]. The system includes a wind turbine (WT), a permanent magnet synchronous generator, a three phase diode rectifier bridge, a step up DC/DC converter, and a current controlled pulse width modulated (PWM) voltage source inverter. The PMSG has high performance, higher efficiency, no exciting current, smaller in size and less in weight in comparison to other types of generators. A multi-pole direct driven PM generator, connected to the grid through a full scale converter, can be operated at low speeds, so that the gearbox can be omitted. Direct driven applications are increasingly useful due to the fact that a direct driven generator has lower installation and maintenance cost, a flexible control technique and quick response to wind fluctuation and load variation [Najafi et al. (2011)].

1.3.2 PV Generator and Configurations of PV systems

There are normally two ways to generate electricity from sunlight through photovoltaic and solar thermal systems. In this dissertation, only photovoltaic energy and system will be discussed. Just like the growth of wind energy, PV energy is another fast growing renewable energy technology. For PV systems, the power electronic interface has two key tasks. The first one is to control the terminal conditions of the PV arrays so as to track the maximum power point (MPP) for maximizing the energy capture. The other is to convert the generated DC voltage into

a suitable AC current for the utility supply. The photovoltaic technology uses semiconductor cells, the photovoltaic effect results in the generation of direct voltage and current from the light falling on the cell. The PV cells are assembled in modules to produce sufficient voltage and current. The PV module or array is an unregulated DC power source [Jhunjunwala et al. (2013)]. Mainly in autonomous and small installations, a battery storage system may be used at the DC bus. Most of the individual range of PV module ranges from 20 W to 100 kW [Ackermann et al. (2001)]. The disadvantages of PV systems are requirement of larger significant area, higher installation cost than other DG technologies and intermittent output with a low load factor [Borbely and Kreider (2001)]. It is already well established in many countries including India and is one of the key technologies of the 21st century. In January 2015, the Indian government significantly expanded its solar plans and has targeted 100,000 MW of solar capacity by the year 2022. The installed solar PV power capacity in India for the past 5 years is given in Table 1.2.

Table 1.2: Installed solar PV power capacity in India

Year	Installed PV power capacity (Cumulative capacity in MW)
2010	161
2011	461
2012	1,205
2013	2,319
2014	2,632

There are different configurations for connecting PV modules to the utility network [Frede Blaabjerg et al. (2004)]. The centralized inverter system is illustrated in Figure 1.2 (a), where several PV modules are connected in series and/or parallel, and then connected to the single inverter. The reduced version of the centralized inverter system is the string inverter system as shown in Figure 1.2 (b). It has a single string of arrays connected to the individual inverter system. The voltage amplification may be avoided if the input voltage is sufficiently high. The PV module has its integrated power electronic (PE) interface to the utility as shown in configuration of

Figure 1.3 (a). For multiple PV modules, generally two types of topologies are used. They are single stage and two stage configurations. The single stage inverter for multiple modules is depicted in Figure 1.3 (b).

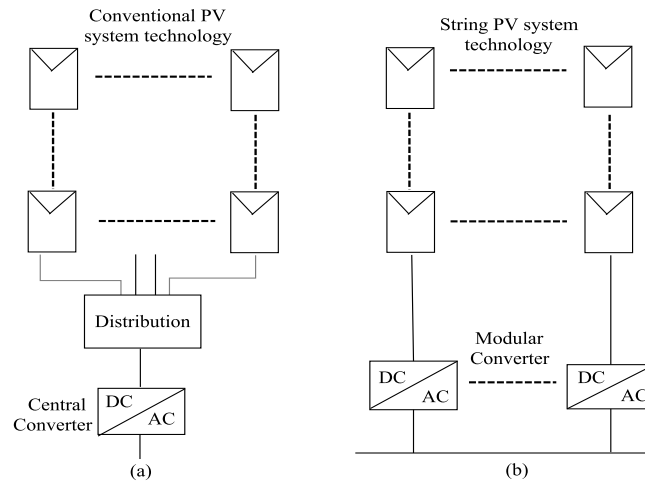


Figure 1.2: Configurations of PV systems (a) Centralized scheme (b) String technology

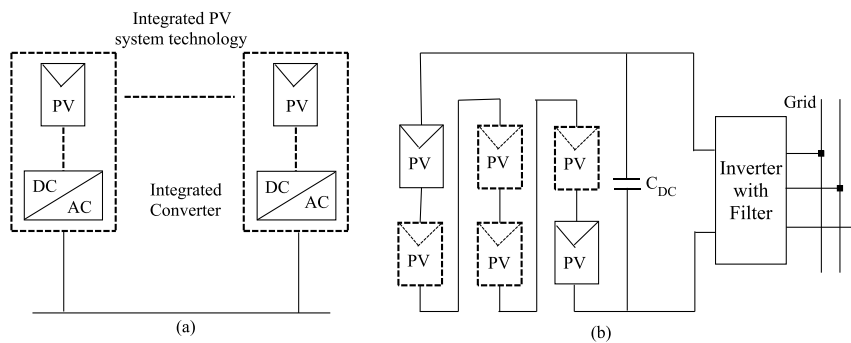


Figure 1.3: (a) Integrated PE interface (b) Single stage inverter for multiple modules

In two stage configurations, the connection of the modules and the inverter may be classified into two categories. In the first category, the PV modules are connected in series and then connected to a grid tie inverter plus a simple DC/DC converter as shown in Figure 1.4 (a). If isolation is not required, buck, boost or buck-boost can be used for the DC/DC conversion stage. The second category includes a DC/DC converter for each string and a common grid connected inverter as shown in Figure 1.4 (b). The overall efficiency is expected to be better because these strings can operate at their individual MPP conditions.

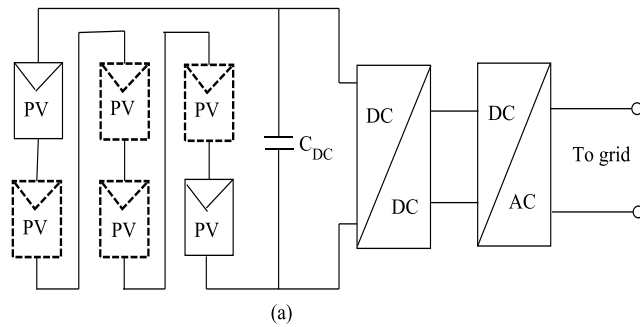


Figure 1.4: (a) Common dual stage inverter

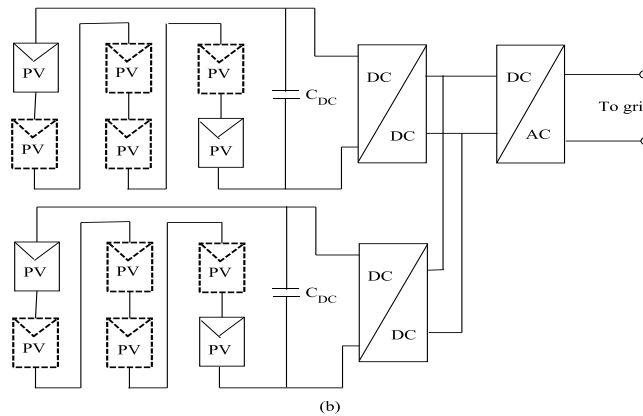


Figure 1.4: (b) Strings with individual DC/DC converter and a common inverter

1.3.3 Small Hydro Power Plant

In developing and hilly countries where small rivers are available, a small hydro power plant (SHPP) can serve a small community or industrial plant. It is possible to construct the SHPP with or without a water reservoir (WR). A disadvantage of the SHPP without WR is that the water is not utilized in its full capacity and the generator runs always in full load condition without delivering active power. A hydroelectric facility requires a dependable flow of water and a reasonable height of fall of water, called the water head. In a typical installation, water is fed from a reservoir through a channel or pipe into a turbine. The pressure of the flowing water on the turbine blades causes the shaft to rotate. The rotating shaft is connected to an electrical generator which converts the motion of the shaft into electrical energy. The definition of a small hydro project varies but a generating capacity of up to 10 MW is generally accepted as the upper limit. Small hydro can be further subdivided into two categories: mini hydro, usually defined as less than 1,000 kW and micro hydro which is less than 100 kW [Borges and Pinto (2008)]. Micro hydro is usually

the application of hydroelectric power sized for smaller communities, single families or small enterprises.

Small hydro plants may be considered as a source of low cost renewable energy connected to conventional electrical distribution networks. Alternatively, small hydro projects may be built in isolated areas that would be uneconomic to serve power from a utility grid network, or in areas where the national electrical distribution network is not available. Since small hydro projects usually have minimal reservoirs and civil construction work, they are seen as having a relatively low environmental impact compared to large hydro power plants and hence decrease the environmental impacts. Small hydro power plants use either synchronous or asynchronous generators. For isolated plant operation synchronous generators are used. And the small hydro plants connected to an electrical grid system can use economical induction generators to further reduce installation cost and simplify their control and operation. The stability of an isolated grid is maintained through controlled units associated with synchronous generator at varying load profile.

1.3.4 Wave Energy Conversion

Ocean wave energy is a renewable energy source with a large potential that may contribute to the increasing demand for power worldwide. Almost 75% of the earth is filled with water, a large proportion of which are the world's seas and oceans. These oceans contain a huge amount of energy in the form of ocean waves and tides. Both kinetic and potential energy associated with these travelling water waves can be exploited. For a given wave, the power is approximately proportional to its square of amplitude and to the period. The high concentration of continuously oscillating water results in high energy densities, making it a favorable form of hydro power. Wave power conversion technologies involve three main designs, on-shore or embedded near the harbor, near shore in close proximity to the seashore standing on the sea bed and off-shore in the deep waters. For large scale deployments, off-shore installments are found to be more appropriate. Wave energy can be used to generate electricity much in the same way as a traditional hydroelectric power plant by constructing a dam or barrage across a narrow bay. The turbines and gates are installed at different points along the barrage, and when there is a difference in hydrostatic head on both

sides of the dam, the gates open and water flows in, rotating the turbines which are connected to generators to generate electrical power [Previsic et al. (2005)].

1.3.5 Geothermal

Geothermal power plants use natural hot water and steam from below the earth's surface to rotate turbine generators to produce electricity. Geothermal power plant is a recoverable energy resource and is very site specific. Geothermal power plant can range from hundreds kW to hundreds MW [Bloomquist (2002)]. After hydropower and biomass, geothermal energy is the third most exploited energy source. Geothermal power plays a fairly significant role in the energy balance of certain areas of the world. Unlike fossil fuel power plants, no fuel is burned in these plants. Hence, geothermal power plants emit water vapors but produce no smoky emissions. The schematic diagram of geothermal power plant is shown in Figure 1.5 [Hammons (2003)].

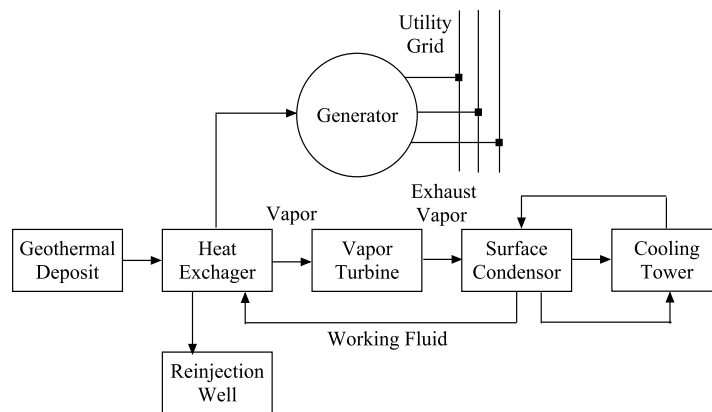


Figure 1.5: Schematic diagram of geothermal power plant

Geothermal electricity can be used for the base load power as well as the peak load power demand. There are three basic designs of geothermal power plants. All these basic designs extract hot water and steam from earth's crust, utilize the heat content and return the warm water to the heat source to extend its life [Barun and McCluer (1993)]. In the simplest design, the steam directly goes to the turbine and then to the condenser where it is condensed into water. In the second approach, the steam and hot water are separated and while the steam is used to drive the turbine, the water is sent back to underground. In the third approach known as binary system, the hot water and steam is passed through a heat exchanger where the heat is extracted to

heat up a second liquid (organic fluids) in a closed loop and then is used to drive the turbine. The choice of the approach to be used to generate electricity is determined solely by the type of the resource and the availability of steam or water from it.

1.3.6 Fuel Cells

Fuel cell (FC) is an electrochemical energy conversion device, where the chemical energy is converted directly into electrical energy along with the heat and water as by products. Approximately a fuel cell can produce 0.6 to 0.75 V and current in the range of 1500-3000 amp/m² of the cell depending on the operating temperature and pressure. This is equivalent to 900-1800 W/m² of cell area in the stack. In order to achieve the desired output, a group of stack may be connected in series/parallel combination. The power and voltage level can range from 2 kW to 50 MW and a few volts to 10 kV respectively. A fuel cell works much similar to a battery. Both batteries and fuel cells have two electrodes, an anode and cathode, separated by an electrolyte. The battery storage contains all the substances involved in the electrochemical oxidation-reduction reactions and has a limited capacity. Whereas a fuel cell is supplied with its reactants externally and it can operate continuously as long as fuel is supplied. The energy savings result from the high conversion efficiency, typically 40% or higher depending on the type of fuel cell. When utilized in cogeneration applications, energy efficiency can be of the order of 85% or more. Currently there are five types of FC technologies: phosphoric acid fuel cell, proton exchange membrane fuel cell, molten carbonate fuel cell, solid oxide fuel cell and alkaline fuel cell. The main challenge in making fuel cells widely used in the DG market is to make them more economically competitive with the current technologies [Ellis et al. (2001)].

Using power electronics based converters topology, a fuel cell is interfaced to the customer load or to the utility network [Frede Blaabjerg et al. (2004)]. Most of the fuel cell system consists of a DC/DC converter and a DC/AC inverter combination as its power conditioning circuit as shown in Figure 1.6 (a). The other possible configuration of the fuel cell system comprises a DC/AC converter which converts the voltage into AC voltage at a high frequency and then a cyclo-converter is used to get AC voltage at a power frequency as shown in Figure 1.6 (b).

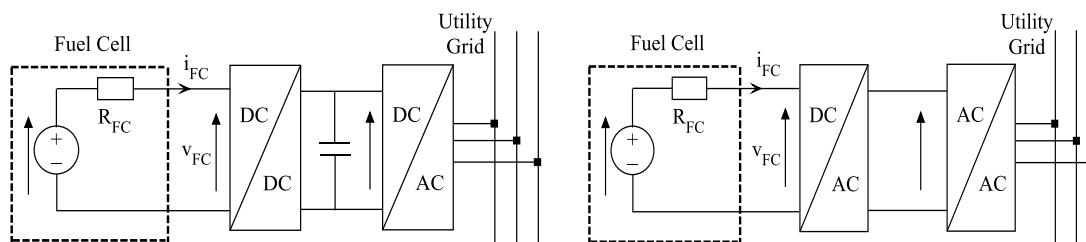


Figure 1.6: Fuel cell systems with (a) DC/DC and DC/AC conversion (b) DC/AC and AC/AC conversion

1.3.7 Microturbines

Microturbines are the progress of gas turbine technology with smaller size, low inertia and high speed operation. A microturbine based generation (MTG) system can generate power in the range of 25 kW to 500 kW. Today's microturbine technology is the result of development work in small stationary and automotive gas turbines, auxiliary power equipment and turbochargers. The DG systems based on microturbine are clean, reliable, energy efficient and provide a supplement to traditional forms of power generation. The basic components of a microturbine are the compressor, combustor, turbine generator and recuperator. In a microturbine, the turbo-compressor shaft generally turns at high rotational speed as high as 1, 20,000 RPM based on the power rating. The microturbine utilizes gas foil bearings (air bearings) for high reliability, low maintenance and safe operation. This needs minimum components and no liquid lubrication is necessary to support the rotating group. Recuperators are heat exchangers that use the hot exhaust gas of the turbine (typically around 1,200°F) to preheat the compressed air (typically around 300°F) going into the combustor. This reduces the fuel needed to heat the compressed air to turbine inlet temperature. The microturbine efficiency can go above 80% with recuperator [Scott (1998)].

There are two kinds of microturbine designs available, based on position of compressor, turbine and generator [Gaonkar et al. (2008)]. Figure 1.7 (a) shows a high speed single shaft design with the compressor and turbine mounted on the same shaft along with the permanent magnet synchronous machine. The generator generates power at very high frequency ranging from 1500 to 4000 Hz. The high frequency

voltage is first rectified and then inverted to a normal AC power at 50 or 60 Hz. Another design is shown in Figure 1.7 (b), in which the turbine on the first shaft directly drives the compressor, while a power turbine on the second shaft drives the gearbox and conventional electrical generator (usually induction generator) producing 60 Hz power. The two shaft design features more moving parts but does not require complicated power electronics to convert high frequency AC power output to 60 Hz.

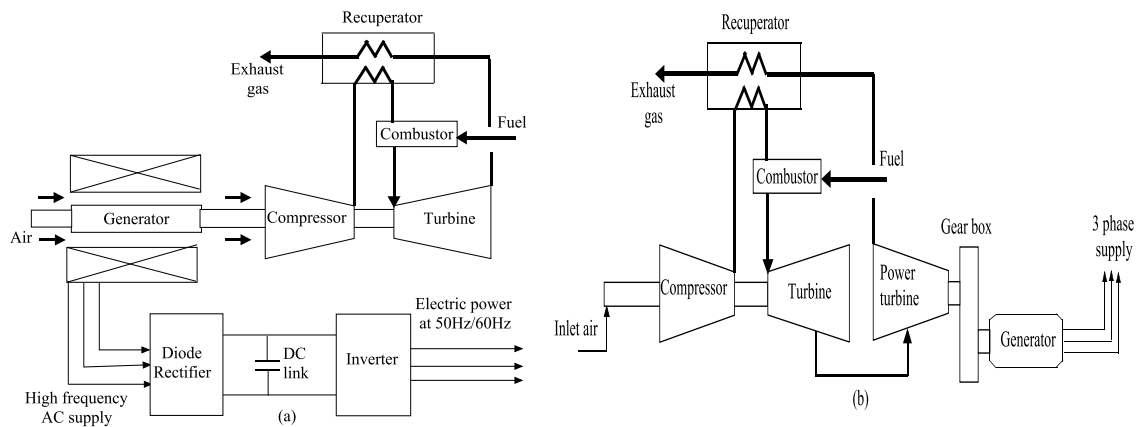


Figure 1.7: Schematic of (a) Single shaft MTG system (b) Split shaft MTG system

1.3.8 Internal Combustion Engine

Reciprocating internal combustion engines (ICEs) convert heat resulting from combustion of a fuel in to rotary motion which drives a generator in a distributed generation system [Pandiaral and Fox (2000)]. These engines can be of either spark ignition type or compression type. The spark ignition type uses natural gas, propane, or gasoline and the compression types use diesel fuel or heavy oil. They provide advantages such as low capital cost, large size range, from a few kW to MW, good efficiency, possible thermal or electrical cogeneration in buildings and good operating reliability. These characteristics combined with the engine ability to fast start-up during a power outage, make them the main choice for emergency or standby power supplies. The electrical generator is usually induction or synchronous type. It is connected directly to the electrical power system without any additional interconnection device. The key barriers to ICE usage are high maintenance cost, which is highest among the DG technologies, high nitric oxide emissions and a high noise level.

1.4 ENERGY STORAGE DEVICES

The energy storage is integral part of the DG system. The storage devices are required to store the energy during times when production exceeds consumption and the stored energy is used at times when consumption exceeds production. They are also used to mitigate the power fluctuations and balance power during variation in availability of natural resources and also during the load transients. Intermittent energy sources are by nature unpredictable and the amount of electrical energy they produce varies over time and depends heavily on random factors such as the weather conditions. To compensate or absorb the difference between the generated wind power and the required grid power, energy storage devices are used. The different energy storage devices like battery, flywheel, supercapacitor technologies and their interfacing systems are discussed in [Ribeiro et al. (2001); Illindala (2012)]. As the renewable energy sources usage increased the most common choice for storing energy is by using battery and ultracapacitor. Battery energy storage system uses a power converter module to convert the battery DC energy into AC grid compatible energy. These units present fast dynamics with response times near 20 milliseconds and efficiency from 60% to 80% [Robert B. Schainker (2004)]. Ultracapacitors or electrochemical double layer capacitor (EDLC) are devices that can be used as energy storage systems, that have high energy and power densities, a high efficiency, nearly 95% and a large life expectancy [Burke (2000)]. The storage device is connected to the DC link through a bidirectional DC/DC converter [Narasimharaju et al. (2012)]. The control of buck and boost operation of converter can be achieved from same controller. This converter controls charging and discharging of energy storage device depending upon load condition [Samosir and Yatim (2010)].

1.4.1 Battery

A battery system is very important in all standalone PV, wind and hybrid systems and it is used to minimize the demand-generation mismatch of the system. The main objective of battery controller is to store excess energy in it during high wind and irradiation condition and discharge the energy temporarily when wind and solar power falls. Energy can flow in two directions to balance the energy between sources and load. The interfacing of battery on DC link is achieved with the help of

buck-boost DC/DC converter [Nishad Mendis et al. (2012)]. For mitigating the fluctuation in power production due intermittent nature of energy sources the battery storage devices are utilized.

1.4.2 Ultracapacitors

The Ultracapacitors are high power density devices which deliver high power for short duration of time. These devices have very high charging and discharging cycles. The basic operating principle, construction, design are described in [Bullard et al. (1989)]. The electric double layer capacitor technology and circuit models are presented in [Nelms et al. (2003)]. In integration of renewable energy sources, one of the major challenges is mitigating of output power fluctuations. Hence, before delivering power to the utility grid it is essential to smooth the power fluctuations. The ultracapacitor storage system (UCSS) is the current typical means of smoothing intermittent solar and wind power generation. The ultracapacitors are ideal for seconds to minutes (short-term) energy storage that enables wind turbine generators to compensate for fast changes in the power output [Liyan Qu and Wei Qiao (2011)]. The combination of battery and UCs has advantage over using one of them. The battery is energy dense device which can supply power for longer period while UCs can deliver large burst of power for short duration of time. These two devices are required in renewable energy based power generation system.

1.4.3 Other Storage Devices

The electricity demand fluctuates depending on the time of the day and the time of a year. As the concept of microgrid is a mixed power system make the best usage of the different types of local generations. Some forms of generations have large response time and others can start up very quickly to provide energy depending the real-time load demand pattern. Provided these reasons clearly, the energy storage is beneficial in managing such a system. A desired form of energy storage is expected to provide the required power into the power system and store up sufficient energy at low electricity consumption. Other types of short term storage are flywheel, pumped hydro storage and superconducting magnetic energy storage [Meghdad Fazeli (2010)]. The flywheels are typically useful when there is a mismatch between the power generated and the load power demand. It can provide power for maximum

acceleration and can handle the power requirements of the peak load and store the energy during low load demand. These storage devices have a relatively fast response time. The pumped hydro storage type stores energy in the form of water. Pumping is done at time when the supply is more than the demand. The water is pumped from a lower elevation reservoir to a top reservoir using the low cost electric power. In superconducting magnetic energy storage the energy is stored in form of a DC current circulating in a large inductor. The resistance of a superconductor is zero so the current can flow without reduction in its magnitude. This variable current through the superconducting coil is converted to a voltage, which can be connected to an inverter to produce power.

1.5 MICROGRID SYSTEMS

A microgrid is a group of microsources and loads operating as a single controllable system that provides power to its local area. To the utility system, the microgrid can be thought of as a single controllable load that can respond in seconds to meet the requirements of the transmission system. To the customers, the microgrid can meet their special needs like enhancing reliability, reducing feeder losses, supporting local voltages providing increased efficiency. The output power the microgrid must have high reliability and power quality than normally supplied by the utility system. These technologies require power electronics devices to interface with the power network and its loads. In many of the cases, there is a DC voltage source like PV, FC etc. which must be converted to an AC voltage at the required frequency, magnitude and phase angle. This conversion will be performed using a voltage source converter using a possible pulse width modulation to provide fast control of voltage magnitude. The reliability, economic operations, control methods and planning of microgrid are investigated in [Bae and Kim (2007)].

The main components of a microgrid are distributed generators such as PV arrays, small wind turbines, fuel cells, internal combustion engines, microturbines, etc., energy storage devices like flywheels, superconductor inductors, supercapacitors, compressed air systems, batteries, etc., and loads. Based on interfacing techniques, the generators can be (i) generators that consist of direct coupled conventional rotating machines and (ii) electronically interfaced generators. The energy storage devices are

used to compensate for the power shortage within the microgrid, mainly in the islanded mode if the generators are not able to satisfy the total load demand. They also prevent transient instability of the microgrid by providing power in transients.

Microgrid control can be mainly divided into (i) supervisory control and (ii) local control [Mohammad Bagher Delghavi (2011)]. In the grid connected mode, the microgrid voltage magnitude or frequency is imposed by the utility grid. However, they can be controlled to exchange pre-specified amounts of real and reactive powers with the rest of the microgrid. But in the isolated mode of operation, the DG systems are primarily controlled to regulate the microgrid voltage magnitude and frequency and are the function of the local control. In the absence of a utility network, a sustained islanded mode operation also implies that the sum of DG system power outputs equals the total load power. The supervisory control is implemented centrally, through the microgrid central controller (MCC). It requires a communications network to exchange information with the DG systems and loads. The main function of the local control is to ensure the stability and robustness of the microgrid, during transients as well as steady states. Thus, the local control ensures that the DG systems operate in synchronism with the grid in the grid connected mode of operation. In the islanded mode of operation it ensures that, the aggregate of the DG system power outputs tracks the total load power, the microgrid voltage magnitude and frequency are regulated while the DG systems properly share the total load both in transient and steady state conditions. Further, the local control ensures that the DG systems operate within their limits and are protected against network faults, irrespective of the operating mode.

1.5.1 Benefits and its Control

The main benefits of microgrids are high energy efficiency through the application of combined heat and power (CHP), high quality and reliability of the delivered power and environmental and economic benefits [Assano et al. (2007)]. The waste heat from the conversion of fuel to electrical power in small generators can be used by local consumers, through the CHP technology in order to increase the efficiency. In a microgrid, however, most DERs employ power electronic converters which can rapidly correct voltage sags or rise, harmonics, etc., even in the presence of

nonlinear or unbalanced loads. Some of the basic technical issues that need to be addressed are,

Control: A major issue in DG is the technical difficulties related to control of a significant number of microsourses.

Operation and investment: The economy of scale favors larger DG units with a ratings of a microsource have a connection cost much less per kW since the protection cost remains essentially fixed. The microgrid concept allows for the same cost advantage of large DG units by placing many microsourses to a single DC bus with single voltage source converter interface. As well, smaller generators have economic benefits such as shorter construction times and transmission lines.

Power quality and reliability: DG has the potential to increase the power quality and the system reliability due to the decentralization of supply. If DG is allowed to operate autonomously in transient conditions, reliability levels can be increased.

1.5.2 Topologies for Interfacing DG Systems

The combination of two or more power generation technologies to make use of their best operating characteristics and to attain higher efficiencies than that could be gained from a single power source is termed as hybrid power system. There are many combinations of different alternative energy sources and storage devices to build a hybrid system. Some of the important combinations for hybrid DG system are [Caisheng Wang (2006)]

- Microturbine/FC system
- Microturbine/Wind system
- Diesel/FC system
- PV/FC/Electrolyzer system
- Wind/FC system
- Wind/Diesel system
- Wind/PV/Diesel system
- Wind/PV/FC system

There are two main categories to integrate different alternative energy sources to form a hybrid system. They are DC coupling and AC coupling. In a DC coupling

configuration of hybrid system, different alternative energy sources are connected to a DC bus through suitable power electronic interfacing devices shown in Figure 1.8. Then the DC energy is converted into AC through a DC/AC converter or inverter [Oystein Ulleberg (1998)]. In AC coupling scheme, different energy sources are integrated through proper power electronic interfacing circuits to a power frequency AC bus shown in Figure 1.9. Different coupling schemes find their own suitable applications. The DC coupling scheme is the simplest and the oldest type of integration. A single-wire transmission line (or single wire method) is a method of transmitting electrical power or signals using only a single electrical conductor. The AC coupling scheme is more modular than DC coupling configuration and is ready for grid connection [Strauss and Engler (2003)]. Table 1.3 summaries the advantages and disadvantages of DC and AC integration schemes.

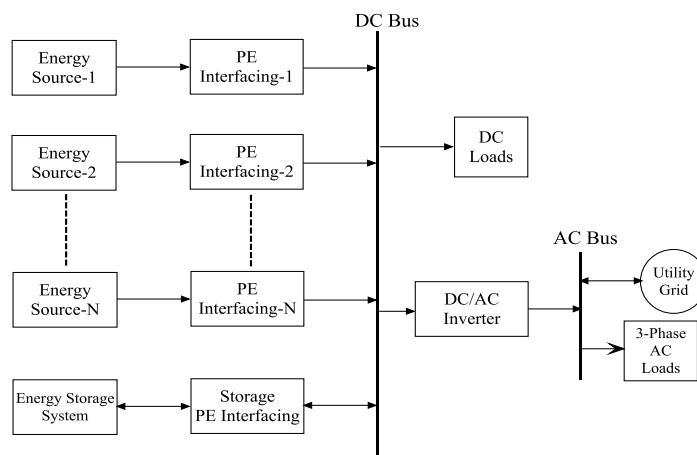


Figure 1.8: DC coupling configuration

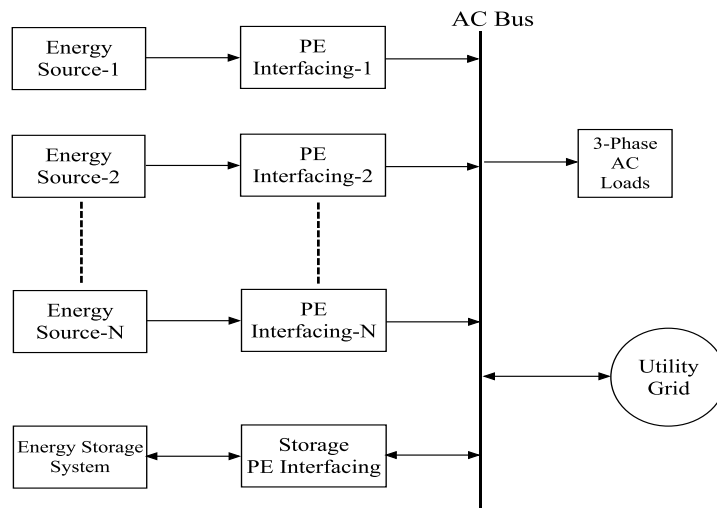


Figure 1.9: AC coupling configuration

Table 1.3: Comparisons between DC and AC integration schemes

Coupling Configuration	Advantages	Disadvantages
DC coupling	<ol style="list-style-type: none"> 1. Synchronism not needed. 2. Suitable for long distance transmission 3. Single-wired connection 4. Less transmission losses 	<ol style="list-style-type: none"> 1. Difficulties on the voltage compatibility 2. Corrosion concerns with the DC electrodes. 3. High installation and maintenance costs for non-standard connection. 4. The complete system fails to supply AC power, if the DC/AC inverter is out of service.
AC coupling	<ol style="list-style-type: none"> 1. If one of the energy sources is out of service, it can be isolated from the system easily and thus more reliable. 2. Ready for grid connection. 3. Standard interfacing and modular structure. 4. Easy multi-voltage and multi-terminal matching. 	<ol style="list-style-type: none"> 1. Synchronism required. 2. The power factor and harmonic distortion correction are needed. 3. Not suitable for long distance transmission.

1.5.3 Advantages of Combined wind/PV Power System

Both wind and PV power sources are pollution free and abundant. But unfortunately, they are not very reliable. Generally, PV power and wind power are complementary since sunny days are usually calm and strong winds often blow during cloudy days or night. Hence, the hybrid PV/wind power system has higher availability and reliability to deliver continuous power than individual source. The hybrid wind/PV power systems have noticeable advantages from an ecological perspective. They may become a cost competitive option in areas where wind and solar patterns match each other significantly. Combining wind and solar power sources together with storage batteries to cover the periods of time without sun or wind provides a realistic form of power generation. Moreover, the size of battery storage can be reduced to some extent as there is less dependence on only one method of power

production. The main advantage of this hybrid system is that it meets the basic power requirements of non-electrified remote areas, where grid power has not yet extended. Thus, wind/PV hybrid system is the best technique to utilize not just one local available renewable energy resource but multiple renewable energy resources converts them into useful energy services.

1.6 LITERATURE REVIEW

In this work, the study of microgrid with wind and PV based DG system is considered due to its advantages discussed in the previous sections. This section gives the detail about the research developments on modeling and performance study of wind, PV and microgrid system operation of both of these power sources, storage devices, microgrid configurations and its operation in isolated/grid connected mode. Also the necessity of power smoothing and different methods of power smoothing of grid integrated DG system are discussed.

- **Wind Power Generation System**

With its abundant, inexhaustible potential, its increasingly competitive cost, and environmental advantage, wind energy is one of the best technologies available today to provide a sustainable supply to the world development. The principal components of a typical modern wind energy system are turbine rotor, gearbox, generator and tower. The typical block diagram grid connected wind energy conversion system with MPPT controller is shown in Figure 1.10. The use of the variable speed PMSG in wind turbine application can increase the energy capture from wind, resolve other problems such as noise, and improve efficiency [Higuchi et al. (2000)]. In order to determine the optimal operating point of the wind turbine, it is essential to include a maximum power point tracking (MPPT) algorithm in the system. A MPPT algorithm increases the power conversion efficiency by regulating the turbine rotor speed according to actual wind speed [Raza Kazmi et al. (2010)]. For extracting maximum power of turbine and delivering an appropriate energy to grid are two important purposes in wind turbines, AC/DC/AC converter is used in [Arifujjaman et al. (2006) and Chinchilla et al. (2006)] to convert the power in wind turbines. In this structure, inverter satisfies the requirements related to grid connection and boost converter provides the ability of extracting maximum power using DC bus control in output of

rectifier. Applying power electronics converters to transfer the power to grid with the possibility of speed variation in a great range of values is preferred because of their great advantages. Various methods are presented in [Senjyu et al. (2004); Kelvin Tan and Sayed Islam (2004)] to control the maximum power where almost all of the efficient methods apply rotor speed feedback. A novel control strategy for a variable speed wind turbine with a permanent magnet synchronous generator is presented in [Md. Enamul Haque et al. (2010)]. The control strategy for the generator side converter with maximum power extraction is presented with simulation results.

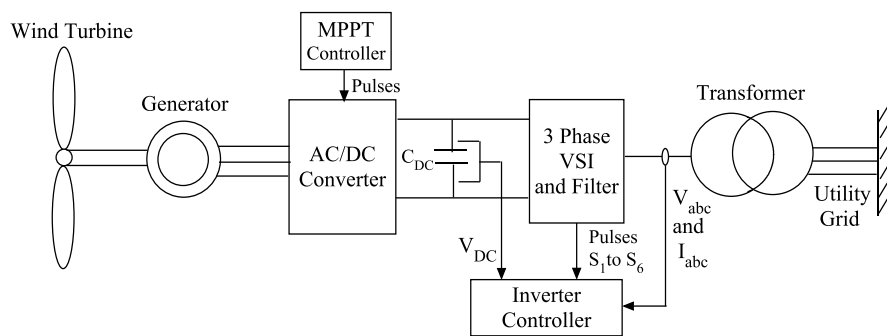


Figure 1.10: Schematic diagram of WECS with MPPT controller

A method to control of variable speed wind generation system connected to permanent magnet synchronous generator is reported in [Najafi et al. (2011)]. In [Haque et al. (2010)], a novel control strategy for the operation of a permanent magnet synchronous generator based standalone variable speed wind turbine is presented. The mathematical modeling and control strategy for the grid connected PMSG based small wind turbine systems are presented in [Md. Arifujjaman (2010)]. A robust and reliable grid power interface system for wind turbines using a permanent magnet synchronous generator is proposed in [Shao Zhang et al. (2011)], in which a Z-source inverter is employed as a bridge between the generator and the grid.

- **PV Power Generation System**

The production of electricity from renewable energy sources like photovoltaic has increased in recent years due to environmental problems and the shortage of traditional energy sources. The isolated PV generation units can feed local loads in many of the remote areas, and thus improve reliability of power with low capital investment [Agustoni et al. (2003)]. Some standalone PV generation systems with

energy storage are developed for residential and rural applications [Hiroaki Nakayama et al. (2008)]. The standalone PV system requires battery for energy storage to supply the load power when solar power is not available [Chiang et al. (2009)]. In addition, for longer life of battery, the battery charging controller is essential. The rechargeable batteries are widely used in standalone photovoltaic systems to store the energy.

The conversion efficiency of the PV cell is low and to increase its operating efficiency a maximum power point tracking algorithm is required. Several maximum power point tracking algorithms for photovoltaic systems have been developed [Esrasm and Chapman (2007)]. The MPP is tracked by means of a MPPT device, based on one of the following schemes: perturb and observe method, incremental conductance, parasitic capacitance or constant voltage [Hohm and Ropp (2000)]. As known from a power-voltage curve of a solar panel, there is an optimum operating point such that the PV delivers the maximum possible power to the load. The optimum operating point changes with solar irradiation and cell temperature. In this work incremental conductance MPPT algorithm method is used due to its simple approach [Hussein et al. (1995)]. Also, this algorithm can track rapidly increasing and decreasing irradiance conditions with higher accuracy than other methods [Mutoh et al. (2006)]. In incremental conductance method, the array terminal voltage is always adjusted according to the MPP voltage, and it is based on the incremental and instantaneous conductance of the PV module. This method exploits the condition that the ratio of change in output conductance is equal to the negative output instantaneous conductance. Figure 1.11 shows the typical block diagram for interconnection of PV power generation system to the utility grid.

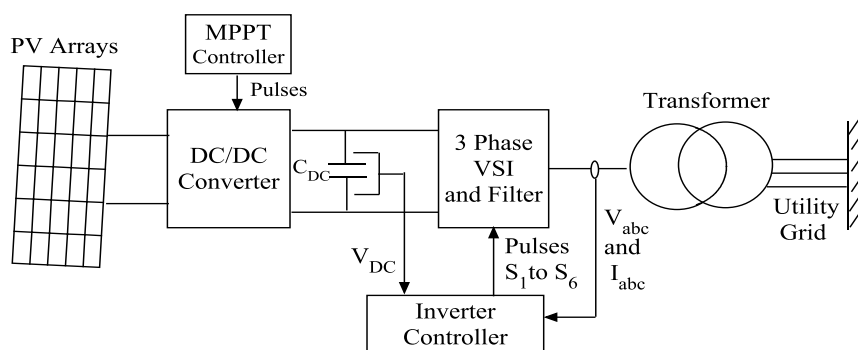


Figure 1.11: Schematic block diagram for interconnection of PV arrays

Presently, grid connected photovoltaic systems are becoming the most important application of PV systems [Doolla and Banerjee (2010)]. The design, simulation and implementation of a novel high performance power conditioning system (PCS) of a three-phase grid connected PV system and its control scheme for applications in DG systems is described in [Molina and Luis E. Juanico (2010)]. The detailed transient models of the grid connected PV/Battery hybrid generation system, and all these models are simulated by using Matlab/Simulink is discussed in [Fei Ding et al. (2010)]. New strategies of design and control of a three-phase grid connected photovoltaic system which consists of PV generator, buck-boost DC/DC converter, DC bus, three-phase voltage inverter, grid filter and utility grid is presented in [Rym Marouani et al. (2011)].

- **Microgrid Configurations**

In remote and rural areas, connecting the electric grid is very uneconomical to carry out. Thus, it is more economical to electrify these areas by means of a microgrid system with existing renewable energy sources available locally. The microgrid configuration represents the energy distribution architecture from the generating sites to the consumers and finally the interconnection between numerous sites and a number of consumers. This section briefs about different microgrid configurations studied, developed and implemented worldwide to meet the energy demands of off-grid modern societies.

A microgrid can be realized as a semi-independent grouping of generating sources (like wind, PV, conventional generator sets, micro turbines, fuel cells, small scale renewable generators) and controllable loads. In several research works, several microgrid configurations have been presented. Figure 1.12 (a) represents a simplest microgrid architecture which may be part of a distribution system with a group of radial feeders [Piagi and Lasseter (2006)]. The single point of connection to the utility is termed as the point of common coupling (PCC). The A, B and C are representing feeders with sensitive loads, which need local generation also. There is no local generation for non-critical load feeders. By using the static switch the feeders A to C can be isolated from the grid. The general architecture of a microgrid consisting of a radial connection of four feeders named A, B, C and D with a set of micro sources

and associated loads along with energy manager is shown in Figure 1.12 (b) [Vechiu et al. (2009)].

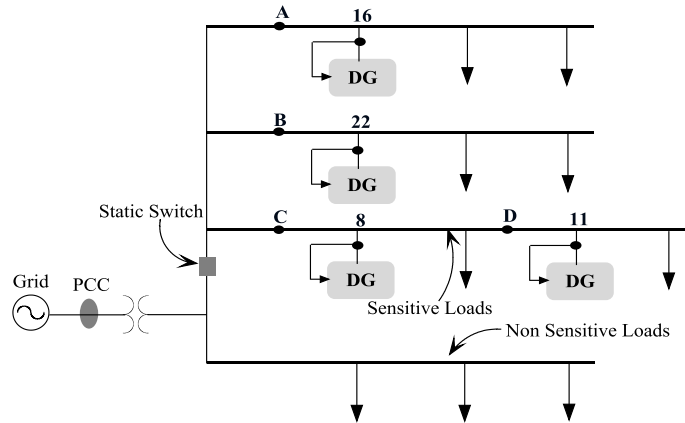


Figure 1.12: (a) Microgrid architecture [Piagi and Lasseter (2006)]

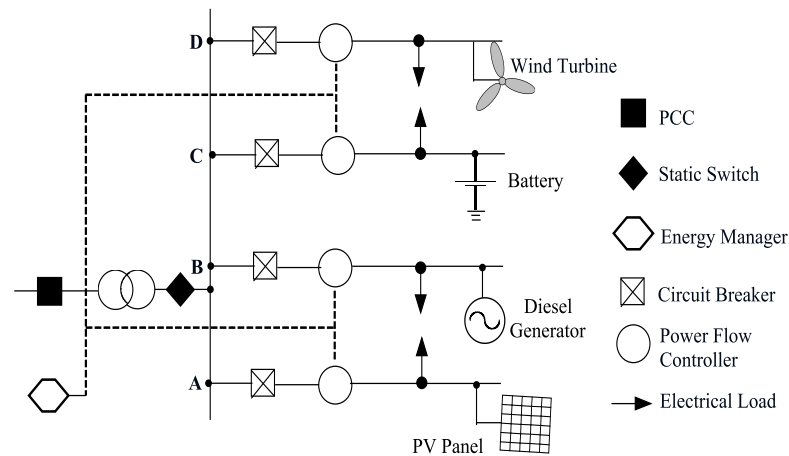


Figure 1.12: (b) General microgrid configuration with energy manager [Vechiu et al. (2009)]

If the higher power or energy is demanded, numerous generators must be connected into the system. In [Cramer et al. (2003)], different AC energy sources, such as wind generators and other generator sets are converted to DC and also coupled to the battery. The power range for a DC coupled configuration is extremely broad and can be used for various off-grid applications. This configuration of representing the microgrid is very cost effective and is depicted in Figure 1.13. In general, if the systems size increases, these generating sources are implemented as AC coupled hybrid systems. In this configuration, the DC coupling is completely avoided

and batteries, as well as PV modules, are equipped with extra power electronics as shown in Figure 1.14 [Meinhardt et al. (2004)].

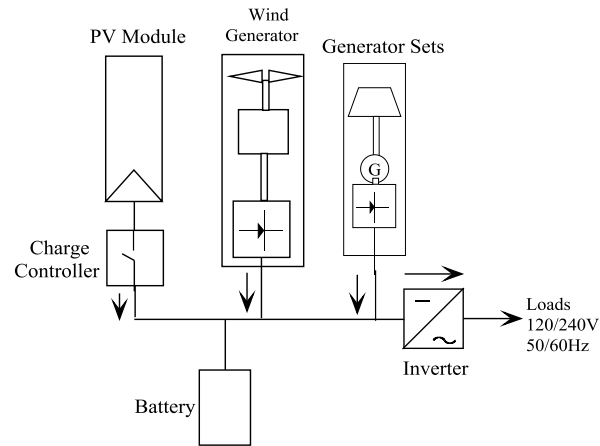


Figure 1.13: DC coupled configuration [Cramer et al. (2003)]

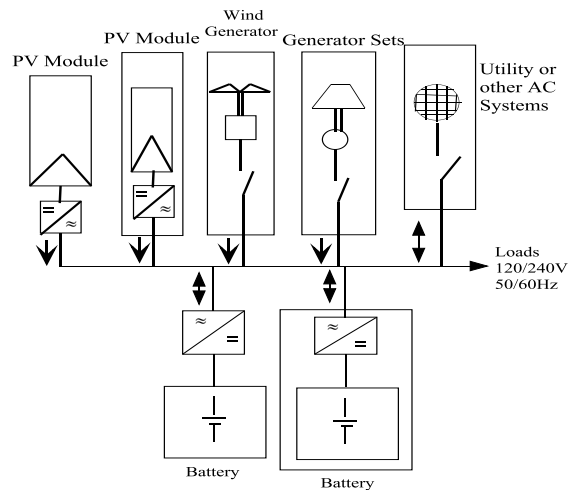


Figure 1.14: A modular AC coupled configuration [Meinhardt et al. (2004)]

As stated earlier, The DC coupling scheme is the simplest natural solution in small systems, but in large systems, AC coupling is more advantageous. It is also possible to combine AC and DC coupled in one system, namely, an AC and DC coupled configuration [Moutawakkil and Elster (2006)]. This type of configuration is used to supply remote or rural consumers like farms, small villages, etc. This technology has emerged due to the need to supply (medium power) AC loads by DC power sources and to charge the battery on the DC side also through combustion generators such as diesel generator sets, as represented in Figure 1.15. The range of DC voltage is between 12 and 48 V and the power range is between 1 and 5 kW.

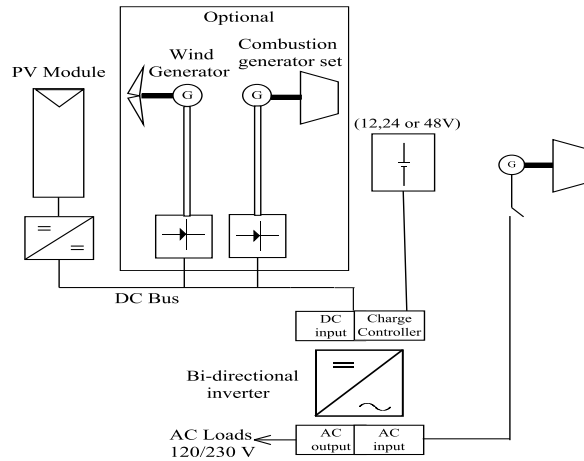


Figure 1.15: AC and DC coupled configuration [Moutawakkil and Elster (2006)]

Figure 1.16 presents the one-line diagram of the CERTS microgrid test bed [Joseph et al. (2008)]. The CERTS test bed is a full-scale test bed built near Columbus, Ohio and operated by American Electric Power. This test bed has three feeders. One feeder has two 60 kW converter based sources driven by natural gas. Other feeder has a single source of same type and capacity. Third feeder is connected to the utility but, it could be powered by the DGs when static switch is closed without injecting power to the utility. Each generator set is provided with battery energy storage at its DC bus.

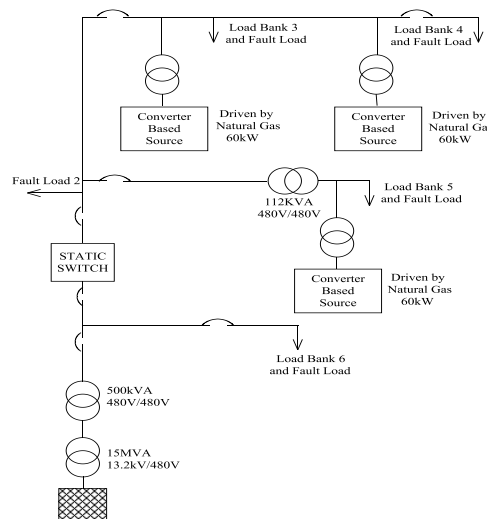


Figure 1.16: CERTS microgrid test bed [Joseph et al. (2008)]

A central communication system is used to connect the Energy Management System (EMS) and the generator sets to dispatch DG set points. However, this communication network is not used in dynamic control of the microgrid. Thus, the

power sources are in autonomous control with plug-and-play capability. There is no central controller in the CERTS microgrid allowing the power sources to be operated in peer-to-peer fashion.

- **Microgrid with Wind and PV power System**

Due to the rapid growth of the power electronics techniques, the wind and photovoltaic power generations system has increased rapidly. Recently an interest is increasing rapidly about the small scaled grid system based on several tens kilowatt of photovoltaic power generation and wind power generation. Such a grid system, which is called a microgrid, has advantages to increase an operational efficiency and economics when it is connected to grid or supply a secured electric power at islands, mountains and remote areas without the connecting grid [Lasseter and Paigi (2004); Solero et al. (1996)]. In [Kai Strunz et al. (2014)], an aggregated model of renewable wind and solar power generation forecast is proposed to support the quantification of the operational reserve for day-ahead and real-time scheduling. Also, the operational controls are designed to support the integration of wind and solar power within microgrids. The two most popular RESs are wind and PV. The combination between these two sources can also form one of the suited hybrid systems because wind and PV can counterpart each other meteorologically. Similarly, standalone system with wind or PV can combine with dispatchable DG such as a diesel generator or energy storage such as a battery to form another type of hybrid system.

- **Microgrid Operation in Isolated/Grid Connected Mode**

A microgrid system could be designed to operate either in isolated mode or in grid connected mode if utility grid is available, through power electronic interface. For a standalone application, the system needs to have sufficient storage capacity to handle the power variations from the alternative energy sources involved. This kind of microgrid system has its own generation sources and connected loads [Lasseter (2002)]. For a grid connected application, the alternative energy sources in the microgrid can supply power both to the local loads and the utility grid. Since the grid can be used as system backup, accordingly the capacity of the storage device for these systems can be smaller if they are grid connected. However, when connected to a utility grid, important operation and performance requirements, such as voltage,

frequency and harmonic regulations, are imposed on the system [IEEE Std. 1547 (2003)]. Both isolated and grid connected applications of microgrid are discussed in the later chapters.

For supplying AC loads in these hybrid wind/solar schemes, the varying amplitude and frequency of the stator voltage of the PM alternator and the variable DC voltage of the PV array have to be suitably conditioned using complex power-electronic interfaces [Kim et al. (1997) and Kurozumi et al. (1998)]. The dynamic behavior and simulation results in a standalone hybrid power generation system of wind turbine, microturbine, solar array and battery storage is reported in [Kalantar and Mousavi (2010)]. The hybrid system consists of a 195 kW wind turbine, an 85 kW solar array; a 230 kW microturbine and a 2.14 kAh lead acid battery. A hybrid isolated generating system based on PV fed inverter-assisted wind driven induction generators is presented in [Arul Daniel and Ammasai Gounden (2004)]. The performance of standalone hybrid wind/photovoltaic system with battery storage is reported in [Youssef et al. (2010)] and a squirrel-cage induction generator is used for wind energy system. An efficient standalone wind/photovoltaic hybrid generation system using doubly excited permanent magnet brushless machine proposed for application to remote and isolated areas is shown in Figure 1.17 [Chunhua Liu et al. (2010)].

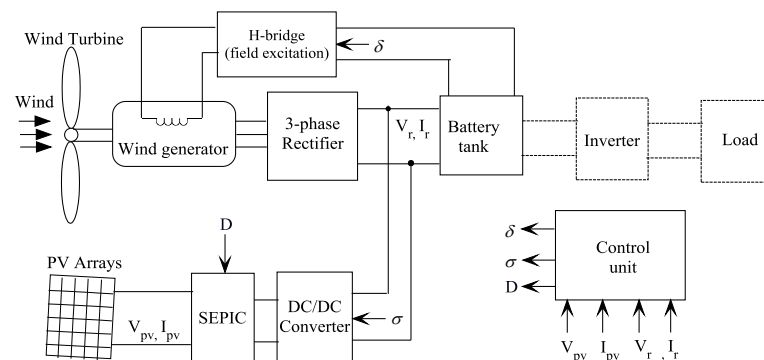


Figure 1.17: Standalone wind/PV hybrid generation system [Chunhua Liu et al. (2010)]

A multi-input inverter for grid connected hybrid PV/wind power system is presented in [Yaow Ming Chen et al. (2007)]. This multi-input inverter consists of a buck/buck-boost fused multi input DC/DC converter and a full bridge DC/AC

inverter. The output power characteristics of the PV array and the wind turbine are introduced. The control strategy for distributed integration of photovoltaic and energy storage systems in DC microgrids is reported in [Eghtedarpour and Farjah (2012)]. The power control of a wind and solar hybrid generation system for interconnection operation with electric distribution system is presented in [Seul Ki Kim et al. (2006)]. This system consists of a variable speed direct driven wind generator with controlled AC/DC converter on wind generator side and photovoltaic system as represented in Figure 1.18.

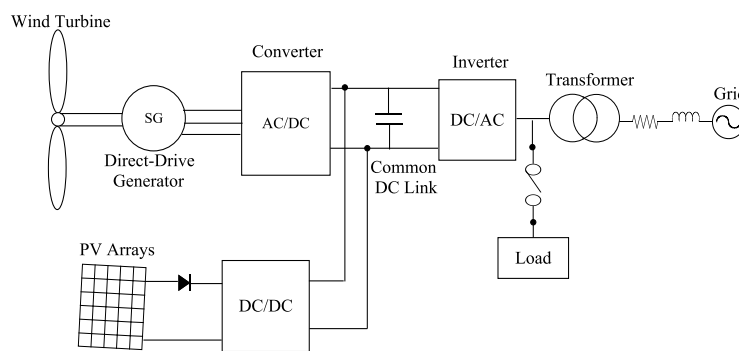


Figure 1.18: Grid connected wind/solar hybrid system [Seul Ki Kim et al. (2006)]

- **Power Smoothing of Grid integrated Microgrid System**

The power output of wind/solar power system varies with changes in weather conditions. These power fluctuations cause adverse effects on the voltage, frequency and transient stability of the utility grid. In the recent years significant attention has been given to generate electricity using wind/solar hybrid system worldwide. The output power of wind and solar system depends upon the weather conditions and fluctuates continuously with variations in wind speed and solar irradiation respectively. The large integration of these intermittent renewable energy (RE) generation sources into the utility grid, may introduce adverse effects on the utility grid [Muhamad Zalani Daud, et al. (2013)]. Thus mitigation of output power fluctuations is one of the major challenges in large integration of wind and solar based generation systems to the utility network. Hence, before delivering power to the utility grid it is essential to smoothen the power fluctuations.

The battery energy storage system can provide flexible energy management solutions that can improve the power quality of renewable energy hybrid power

generation systems [Yoshimoto et al. (2006)]. An intermittent storage medium such as the battery represents a cost-effective and feasible solution, since it can be installed beside the wind energy generator and reduces the energy losses caused by long transformation distances. In [Mohamed Ibrahim et al. (2010)], the technical possibility of using battery storage in order to smoothen the power generated from a grid connected wind energy converter unit is investigated. Also, the battery performance is investigated using fuzzy agent as a degradation estimator model of the battery.

The conventional batteries might be less suited for mitigating these power fluctuations, since they cannot provide the necessary high number of charge cycles. New energy storage technology is energy capacitor system (ECS), which is composed of PE devices and supercapacitor. It is a relatively clean source of energy as it does not contain any toxic material from the environmental viewpoint. It can be cycled millions of time, i.e., it has a virtually unlimited life cycle. Its standby loss is also very low. Therefore, ECS can effectively be used for renewable energy power application [Kinjo et al. (2006)]. A DC coupled wind/hydrogen/supercapacitor hybrid power system is studied in [Tao Zhou and Bruno Francois (2011)]. The purpose of the control system is to coordinate these different sources, particularly their power exchange, in order to make controllable generated power. As a result, an active wind generator can be built to provide some additional services to the grid. A hybrid flow battery supercapacitor energy storage system (ESS), coupled in a wind turbine generator to smoothen the wind power, is studied by real-time hardware-in-the-loop simulation [Li et al. (2010)]. In their work, the prototype controller is embedded in one real-time simulator, while the rest of the system is implemented in another independent simulator.

From the overall literature review, the operation of wind and PV based microgrid system with different integrating configuration, modeling and their interconnection to the unity network has been analyzed. Through the overall literature review, the gap exists mainly to control the output power of wind and PV based microgrid system for grid connected operation. Through the literature review, the control scheme for the output power smoothening of wind and PV based microgrid system has been focused as shortcoming issues. The issue of smoothening of power

fluctuations in wind and PV power generation has attracted dominant research interest and consideration. Thus, the work reported in this thesis presents different control strategies developed for power smoothening of microgrid system which is not found in the existing literature.

1.7 MOTIVATION

Depleting fossil fuels, increasing energy demand and concern over climate change due to CO₂ emission motivate the use of renewable sources. The renewable energy sources have much potential and may be considered strongly for future power supply. Due to the advancement in technology, free of energy cost, less dependence on fossil fuels and cost reductions the DGs such as wind and PV are exploited worldwide. Also these energy sources are preferred for being environmental friendly. However, the power management control strategy for RESs is still challenging due to their weather dependency, high stability and reliable power demand and grid requirements. Due to the rapid growth of the power electronics techniques, the wind and photovoltaic power generation systems have increased rapidly. Most of the studies on wind and PV generation have used only one resource; either wind or PV generation. Recently however, there have been studies on the analysis of wind/PV microgrid system. Usually, two separate inverters for the wind turbine and PV arrays are used for the wind/PV microgrid system. An alternative approach is to use the multi-input inverter for combining these renewable energy sources in the DC end instead of the AC end. It can simplify the wind/PV microgrid system and reduce the costs. Hence, the use of wind and PV based microgrid system strongly contributes to a clean, reliable, efficient and cost effective energy for future power systems. The output power obtained from wind/solar power system fluctuates with changes in weather conditions. These power fluctuations cause adverse effects on the voltage, frequency and transient stability of the utility grid. Thus mitigation of output power fluctuation is one of the major challenges in large integration of wind and solar based generation systems to the utility network. Hence, before delivering power to the utility grid it is essential to smoothen the power fluctuations. Hence we can have increased penetration of the renewable resources into the grid without affecting the grid reliability.

1.8 AUTHOR CONTRIBUTIONS

The author contributions in the thesis are summarized as follows.

- In this thesis, the mathematical model of wind and PV based microgrid system is implemented in Matlab/Simulink environment. The presented wind power system in this work uses the PMSG. The wind system presented by the author uses PMSG with passive rectifier and boost converter combination. This will reduce the switching losses of the system, since there is only one switching device in the boost converter.
- The model presented has a salient feature of integrating wind and PV systems at a common DC link to avoid the use of two separate inverters. It can simplify the wind/PV microgrid system and reduce the cost. The necessary control schemes for power electronics interfacing circuits are implemented for both isolated and grid connected modes of operation of microgrid. The control strategy of DC/DC bidirectional converter for battery is presented. In this work, both photovoltaic panels and the wind generator are controlled to operate at their maximum power point.
- The microgrid model with integration of wind and PV energy system with battery energy storage devices has been implemented for isolated operation. The performance study is analyzed with consideration of DC load, non-linear and induction motor load. The study is focused on the load following, system dynamics and the power sharing among the energy resources in the microgrid.
- The performance study of the microgrid system in grid connected mode of operation is presented using simulation results in this work. The performance results are analyzed for variable nature of the individual DG source. The study presented in the thesis also considers the grid perturbation conditions to ascertain effectiveness of the inverter control scheme of the microgrid system. The balanced voltage dip, unbalanced voltage and polluted grid voltage conditions are considered for the same.
- The control strategies are developed for power smoothing of grid integrated wind/PV microgrid system using ultracapacitors alone and combination of battery and ultracapacitors. In order to observe the real-time performance of energy

storage system in output power smoothing the output power fluctuations, the practical site data for wind speed and solar irradiation are considered. The final result of proposed control strategy is a smooth power output that can be injected to the utility grid.

1.9 ORGANIZATION OF THE THESIS

This thesis is organized into six chapters and brief overview of each chapter is given below.

Chapter 1: This chapter presents the introduction to DG technologies, energy storage devices, microgrid systems and its configurations. The operation and benefits of hybrid wind and PV based DG systems are given. The brief literature review on wind and PV based microgrid system, their integrated operation in isolated and grid connected mode and importance of power smoothing is included. The motivation for wind/PV based microgrid system is presented. The author's contributions and organization of thesis are reported in this chapter.

Chapter 2: In this chapter, the mathematical model of wind/PV based microgrid system with energy storage devices has been given. The detail of modeling of individual components of the microgrid is included in this chapter. The MPPT controllers for wind and PV power systems are reported here. The grid side converter and its control schemes (PQ and VF controller) and the control strategy of DC/DC bidirectional converter for battery are reported. The complete microgrid model implemented in Matlab/Simulink environment is reported in this chapter.

Chapter 3: In this chapter, brief description of wind and PV system with battery for isolated operation is given. The performance study of the microgrid is presented using simulation results in this chapter. The power sharing among the DGs and battery for different loading conditions are reported here. The performance study with DC loads, nonlinear and induction motor considering the variable nature of the individual DG source is given. The simulation results such as wind and solar power, DC link voltage, load voltage, current and system frequency results with source or load change in steps are discussed in this chapter.

Chapter 4: In this chapter, the performance study of the microgrid system in grid connected operation is presented. The grid interfacing operation of wind and PV based microgrid system are given. The simulation result such as the response of microgrid system, power sharing and DC link voltage considering the variation in source or load power are given in this chapter. The microgrid system response to the grid perturbations is also presented using simulation results in this chapter.

Chapter 5: In this chapter, power smoothing of grid integrated microgrid system is presented. The importance of power smoothing of wind/PV microgrid is discussed. The control strategies are developed for power smoothing of the grid integrated microgrid system using ultracapacitors alone and both battery and ultracapacitors have been developed. The simulation results using these control strategies are discussed and presented in this chapter.

Chapter 6 presents conclusions and recommendations for future works.

CHAPTER 2

MODELING OF WIND AND PV BASED MICROGRID SYSTEM

2.1 INTRODUCTION

When many power sources with different characteristics are integrated together in a microgrid system, the complexity in the control mechanism increases. This integration process is carried out first in the powerful Matlab/Simulink software. The complete implemented model is then tested with different meteorological conditions and loading conditions. In order to deal with issues regarding microgrid system planning, interconnected operation and power management, the dynamic model of microgrid system is necessary. This necessitates an accurate and detailed modeling of all the components of microgrid system. The modeling of microgrid for steady state and dynamic performance study has been reported in [Robert Lasseter et al. (2002)]. The operation of a microgrid consisting of wind and photovoltaic system along with battery energy storage during steady state and transient condition is reported in [Kanellos et al. (2005) and Georgakisl et al. (2004)]. The steady-state performance of a rooftop hybrid wind/photovoltaic power system with battery storage for grid connected operation is presented in [Giraud and Salameh (2001)]. The modeling and power control of a solar/wind generation system without wind measurement is reported in [Fernando Valencaga et al. (2003)].

The wind and photovoltaic energy based hybrid systems have received significant attention for contributing renewable power production [Prasad and Natarajan (2006); Kaldellisa et al. (2007)]. In addition to energy sources, a hybrid system may also include DC or AC converters, a storage system, filters and a control system for load management. The power quality control of grid connected hybrid wind/solar system that employs a battery connected in the common DC bus is discussed in [Djamel and Abdallah (2013)]. A fixed speed wind turbine has been employed so power control on high wind speed has been done by stall control. Power control in PV system has been done by employing MPPT tracking that uses perturb

and observe (P&O) method. A hybrid PV/Wind system in which the AC power from the wind is directly supplied to the load via un-interruptible power supply (UPS) is proposed in [Diaf et al. (2008)]. The excess power from wind PV systems, if available, is used to charge the battery. In case of peak load, power is supplied from battery to the load through a DC/AC converter.

In this chapter, the models for the main components of the wind/PV microgrid system are implemented in Matlab/Simulink environment. Namely, they are wind power generation system, PV power system, MPPT controllers, energy storage devices, power electronic interfacing circuits and control schemes for inverter. In this research work, both photovoltaic (PV) panels and the wind generator are controlled to operate at their maximum power point. The presented model of the microgrid system uses a permanent magnet synchronous generator over an induction generator in wind power generation system. The wind system presented in this work uses PMSG with passive rectifier and boost converter combination. This will reduce the switching losses of the system, since there is only one switching device to control in the DC/DC boost converter. In the given microgrid system, the wind and PV system are integrated at common DC link and is connected to the grid using a voltage source inverter. This avoids the use of separate inverters for these two power sources. The necessary control schemes for power electronics interfacing circuits are implemented for both isolated and grid connected modes of operation of microgrid.

2.2 MODELING OF MICROGRID WITH WIND AND PV SYSTEM

The schematic diagram of microgrid system with wind and PV based DG source system considered in this work is shown in Figure 2.1. The microgrid model consists of a wind turbine generator, photovoltaic arrays and a battery energy storage system (BESS), in addition to the DC and AC loads. The wind and PV system are integrated at common DC link and is interfaced to the grid through a three phase voltage source inverter. In this work, RL (resistor-inductor) filter is used to minimize the harmonics generated by the voltage source inverter. The microgrid system can operate in both isolated and grid connected modes. The main converters or inverters have to be controlled to supply high quality and an uninterrupted power to DC and variable AC loads under unpredictable wind speed and solar irradiation conditions for

both operating modes. The battery plays a very important role for both power balance and voltage stability in isolated mode of operation. For different operating conditions, DC bus voltage is maintained stable by a battery converter or buck-boost converter. The stable and high quality AC bus voltage is provided by controlling the main converter. In grid connected mode, the main converter is to provide stable DC bus voltage, and injects only active power to the grid with zero reactive power. When the total power generation is greater than the total load in the microgrid system, it will inject power to the utility grid. Otherwise, the load will receive power from the microgrid and from the utility grid. Thus, the role of battery is not very important in the grid connected mode of operation because the power is balanced by the utility grid.

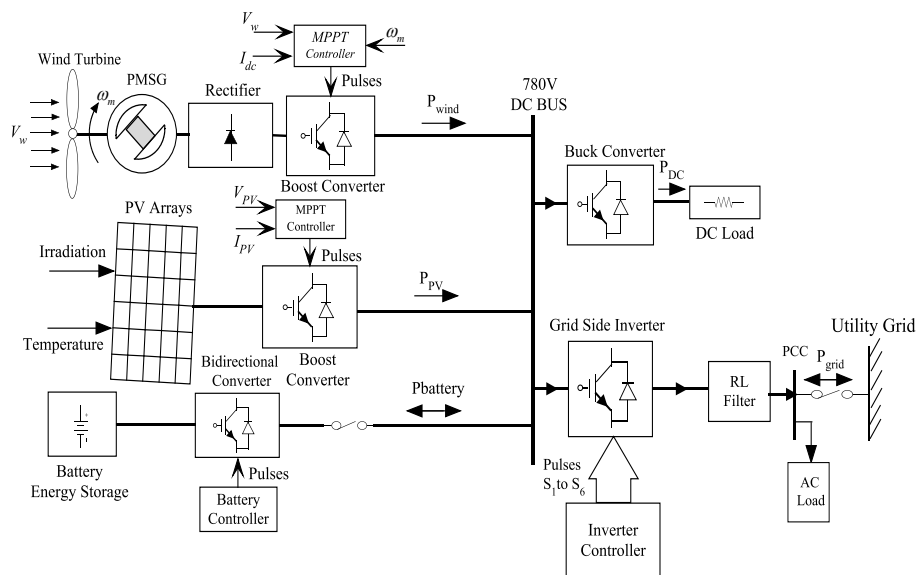


Figure 2.1: Schematic block diagram of the microgrid system

The wind and photovoltaic generators are controlled locally to obtain the maximum power extraction, while the battery energy storage system is controlled using specific control strategy depending on the voltage of the DC bus and energy flow. The PV arrays are connected to DC bus through a DC/DC boost converter and a wind turbine generator (WTG) with PMSG is connected to a DC bus through an uncontrolled rectifier and DC/DC boost converter. A battery is connected to the DC bus through a bidirectional DC/DC converter for isolated operation of the microgrid system. A DC load and 3 phase inductive loads are connected to DC and AC buses

respectively. The rated voltages for DC and AC loads are 500 V and 415 V RMS respectively.

2.2.1 Wind Power Generation System

The wind power system model is composed of a wind turbine, three-phase PMSG and an optimal power extraction by the use of an MPPT algorithm. The modeling of these components of overall wind power system is discussed in the following sections. In this work, the wind power generation system involves a turbine directly coupled to a multi-pole permanent magnet synchronous generator. The wind generating system is then connected to a DC bus through an uncontrolled diode rectifier and DC/DC boost converter. These generators allow gearless coupling, improving the efficiency and robustness of the system [Grauers (1996) and Chen and Spooner (1998)]. Besides, due to variable speed operation capability of PMSG, the power captured from the wind can be optimized by means of an appropriate control strategy.

2.2.1.1 Wind Turbine

With its abundant, inexhaustible potential, its increasingly competitive cost, and environmental advantage, wind energy is one of the best technologies available today to provide a sustainable supply to the world. The principal components of a typical modern wind energy system are turbine rotor, gearbox, generator and tower. The kinetic energy of air of mass ' m ' moving at speed ' V_w ' can be expressed as [Patel (1999)].

$$E_K = \frac{1}{2} m V_w^2 \quad (2.1)$$

During a time period t , the mass (m) of air passing through a given area A at speed V_w is

$$m = \rho A V_w t \quad (2.2)$$

The wind power based on the above two equations is

$$P = \frac{1}{2} \rho A V_w^3 \quad (2.3)$$

The specific power or power density of a wind site is given as

$$P_{den} = \frac{1}{2} \rho V_w^3 \quad (2.4)$$

It is noted that the specific power of a wind site is proportional to the cube of the wind speed. Also, the mechanical power available from a wind turbine [Slootweg et al. (2003)]

$$P_m = \frac{1}{2} \rho A V_w^3 C_p(\lambda, \beta) \quad (2.5)$$

Where P_m = Power in watts, ρ = air density, A = rotor swept area, V_w =wind speed in m/sec, C_p is coefficient of performance. The relationship between rotor speed and wind speed can be given by

$$\lambda = \frac{\omega_m R}{V_w} \quad (2.6)$$

Where R = blade radius in m, ω_m = rotor speed in rad/sec, λ = tip speed ratio (TSR) = ratio between the linear speed of the tip of the blade with respect to the wind speed. The wind turbine torque on the shaft can be calculated from the power [Huang et al. (2009)]

$$T_m = \frac{P_m}{\omega_m} = \frac{1}{2} \rho \pi R^5 \frac{\omega_m^3}{\lambda^3} C_p(\lambda, \beta) \quad (2.7)$$

$$C_p(\lambda, \beta) = 0.5176 \left(\frac{116}{\lambda_i} - 0.4\beta - 5 \right) e^{-\frac{21}{\lambda_i}} \quad (2.8)$$

$$\text{Where } \lambda_i = \left[\frac{1}{\lambda + 0.08\beta} - \frac{0.035}{\beta^3 + 1} \right]^{-1} \quad (2.9)$$

The blade pitch angle β is assumed 0° and using above mathematical expressions the wind turbine model is represented in Figure 2.2.

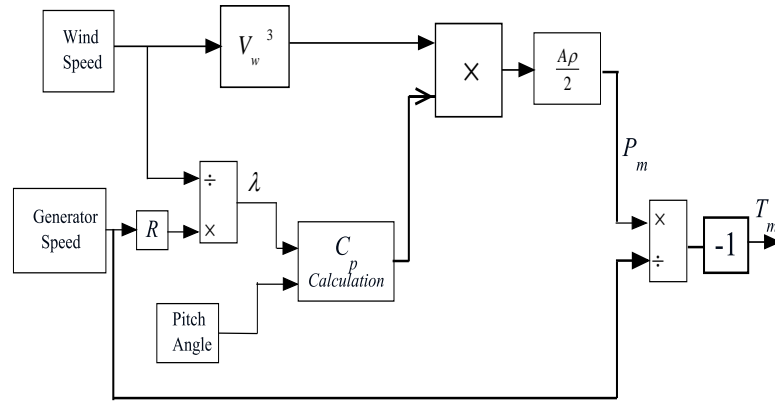


Figure 2.2: Wind turbine model

2.2.1.2 Permanent Magnet Synchronous Generator

In the previous work, most of the researches have considered three phase induction generator or PMSG with controlled rectifier for wind power conversion system of hybrid PV/Wind systems. In this work, the wind turbine directly coupled to a multipole PMSG and the wind generating system is connected to a DC bus through an uncontrolled diode rectifier and DC/DC boost converter. Among the electric generators, PMSG has received much attention in wind energy application because of their property of self-excitation, which allows an operation at a high power factor and high efficiency [Akie Uehara et al. (2011)]. The assumptions made in the modeling of PMSG are

- The saturation of the stator and rotor iron is neglected because of the large air gap usually found in permanent magnet synchronous machines.
- Eddy current and hysteresis losses are negligible
- The induced EMF in the stator windings are sinusoidal

The voltage equations for v_d and v_q of the PMSG in the (d, q) synchronous Park's model are given by [Krishnan (2001); Monica Chinchilla et al. (2006)]

$$v_d = R_s i_d + L_d \frac{di_d}{dt} - \omega L_q i_q \quad (2.10)$$

$$v_q = +R_s i_q + L_q \frac{di_q}{dt} + \omega L_d i_d + \omega \phi_m \quad (2.11)$$

Where i_d and i_q are the d and q -axis machine currents; R_s is the stator resistance; ω is the electrical angular frequency; L_d is the direct axis inductance, L_q is the quadrature inductance; ϕ_m is flux linkages established by the permanent magnet. The expression for the electromagnetic torque in the rotor is written as

$$T_e = \frac{3}{2} p [(L_d - L_q) i_{ds} i_{qs} - \phi_m i_{qs}] \quad (2.12)$$

If the rotor is cylindrical, $L_d \approx L_q = L_s$ so that

$$T_e = \frac{3}{2} p \phi_m i_{qs} \quad (2.13)$$

Where ‘ p ’ is the number of pole pairs of the PMSG. The d and q -axis equivalent circuit model of the PMSG is shown in Figure 2.3.

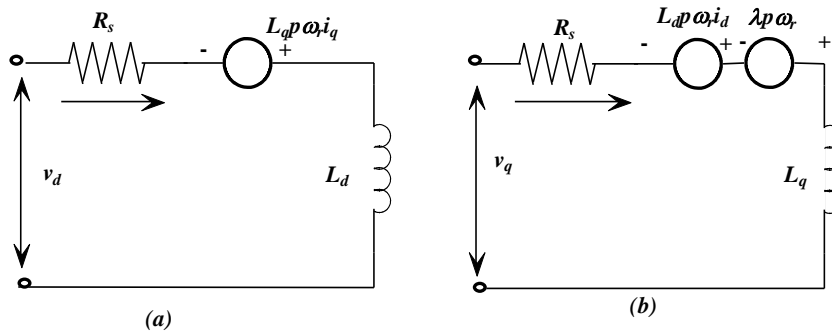


Figure 2.3: d and q -axis equivalent circuit model of the PMSG

2.2.2 PV Arrays

The energy obtained from the sun is the best option for electricity generation as the solar energy can be directly converted into electrical energy by solar photovoltaic module. Electricity from the sun can be generated through the solar photovoltaic modules (SPV). The photovoltaic modules are made up of silicon cells. When many such cells are connected in series we get a solar PV module. Figure 2.4 shows the equivalent circuit of the solar cell composed of a light generated current source, a diode representing nonlinear impedance of the p-n junction, and series and

parallel resistances. The series resistance R_{se} represents the internal losses due to the current flow. The parallel resistance R_{sh} in parallel with the diode, this corresponds to the leakage current to the ground. The basic equation describing the nonlinear current-voltage relationship of the PV cell is [Eghtedarpour and Farjah (2012)]

$$I = I_{ph} - I_D - I_{sh} \quad (2.14)$$

$$I = I_{ph} - I_s \left[\exp \left(\frac{q(V + IR_S)}{akT} \right) - 1 \right] - \frac{V + IR_{se}}{R_{sh}} \quad (2.15)$$

Where I_{ph} is photocurrent of the PV cell; I_s is diode saturation current and R_{se} is the equivalent series resistance, R_{sh} is the equivalent parallel resistance.

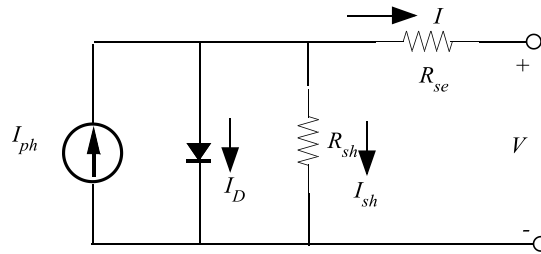


Figure 2.4: Simplified PV cell circuit model

The PV array consists of number of PV modules connected in series and parallel to get an appropriate output power. For modeling, the Solarex MSX-60 PV module was chosen. The MSX 60 PV module has 36 series connected polycrystalline silicon cells and gives 60W of nominal maximum power. The equivalent circuit for the solar cells arranged in N_s -series and N_p -parallel combination is shown in Figure 2.5.

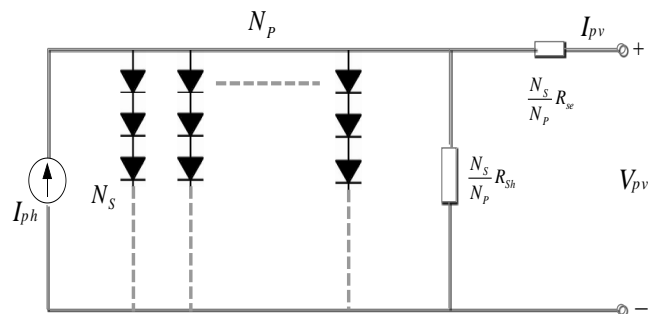


Figure 2.5: Equivalent circuit of a PV array

The relationship between the voltage and current in PV array [Molina and Mercado (2008)] is represented by.

$$I_{pv} = N_p I_{ph} - N_p I_s \left\{ \exp \left[\frac{q}{akT} \left(\frac{V_{pv} + I_{pv} R_{se}}{N_s} + \frac{I_{pv} R_{se}}{N_p} \right) \right] - 1 \right\} - \frac{N_p}{R_{sh}} \left(\frac{V_{pv}}{N_s} + \frac{I_{pv} R_{se}}{N_p} \right) \quad (2.16)$$

Where q is electron charge; k is Boltzmann's constant; T is cell temperature (K); ' a ' is diode quality factor; R_{se} and R_{sh} are cell intrinsic series and parallel resistance. The photocurrent is the function of solar radiation and cell temperature, described as

$$I_{ph} = \frac{G}{G_{ref}} \left(I_{phref} + K_o (T - T_{ref}) \right) \quad (2.17)$$

Where G is the actual solar radiation in W/m^2 ; G_{ref} , T_{ref} and I_{phref} are solar radiation, cell absolute temperature, photocurrent in standard test conditions respectively; K_o is the temperature coefficient of current and is given by

$$K_o = \frac{I_{phref} - I_{ph}(T)}{(T_{ref} - T)} \quad (2.18)$$

The series resistance R_{se} is determined using by

$$R_{se} = - \left[\frac{dV}{dI} \right]_{V_{oc}} + \frac{1}{m} \quad (2.19)$$

$$\text{Where } m = \frac{I_{sref} q}{AkT_{ref}} \exp \left(\frac{qV_{ocref}}{nkT_{ref}} \right) \quad (2.20)$$

The diode saturation current I_s varies with temperature and is represented by the following equation

$$I_s = I_{sref} \left(\frac{T}{T_{ref}} \right)^3 \exp \left[\frac{qE_g}{ak} \left(\frac{1}{T_{ref}} - \frac{1}{T} \right) \right] \quad (2.21)$$

Where E_g is the band gap energy of the semiconductor cell = 1.12 eV depending on the cell material and I_{sref} the diode saturation current in standard test conditions is given by

$$I_{sref} = \frac{I_{sc}(T_{ref})}{\exp\left(\frac{qV_{oc}(T_{ref})}{akT_{ref}} - 1\right)} \quad (2.22)$$

Considering all modeling equations of the PV arrays, the Matlab/Simulink based model of PV array is shown in Figure 2.6.

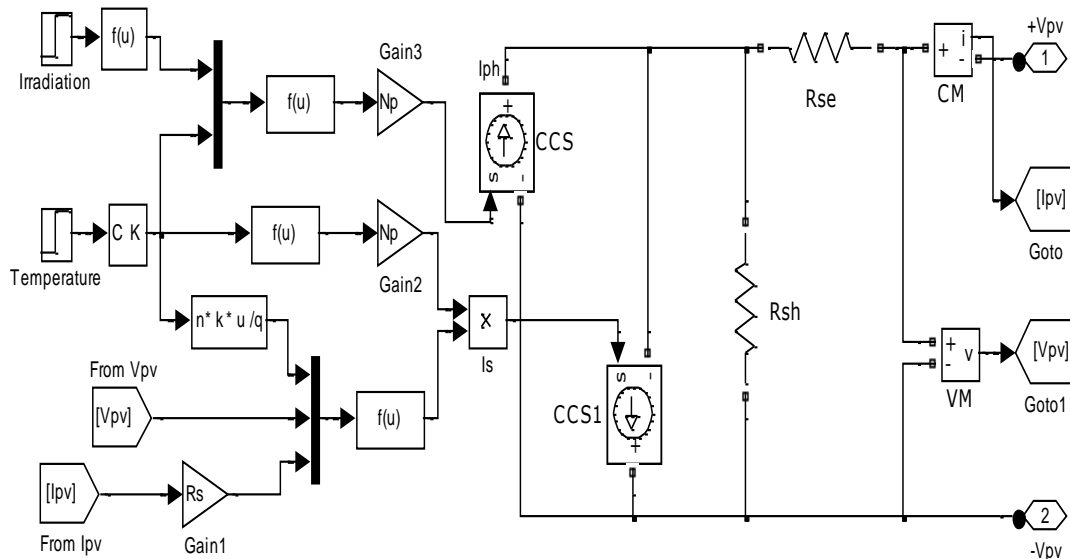


Figure 2.6: Matlab/Simulink model of PV array

2.3 MAXIMUM POWER POINT CONTROLLERS

Three basic types of MPPT algorithms used for the wind power systems are namely, perturb and observe technique, Tip Speed Ratio (TSR) control and Optimum Relationship Based (ORB) control [Wang and Chang (2004)]. P&O control technique adjusts the turbine speed toward the MPP, according to the result of comparison between successive wind turbine generator output power measurements. TSR control directly regulates the turbine speed to keep the TSR at an optimal value by measuring wind speed and turbine speed [Kazmi et al. (2011)]. ORB control ensures MPPT with the aid of knowledge of optimum relationships between system parameters. In [Haque et al. (2010)] the relationship between electrical torque and rotor speed is employed to

track maximum power point. The maximum power point algorithm suitable for large inertia systems and it is operated at without measurement values of wind speed [(Yuanye Xia et al. (2011))]. In this work, perturb and observe technique is used for wind power generation system. The generated AC power from PMSG is converted to DC power through a diode bridge which is simple, robust, requires no control circuit and cheap. Since only one power switching device is used in DC/DC converter, resulting in low cost and simple control.

A MPPT controller is essential in case of PV power systems to deliver the maximum possible power to the load. There are different approaches like fractional open-circuit voltage method, fractional short-circuit current method, perturb and observe, incremental conductance, etc. to track the maximum power [Esram and Patrick Chapman (2007)]. In this work, the incremental conductance method is used because of its ability to track the maximum power under fast changing atmospheric conditions.

2.3.1 Wind Power System

In order to determine the optimal operating point of the wind turbine, it is essential to include a maximum power point tracking algorithm in the system [Raza Kazmi et al. (2010)]. A MPPT algorithm increases the power conversion efficiency by regulating the turbine rotor speed according to actual wind speeds [Yuanye Xia et al. (2011)]. The maximum power point (P&O technique) algorithm operated at without measurement values of wind speed and it is suitable for large inertia systems.

The MPPT algorithm keeps the power coefficient C_p at its maximum, $C_p=C_{pmax}$, corresponds to λ_{opt} [Majid A. Abdullah et al. (2011)].

$$\text{Where } \omega_{ref} = \frac{V_w \lambda_{opt}}{R} \quad (2.23)$$

We deduce

$$P_m = 0.5 \rho A C_{pmax} \left(\frac{R \omega_{ref}}{\lambda_{opt}} \right)^3 \quad (2.24)$$

The reference turbine speed ω_{ref} is generated by the MPPT code using perturb and observe technique. Let the output power of the generator is P_{ref} corresponding to initial reference speed for rotor ω_{ref} . The reference rotor speed (ω_{refnew}) increased or decreased by one step and corresponding output power (P_{refnew}) is calculated again. The change in rotor speed ($\Delta\omega = \omega_{refnew} - \omega_{ref}$) and corresponding power ($\Delta P = P_{refnew} - P_{ref}$) are calculated. The signs for calculated values of $\Delta\omega$ and ΔP are assigned as follows.

If $\Delta\omega > 0$ then $\text{sign}(\Delta\omega) = 1$, else $\text{sign}(\Delta\omega) = -1$;

If $\Delta P > 0$ then $\text{sign}(\Delta P) = 1$, else $\text{sign}(\Delta P) = -1$;

The new speed is determined using the following equation and the entire procedure is repeated to reach to optimum operating point of the system.

$$\omega_{ref}(n) = \omega_{ref}(n-1) + \text{sign}(\Delta P) * \text{sign}(\Delta\omega) * \omega_{step} \quad (2.25)$$

Let us assume the initial wind speed is V_{w1} and operating point of the turbine represented as (ω_1, P_1) in P verses ω characteristic curve. Also, let us now assume that the turbine speed is increased by ω_{step} , due to change in wind speed V_{w2} which results in a new speed ω_2 .

$$\Delta\omega = \omega_2 - \omega_1 > 0; \text{ then } \text{sign}(\Delta\omega) = 1$$

$\Delta P = P_2 - P_1 > 0$; then $\text{sign}(\Delta P) = 1$; Therefore, $\omega_2 = \omega_1 + \omega_{step}$. Hence the operating point of the turbine changes and this new operating point will be given by (ω_2, P_2) . The flowchart for maximum power point tracking algorithm used for tracking maximum power output from wind system is given in Figure 2.7. The schematic block diagram of wind energy conversion system with PMSG and MPPT controller is shown in Figure 2.8.

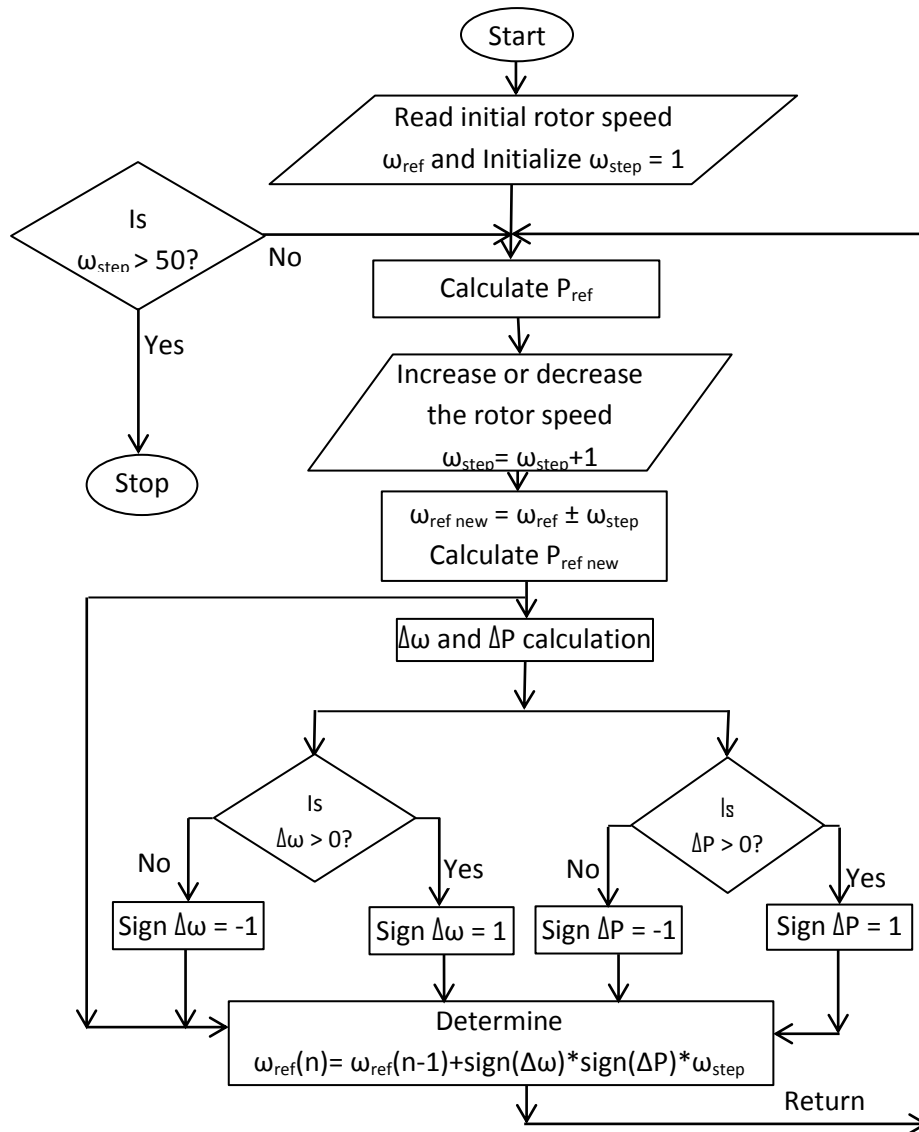


Figure 2.7: Flowchart for maximum power point tracking algorithm

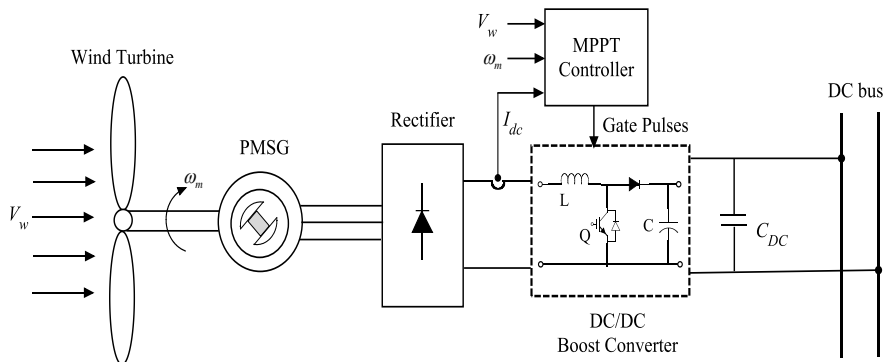


Figure 2.8: Schematic diagram of WECS with PMSG and MPPT controller

2.3.2 PV System

MPPT algorithm based on incremental conductance is used to get maximum power output. Also, this algorithm can track rapidly increasing and decreasing irradiance conditions with higher accuracy than other methods [Mutoh et al. (2006)].

In this method, the PV module terminal voltage is adjusted according to the MPP voltage based on the incremental and instantaneous conductance of the PV module. The relationship between dI/dV and $-I/V$ is based on the fact that when MPPT is towards the right side of the MPP, dP/dV is negative and when it is towards the left side of the MPP, dP/dV is positive. This algorithm can determine the MPPT has reached the MPP or not, while operating point oscillates around the maximum power point. Figure 2.9 shows P-V characteristics of 40 kW solar power system.

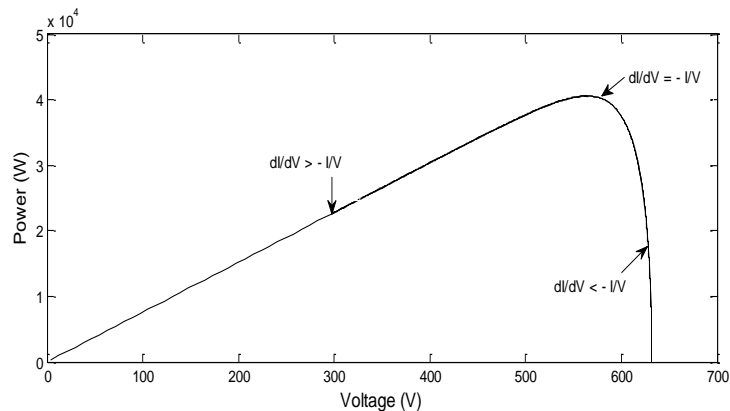


Figure 2.9: P-V Curve of 40 kW solar system

From Figure 2.9 it is observed that the slope of the P-V curve is equal to zero at the point of MPP, positive on the left of the MPP and negative on the right of the MPP. Since $dP/dV=0$, at the point of maximum power, in terms of V and I, the equation could be written as $dP/dV = [d(VI)]/dV = 0$;

$$\therefore dI/dV = - I/V$$

The PWM control signal of the converter is regulated by the MPPT algorithm until the condition $(dI/dV)+(I/V)=0$ is achieved. The schematic diagram for interconnection of PV power generation system with MPPT controller is represented as shown in Figure 2.10.

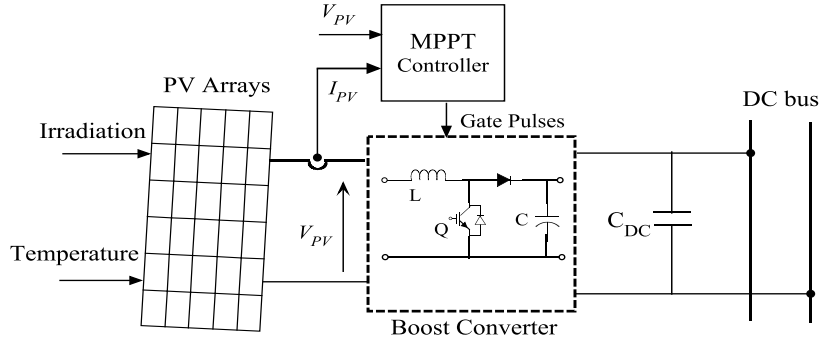


Figure 2.10: Schematic block diagram for interconnection of PV arrays with MPPT controller

2.4 ENERGY STORAGE DEVICES

2.4.1 Battery

The design of proper controller is another challenge because of the nonlinear characteristic of battery. The simplest and commonly used model of a battery with an ideal voltage source in series with a constant internal resistance is reported in [Durr et al. (2006)]. The Thevenin model of representing the battery is presented in [Salameh et al. (1992); Appelbaum and Weiss (1982)] which consists of an ideal no-load battery voltage, series internal resistance in series with parallel combination of overvoltage resistance and capacitance as shown in Figure. To avoid excessive complexity while considering the dynamics of the battery, a generic dynamic battery model is proposed in [Tremblay et al. (2007) and] and this includes the current flowing across the battery and the battery state of charge (SOC). In this research work, the lead acid battery is used where it is modeled by a constant resistance connected in series with a controlled voltage source. The simplest of the equivalent circuit models used for batteries is the Thevenin battery model as represented in Figure 2.11 (a). The controlled source is described in the following equations [Yasin et al. (2011)].

$$E_{batt} = E_o - K \frac{Q_b}{Q_b - \int idt} + A \exp(-B \int idt) \quad (2.26)$$

$$V_{batt} = E_{batt} - R_{batt} I_{batt} \quad (2.27)$$

The state of charge of the battery is given by the following equation,

$$\%SOC = [1 - \frac{1}{Q_b} \int_0^t i(t) dt] \times 100 \quad (2.28)$$

Where E_{batt} = No load voltage (V); E_o = Battery constant voltage (V); K =Polarization voltage (V); Q_b =Battery capacity (Ah); A = The exponential zone amplitude (V); B = The exponential zone time constant inverse (Ah⁻¹); $\int idt$ =charge drawn/supplied by the battery (Ah); I_{batt} = Battery charging and discharging current (A); R_{batt} = Internal resistance of the battery (Ω); V_{batt} =Terminal voltage of the battery (V). The equivalent electrical circuit model is represented in Figure 2.11 (b).

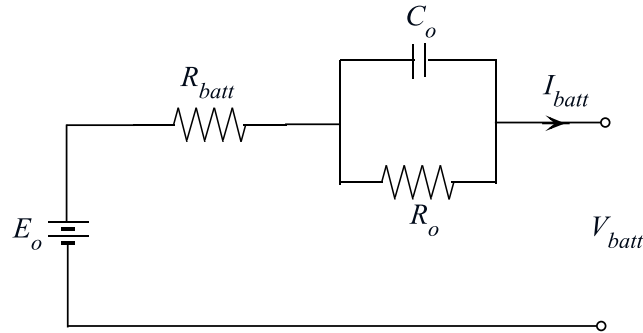


Figure 2.11: (a) Thevenin Battery Model [Appelbaum and Weiss (1982)]

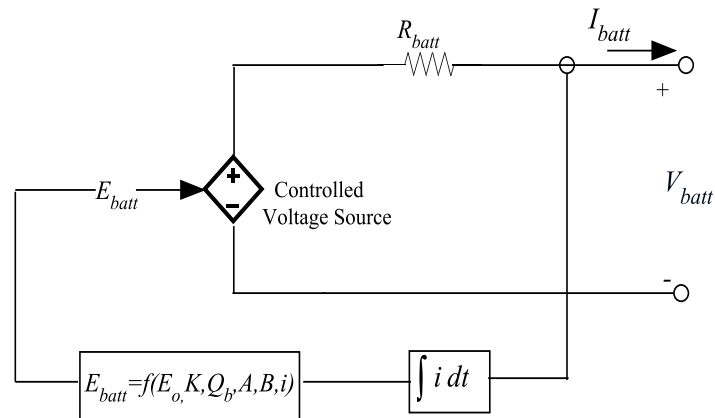


Figure 2.11: (b) Equivalent electrical circuit of battery

2.4.2 Control Strategy of DC/DC Bi-directional Converter for Battery

The primary goal of the battery converter is to regulate the common DC bus voltage in isolated mode of operation of microgrid. The battery current changes accordingly to changes in weather conditions and load power requirements. The

control of the bi-directional DC/DC converter is the key factor of the power management of the microgrid system. A battery bank is used to supply the power to fast source or load variations, ripples and spikes in standalone applications. A DC/DC bi-directional converter works in a buck mode to charge the battery with excess power and in a boost mode to discharge it to fill up the gap of power deficiency. The charging or discharging of battery maintains the power balance between fluctuating wind, PV power and time varying load. The DC link voltage and battery current are regulated by two control loops. The outer voltage loop regulates the voltage and the error is passed through a PI controller to obtain a reference battery current. The reference battery current is compared with the measured battery current and error is passed through another PI controller and generates the necessary PWM signal for switching of the buck-boost DC/DC converter. In addition, a safety feature is integrated to monitor the state of charge (SOC) of the battery storage system during its operation. The SOC should be regulated within predetermined limits ($SOC_{min} \leq SOC \leq SOC_{max}$) as described in [Yoshimoto et al. (2006)]. The schematic of the DC/DC converter controller used to regulate the charging or discharging current of the battery to maintain the DC bus voltage constant is shown in Figure 2.12.

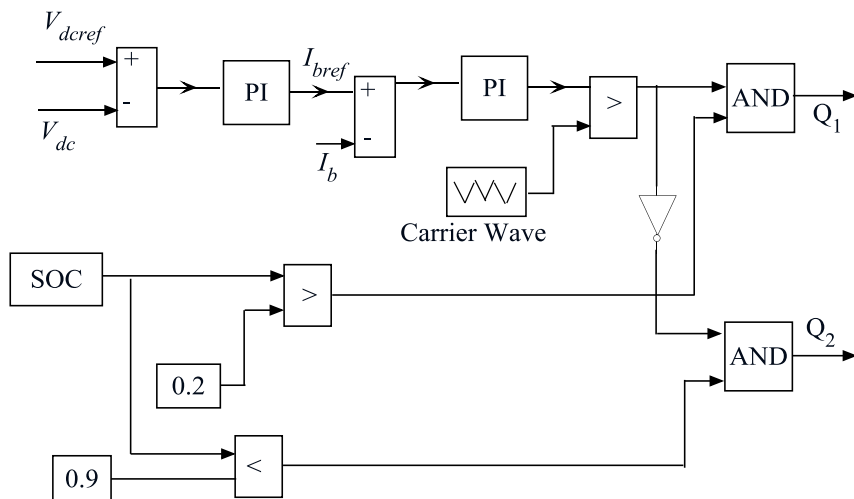


Figure 2.12: Control scheme of Buck-Boost Converter of the Battery

2.4.3 Ultracapacitors

The ultracapacitors also known as electric double layer capacitors are large capacitance devices, with capacitances of several thousand farads. They are high power density devices. Figure 2.13 (a) shows the image of Maxwell Boostcap

ultracapacitors. The classical equivalent circuit model of ultracapacitor consists of three electrical components [Uzunoglu and Alam (2006)]. They are capacitor C , resistance in series ESR (Equivalent Series Resistance, R_{esr}) and resistance in parallel EPR (Equivalent Parallel Resistance, R_{epr}) as shown in Figure 2.13 (b). C is the charge storage capacity of the ultracapacitor, ESR is the internal series resistance and EPR is used to model the leakage current.



Figure 2.13: (a) Maxwell Boostcap ultracapacitors

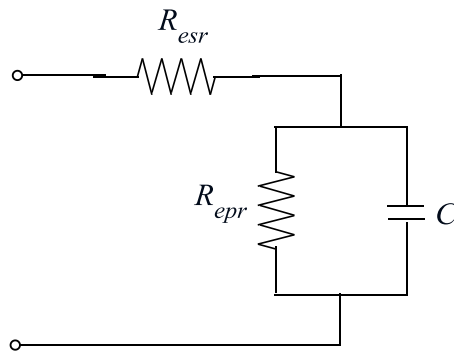


Figure 2.13: (b) Classical equivalent circuit model of ultracapacitor

In this work, the ultracapacitor (UC) storage system is modeled by the nominal capacitance (C) in series with an ESR (R_{esr}) [Yanzhu Ye et al. (2013)] as shown in Figure 2.14 (a). The energy stored in the UC is a function of capacitance and voltage. The voltage across UC effectively determines the SOC because the value of capacitance is relatively stable. Let E_{max} be the maximum stored energy and E_{inst} be the instantaneous stored energy of UC, the percentage SOC is determined using following expressions.

$$E_{\max} = 0.5C(V_{\max})^2 \text{ and } E_{inst} = 0.5C(V_{inst})^2 \quad (2.29)$$

$$\%SOC = \frac{E_{inst}}{E_{\max}} \times 100 \quad (2.30)$$

During the system operation, the present UC voltage and current are essential to be monitored to follow the following constraints.

$$V_{\min} < V < V_{\max} \text{ and } I_{Ch,max} < I < I_{Dis,max} \quad (2.31)$$

Where V_{\min} and V_{\max} are minimum and maximum working voltage of the ultracapacitor respectively. And $I_{Ch,max}$ and $I_{Dis,max}$ are the maximum charging and discharging current of UC separately. The UC current is negative for charging and is positive for discharging. Figure 2.14 (b) shows the connection of UC units to build a UC bank that is capable of providing required amount of power. If the number of capacitors connected in series is n_s and number of series strings in parallel is n_p then the total UC system capacitance and resistance of the UC bank are determined as

$$R_{uc\ total} = n_s \frac{R_{esr}}{n_p} \quad (2.32)$$

$$C_{uc\ total} = n_p \frac{C}{n_s} \quad (2.33)$$

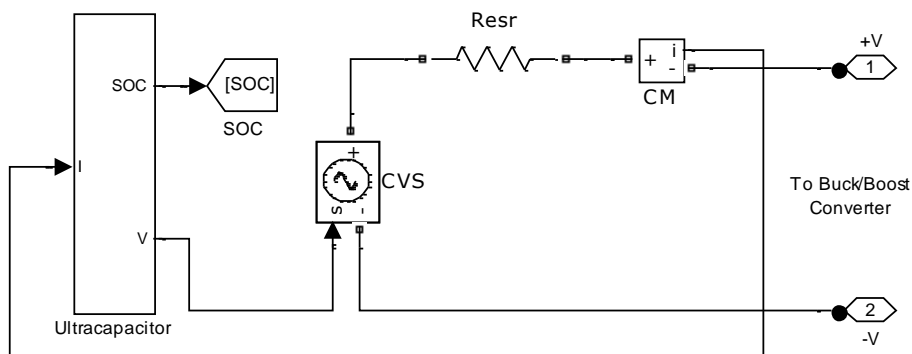


Figure 2.14: (a) Equivalent circuit of UC unit

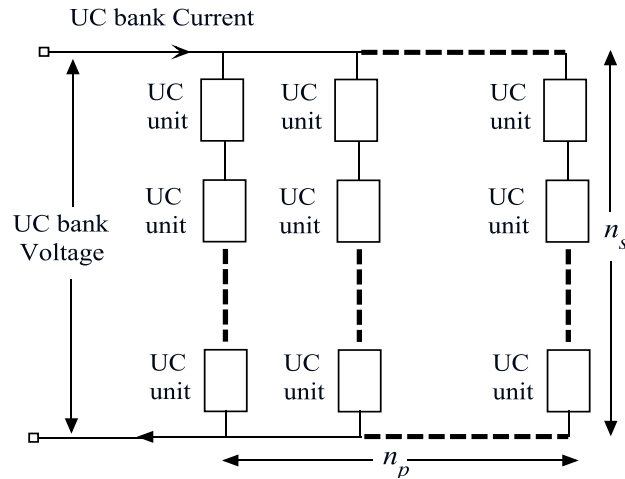


Figure 2.14: (b) Arrangement of capacitors in a UC bank [Uzunoglu and Alam (2006)]

2.5 CONTROL SCHEMES FOR INVERTER

To convert the DC link voltage to AC output voltage a voltage source inverter (VSI) using pulse width modulation topology is implemented [Bose Bimal (2002)]. It consists of six insulated gate bipolar-junction transistors (IGBT). Furthermore, the SPWM is used in order to generate the gating pulse for applying to the gates of the IGBT. In order to operate voltage source inverter, typically two types of control schemes are adopted. They are (i) the active and reactive power control scheme and (ii) Voltage and frequency control. When the inverter is operated to inject a real and reactive power generated from microgrid system to the utility grid, the PQ control scheme is used [Caldon et al. (2003)]. For standalone operation of microgrid system the inverter is controlled to supply the load with fixed values of voltage and frequency. The inverter control schemes for the microgrid system have been implemented in the Matlab/Simulink environment.

2.5.1 Active and reactive power control

The control scheme of the grid side voltage source inverter (VSI) is shown in Figure 2.15. In this type of inverter, the IGBTs are used as switching operation devices. To minimize the harmonics generated by the inverter the series resistor and inductor (RL) filter is used.

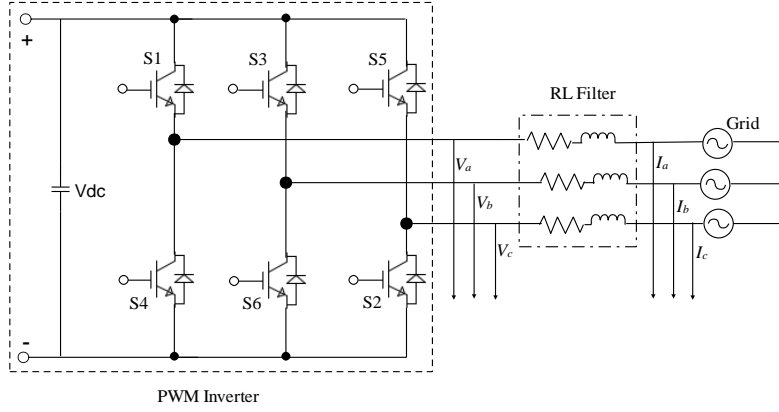


Figure 2.15: Grid side inverter

The total instantaneous power in a three-phase system is given by

$$p(t) = v_a i_a + v_b i_b + v_c i_c \quad (2.34)$$

The relations of these powers in synchronous reference frame are as follows

$$P = \frac{3}{2}(V_{gd} i_d + V_{gq} i_q) \quad (2.35)$$

$$Q = \frac{3}{2}(V_{gq} i_d - V_{gd} i_q) \quad (2.36)$$

If the reference frame is synchronized with the grid voltage, the grid voltage vector is $V_g = V_{gd} + j0$, the expressions for active and reactive power are given by

$$P = 1.5(V_{gd} i_d) \text{ and } Q = 1.5(V_{gd} i_q) \quad (2.37)$$

The d and q -axis components in synchronous reference frame with decoupling terms can be represented as

$$u_d = R_f i_d + L_f \frac{di_d}{dt} + V_{gd} - \omega L_f i_q \quad (2.38)$$

$$u_q = R_f i_q + L_f \frac{di_q}{dt} + V_{gq} + \omega L_f i_d \quad (2.39)$$

The objective of the grid side inverter control strategy is to maintain the DC link voltage constant and to transfer the total maximum power produced to the grid at unity power factor. In this control scheme, the active and reactive power control can be implemented by controlling the direct and quadrature currents respectively with PI controllers. The outer loop of capacitor voltage control is used to set the d -axis current reference for active-power control. The q -axis reference current is specified by desired value inverter reactive power output injected to the grid [Gaonkar and Pillai (2011)]. If the unity power factor is considered, this current would be regulated at zero value. And also to have independent control of the current components i_d and i_q the decoupling voltage components are added to the output of current PI controllers [Rodriguez et al. (2007)]. The phase locked loop (PLL) block which measures the grid voltage phase angle θ_g is used to implement the Park transformation and to synchronize the inverter with the grid. The PQ control scheme presented for grid connected inverter operation using equation (2.36) and (2.37) is shown in Figure 2.16.

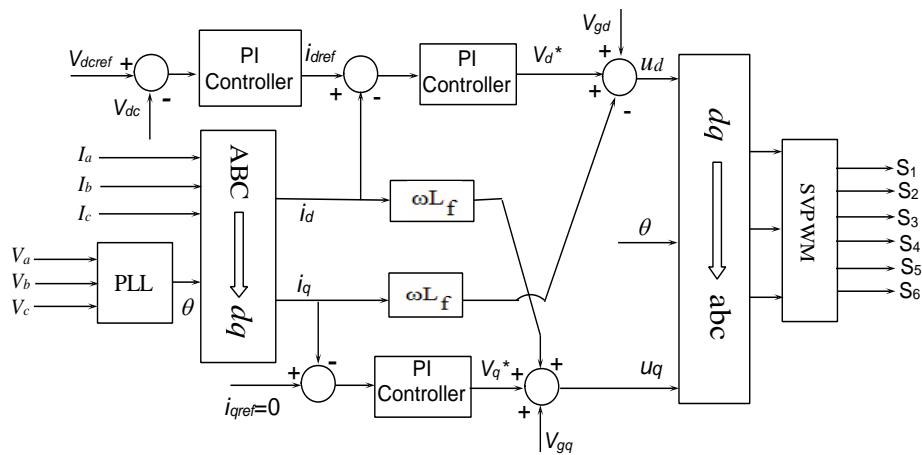


Figure 2.16: Active and reactive power controller

2.5.2 Voltage and frequency control

The isolated mode operation of microgrid system requires a different control scheme from that of the grid connected mode. Since no grid exists in this mode of operation of microgrid system, the output voltage and frequency have to be controlled based on rotating reference frame theory [Haruni et al. (2010)]. By generating a reference angular velocity, the frequency of the system is controlled. This is done by

controlling the amplitude and frequency of the modulating input signal to the PWM inverter. The control structure for the islanding mode is depicted in Figure 2.17.

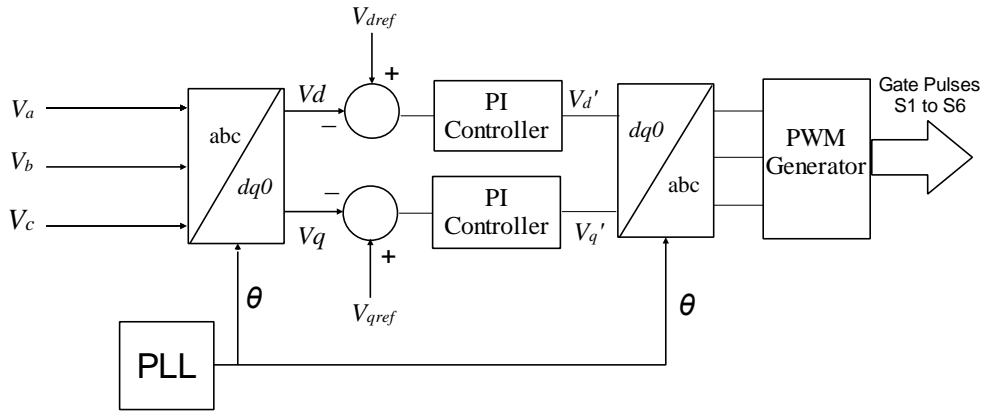


Figure 2.17: Voltage and frequency controller

The inverter must supply power according to the load demand with fixed values of voltage and frequency. When VF control is implemented, it is possible to use a control based on Park transformation and compute the direct and quadrature axis voltage components V_{dref} and V_{qref} , which are considered as the reference values [Haque et al. (2010)]. Since there is no AC side frequency available for reference, an internal voltage signal at the desired frequency must be produced. Moreover, in this control scheme, the voltage errors have to be used to drive two PI regulators producing the signals for the inverter PWM modulation, where V_q is maintained zero. From Figure 2.17, the voltage equations across the RL filter are given by

$$\begin{bmatrix} V_a \\ V_b \\ V_c \end{bmatrix} = \begin{bmatrix} V_{a1} \\ V_{b1} \\ V_{c1} \end{bmatrix} + R_f \begin{bmatrix} I_a \\ I_b \\ I_c \end{bmatrix} + L_f \frac{d}{dt} \begin{bmatrix} I_a \\ I_b \\ I_c \end{bmatrix} \quad (2.40)$$

Where R_f = resistance and L_f = inductance of RL filter and I_a , I_b , and I_c are three phase load currents. The d -axis and q -axis load voltages are given by:

$$V_d' = V_d + i_d R_f + L_f \frac{di_d}{dt} - \omega L_f i_q \quad (2.41)$$

$$V_q' = V_q + i_q R_f + L_f \frac{di_q}{dt} + \omega L_f i_d \quad (2.42)$$

The voltage V_d' and V_q' are given to PWM signal generator so that the output voltage is controlled as shown in Figure 2.17.

2.5.3 DC link and Filter

A lower bound on the DC bus voltage can be determined from the following equation at a unity power factor [Mohan et al. (2010)]

$$0.6124m_a V_{DC} \geq \sqrt{(V_{acLL})^2 + 3(\omega L_f I_{AC})^2} \quad (2.43)$$

Where V_{acLL} = Line to Line RMS voltage on inverter side.

L_f = Filter Inductance.

I_{ac} = Maximum possible RMS value of the AC load current.

m_a = Modulation Index of the Inverter.

The value of the DC link voltage is 780 V for RMS voltage of 415 V on inverter side. The electrolytic DC link capacitor is included for power decoupling between the microgrid and the grid. When the power flows into the DC link is constant and the power drawn from the DC link follows a $\sin^2(\omega t)$ waveform, the size of this decoupling capacitor can be determined.

$$C_{DC} = \frac{P_{DC}}{2\omega V_{DC} \bar{v}_{dc}} \quad (2.44)$$

Where P_{DC} is the average DC link power, ω is the grid frequency (314 rad/sec); V_{dc} is the DC link voltage and \bar{v}_{dc} is the amplitude of the ripple voltage. If the DC link voltage is less than the peak grid voltage plus the voltage drop across the semiconductors and filter, the grid current cannot be controlled. The maximum DC link voltage selected is 800 V and the amplitude of the ripple voltage is 30 V

respectively [Kjaer (2005)]. The size of the DC link capacitor is computed by above equation is to be nearly 4000 μF and the DC link capacitor size of 5000 μF is selected in order to allow for some over voltages, without damaging the capacitor.

To reduce the high frequency harmonics content of the line current caused by the switching operation of the inverter, the line filters are used [Gaonkar et al. (2008)]. Normally, a line filter consists of LC (inductor-capacitor), RL (resistor-inductor), RC (resistor-capacitor) or LCL (inductor-capacitor-inductor) [Mustapha and Moulay (2004)]. In this work, series RL filter is used to reduce the harmonics generated by the voltage source inverter as shown in Figure 2.18.

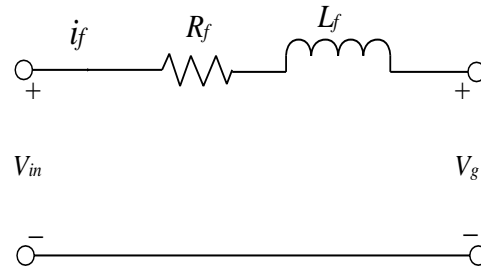


Figure 2.18: Series RL filter

The equation for grid voltage V_g is given by applying Kirchhoff's voltage law to the circuit of Figure 2.16 is,

$$V_g = V_{in} + i_f(R_f + j\omega L_f) - L_f \frac{di_f}{dt} \quad 2.45$$

Where i_f is the filter current (A), V_{in} is the voltage at the terminal of the converter (V).

2.6 MICROGRID SYSTEM MODEL IMPLEMENTED IN MATLAB/SIMULINK

The model of microgrid with wind and PV based DG system implemented in Matlab/Simulink environment is shown in Figure 2.19. Both PV panels and the wind generator are controlled to operate at their maximum power point using MPPT controllers. The wind and PV power system are integrated at common DC link and this DC link power is delivered to the grid/load using a three phase voltage source inverter. In order to minimize the harmonics generated by the inverter the RL filters are used. The modeling and simulation parameter of microgrid system and control schemes are given in Appendix A.

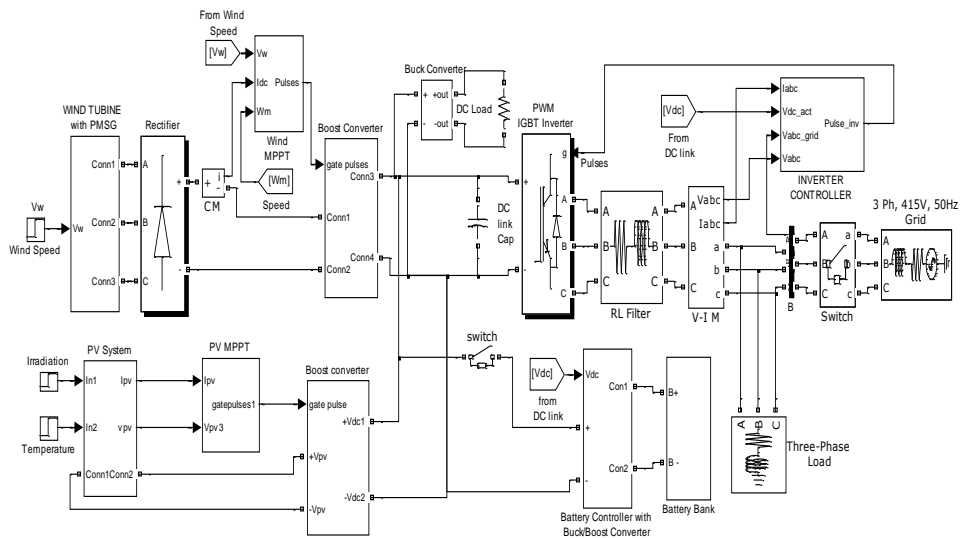


Figure 2.19: Model of microgrid system in Matlab/Simulink with MPPT controllers

2.7 CONCLUSIONS

To analyze the dynamic behavior of microgrid system, proper and accurate models are required for various components. Thus, this chapter presents the detailed modeling of wind and PV based DGs, storage devices like battery and ultracapacitors and design of MPPT controllers. Following this, the detailed model of PMSG and power electronics converter interfacing along with control strategies have been described. All the models obtained from theoretical equations have been built in Matlab/Simulink environment. The detail model presented is used to study both isolated and grid connected operation microgrid system. The model presented has a salient feature of integrating wind and PV power system at common DC link to avoid the use of separate grid connection requirements for each of the power sources. Also, the model implemented is used for studying the power smoothing using energy storage devices when the microgrid system is connected to the utility grid.

CHAPTER 3

PERFORMANCE ANALYSIS OF MICROGRID IN ISOLATED MODE OF OPERATION

3.1 INTRODUCTION

Both wind and PV based distributed generation systems may become a dominant source of power in the near future for residential and remote applications because of their efficiency and cleanness. Also these energy sources are preferred for being environmental friendly. The understanding of the dynamic performance of standalone microgrid system is important to the advancements in technology and development of controls for future power systems. Thus, the performance study of microgrid with wind and PV based DG system in an isolated mode of operation becomes significant in dealing with the issues related to system planning, power sharing, control, security and power management. Remote area power supply schemes are now becoming popular in remote areas including islands. However, the design and operation of such a power system are challenging due to the absence of a main grid supply system. When designing and implementing power system for remote areas, voltage and frequency are the most important aspects to be controlled. In addition, coordination between different system components, maximum power extraction from the renewable energy sources and power quality are the other major issues of interest [Nishad Mendis et al. (2003)].

The performance of standalone wind/photovoltaic hybrid system with battery storage is reported in [Youssef et al. (2010)] and employed squirrel-cage induction generator (SCIG) in wind subsystem. A hybrid scheme employing wind turbine permanent-magnet (PM) alternator and PV array was proposed, [Honorati et al. (1996)] in which these power sources were connected in series through DC/DC converters. Subsequently, a simpler configuration connecting the PV and wind generator in parallel was attempted in [Kim et al. (1997)]. Further, for supplying AC loads in these hybrid wind/solar schemes, the varying amplitude and varying

frequency of the stator voltage of the permanent magnet alternator and the variable DC voltage of the PV array have to be suitably conditioned using complex power-electronic interfaces [Kurosumi et al. (1998)].

The performance analysis is an important issue in the standalone microgrid systems based on renewable energy sources. The output power of wind turbines is mostly fluctuating and negatively affects the system frequency. The PV generated power depends on variable solar radiations. The system stability is also affected by variations of the load demand and types of the loads considered. An integration of battery energy storage system (BESS) with renewable power generating system provides active power conditioning features and power quality improvement. The BESS can absorb excess active power when the load is less and can supply power at the time of peak load conditions [Tsai et al. (1995)]. The battery system solves the inconsistencies that renewable energy offers [Bhende et al. (2011) and Fakham et al. (2011)]. Lead acid batteries are ideal for renewable energy systems and applications. Hence, the hybrid generation system forms a highly independent generation system. Over the years, there have been research works on the standalone wind/PV hybrid generation system [Daniel and Ammasai Gounden (2004)] in which the wind generators are focused on induction generators. The analysis performed in this study is based on accurate models with controllable power converters. The frequency deviation, DC bus voltage stability and voltage THD are used as indices for system performance.

In this chapter, the performance analysis of the isolated mode of operation of the microgrid model developed in the previous chapter is described in detail. The performance characteristics like voltage, amplitude and frequency regulation in an isolated mode of operation of the microgrid are studied and analyzed. The power sharing among the DGs and battery for different loading conditions are reported. Moreover the performance study with DC loads, unbalanced loads, nonlinear loads and induction motor load considering the variable nature of the individual DG source is detailed. Further the performance study of the microgrid system is analyzed with individual DG source by disconnecting the PV arrays or excluding wind power generation. The simulation results such as active power, DC link voltage, load

voltage, load currents, percentage THD variations and system frequency for variations in source powers and different types of loads are discussed in this chapter.

3.2 MICROGRID STUDY SYSTEM

In this research work, both power sources and battery bank are connected to common DC bus with a DC link capacitor and supply power to load through single PWM voltage source inverter. The schematic diagram of the microgrid system connected to isolated load implemented in Matlab/Simulink environment is shown in Figure 3.1. The overall control system consists of MPPT controllers for both wind and PV power system, controller for bi-directional DC/DC converter of battery energy storage device and load side inverter controller for voltage and frequency regulation. In this study voltage and frequency control scheme given in Chapter 2 is used to generate the PWM signals for controlling the operation of inverter. The maximum power is extracted from both wind and PV systems for all operating conditions of the microgrid. This is applicable even if the SOC of the battery is reached its maximum limit. The control strategies for the microgrid system are implemented with a view to achieve an acceptable level of voltage and frequency regulation while extracting the maximum power from wind and PV system.

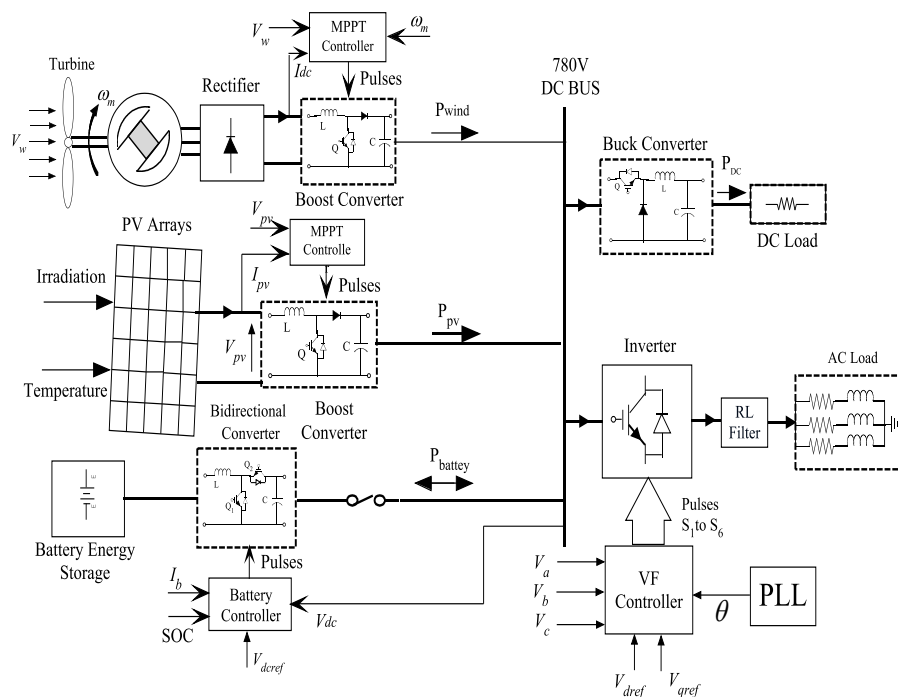


Figure 3.1: Schematic of microgrid system for isolated operation

3.3 PERFORMANCE STUDY AND DISCUSSION

The performance of the microgrid system is investigated in terms of voltage and frequency regulation capability under varying wind speed, solar irradiation and different types of loads. The different types of loads such as DC loads, unbalanced loads, nonlinear loads and induction motor load are considered for the study. The system configuration ratings and parameters are given in Appendix A. In this mode, the DC bus voltage is maintained stable with the help of battery converter. The reference value of DC link voltage is set as 780 V. The initial charge for battery is 60%. The performance evaluation of microgrid system in isolated mode of operation has been analyzed by considering the following case studies. The time domain simulated responses of the microgrid system under different operating conditions are presented in this section.

3.3.1 Performance Characteristics of Wind and PV Systems

The parameters of the wind generation system [Esmaili et al. (2005)] are listed in Appendix A. The characteristic function C_p versus λ , for various values of the pitch angles β is shown in Figure 3.2 (a). Figure 3.2 (b) illustrates the mechanical power versus the rotating-speed of a wind energy conversion system at various wind speed, assuming the blade pitch angle $\beta = 0^\circ$. It is seen that for a given wind speed, there is only one shaft speed at which the captured wind power is maximum which is called optimum or reference shaft speed (ω_{ref}) as explained in Chapter 2.

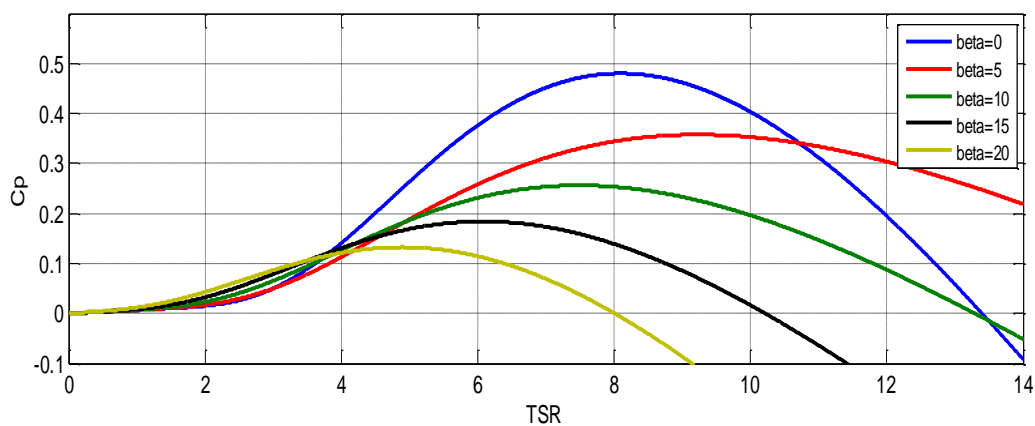


Figure 3.2: (a) C_p vs. λ (TSR) for various pitch angles

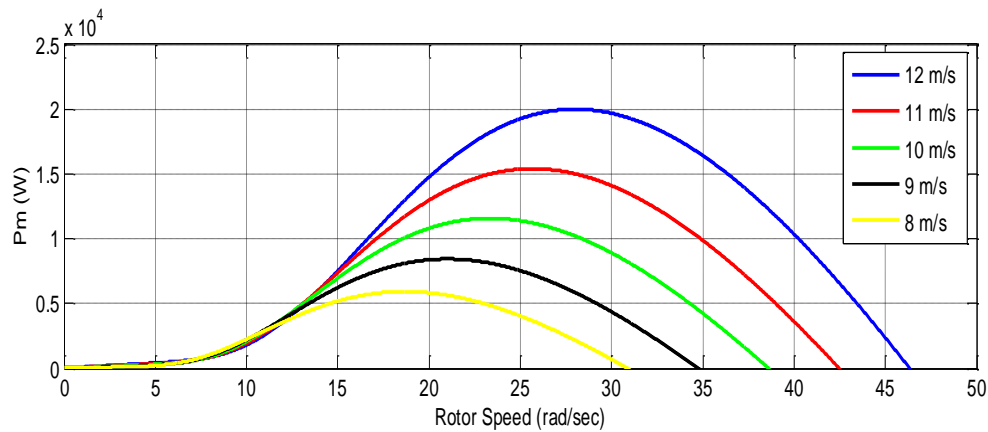


Figure 3.2 (b): Power vs. rotor speed at various wind speed

For PV arrays modeling, the Solarex MSX-60 PV module is chosen and the parameters of MSX-60 PV module are shown in Appendix A [Francisco (2005)]. The following figures show the simulated results for characteristics of the PV module considered in this work. The model I-V characteristic curves under different irradiances are given in Figure 3.3 (a) at 25 °C. From Figure 3.3 (b), it is observed that with decreasing irradiance, there is a negligible change in the maximum output voltage and there is a marginal decrement in output current and hence a noticeable drop in the maximum power point (MPP). The effect of the temperature on the PV model performance is illustrated in Figures 3.4 (a) and 3.4 (b). From these two Figures, it is noted that the lower the temperature, the higher is the maximum power and the larger the open circuit voltage. On the other hand, a lower temperature gives a slightly lower short circuit current.

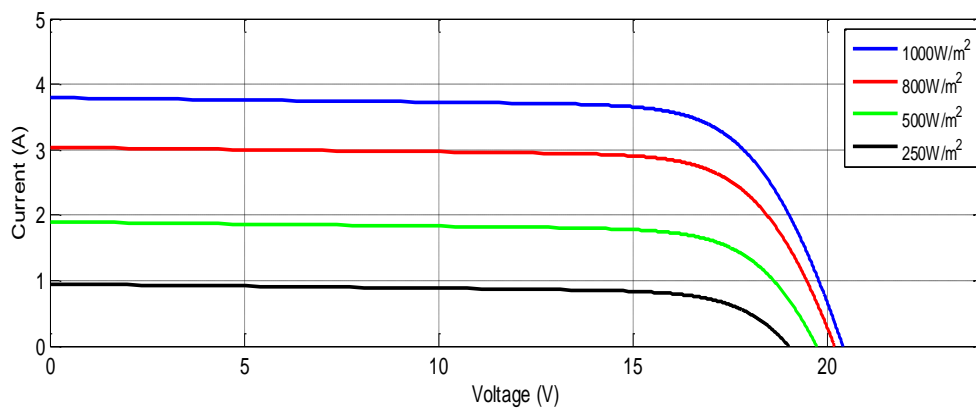


Figure 3.3 (a): I-V characteristics of the PV model under different irradiances

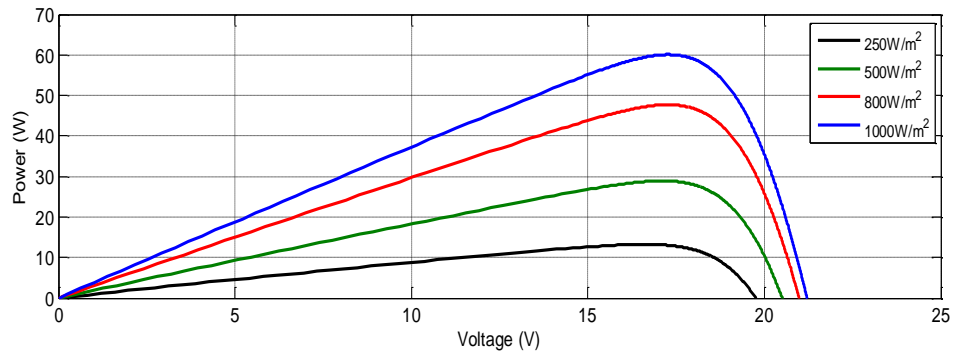


Figure 3.3 (b): P-V characteristics of the PV model under different irradiances

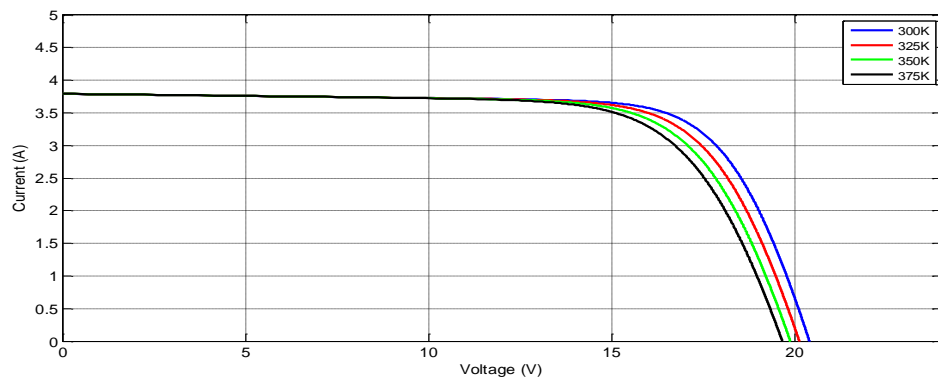


Figure 3.4 (a): I-V characteristics of the PV model under different temperatures

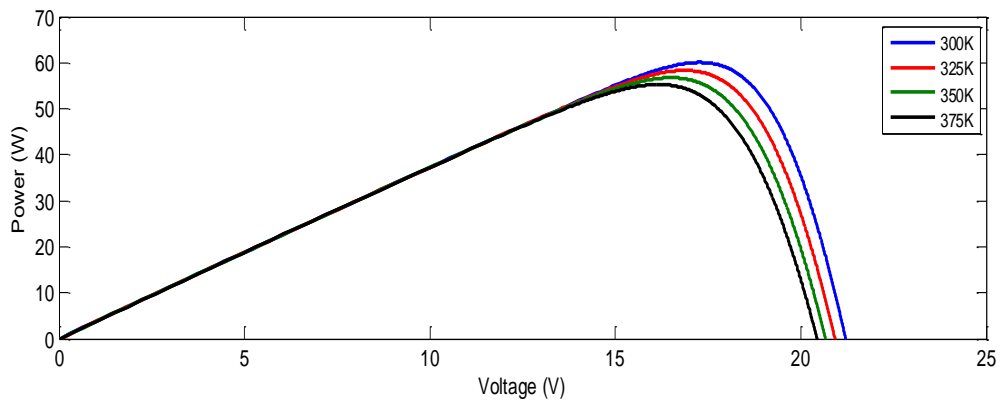


Figure 3.4 (b): P-V characteristics of the PV model under different temperatures

3.3.2 Power Sharing

To evaluate the power sharing among the sources of microgrid system, the following two cases are considered. In the first case, the dynamic behavior of the system with a constant load of 50 kW is studied. Initially the wind speed is 9 m/sec and is increased to 12 m/sec at $t = 1.5$ sec. Also the solar irradiation is varied from 700 W/m^2 to 1000 W/m^2 . Figure 3.5 illustrates the time domain simulated results for

solar irradiation, dI_{pv}/dV_{pv} and $-I_{pv}/V_{pv}$ curves for PV power system. Figure 3.6 shows the simulated results for Active power of wind, PV system, battery and power supplied to load. Due to sudden variations in wind speed, the turbine reference speed ω_{ref} changes. Accordingly the active power output of the wind generation system changes. The wind generator output tracks the corresponding maximum power very successfully as shown in Figure 3.6. The results for percentage State of Charge of battery (%SOC) and Power coefficient C_p of wind turbine for different wind speed are shown in Figure 3.7 (a) and 3.7 (b) respectively. By implementing the MPPT control technique explained in Chapter 2, the rotor speed of PMSG should be adjusted to achieve maximum value of power coefficient (C_p) which remains a constant value of 0.47.

As solar irradiation changes, the active power generation from PV array also varies. From the results from PV system we can observe that incremental conductance MPPT works in such a way that for every instant $\frac{dI_{pv}}{dV_{pv}} = -\frac{I_{pv}}{V_{pv}}$ i.e. PV array is operating at its maximum power point. So the MPPT is able to track the maximum power point. From Figure 3.6 it is seen that if the generated power is decreased and the load demand is still 50 kW, then the excessive load demand is supplied by the battery. Also the extra generated power is utilized to charge the battery in order to maintain the power balance, which is clearly indicated by the negative sign of battery power.

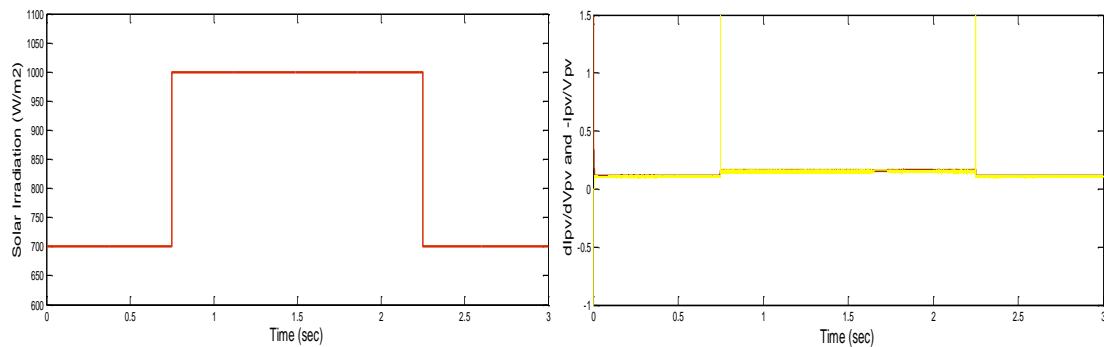


Figure 3.5: Solar irradiation, dI_{pv}/dV_{pv} and $-I_{pv}/V_{pv}$ curves for PV System

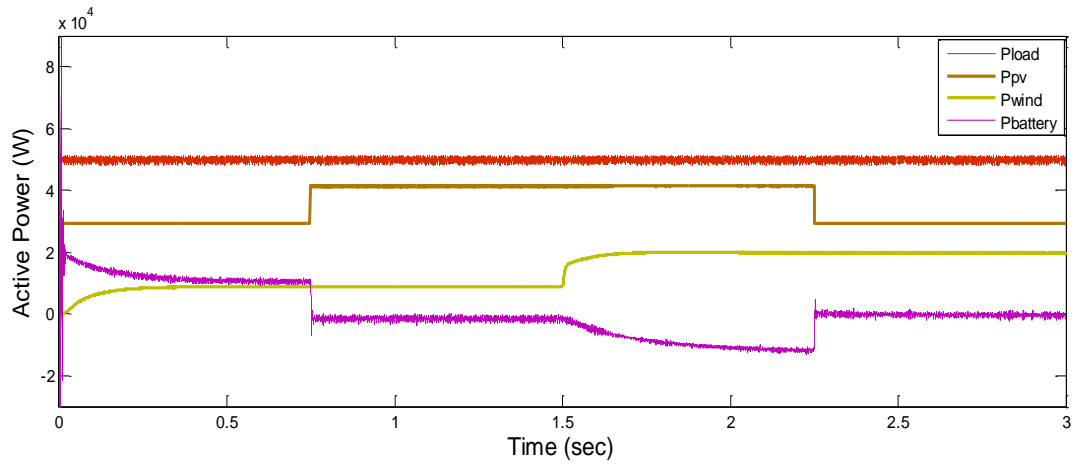


Figure 3.6: Active power of wind, PV system, battery and power supplied to load

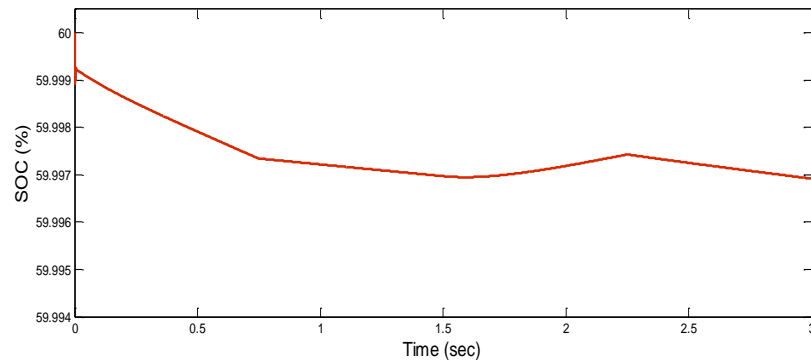


Figure 3.7 (a): State of Charge (%) of battery

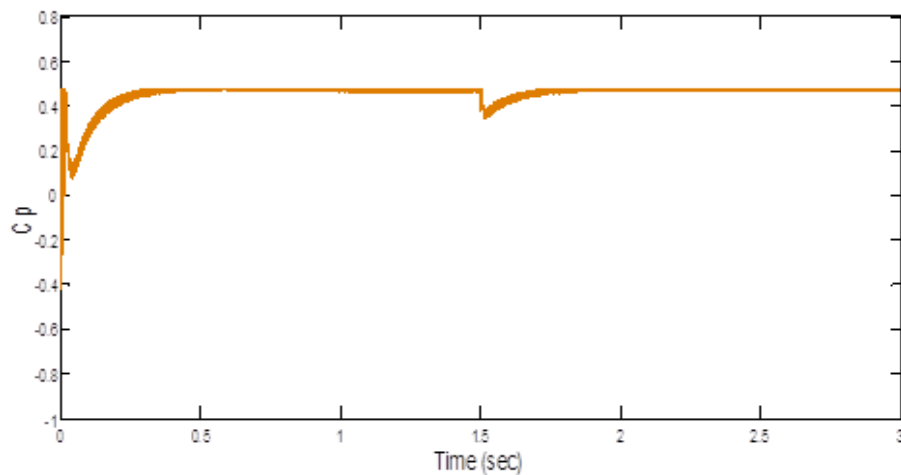


Figure 3.7 (b): Power coefficient C_p of wind turbine

In the second case, initially the load connected to the microgrid is 60 kW and is suddenly decreased to 40 kW at $t=1.5$ sec. The wind speed is kept constant at 12 m/sec and solar irradiation variation considered is same as in Figure 3.5. Figure 3.8

shows the simulated results for Active power of wind, PV system, battery and power supplied to the load for step change in load variation. The power balance between wind, PV power system, battery and load has been maintained while extracting maximum power from both sources. The simulated results for percentage State of Charge of battery and system frequency for different operating conditions are shown in Figure 3.9 (a) and 3.9 (b).

The simulated result for DC link voltage is shown in Figure 3.10. During all kind of source power and load fluctuations, the DC link voltage is well maintained nearly to 780 V. The simulated results for inverter output voltage and load current for variable load are shown in Figure 3.11 (a) and Figure 3.11 (b) respectively. The voltage across the inverter terminals is purely sinusoidal and while maintaining constant voltage and frequency under different dynamic conditions. Thus, the change in the load does not affect the change in the output voltage and hence the voltage across the load remains unchanged.

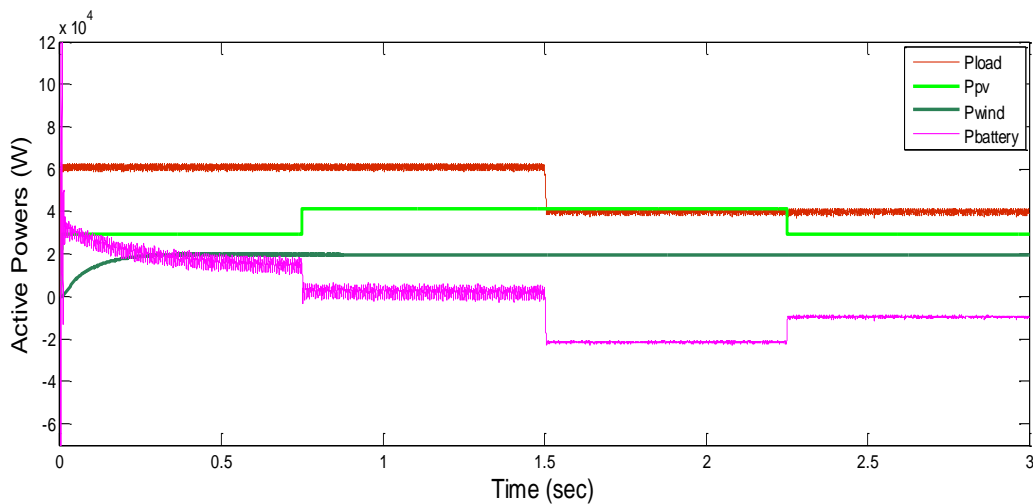


Figure 3.8: Active power of wind, PV system, battery and power supplied to load

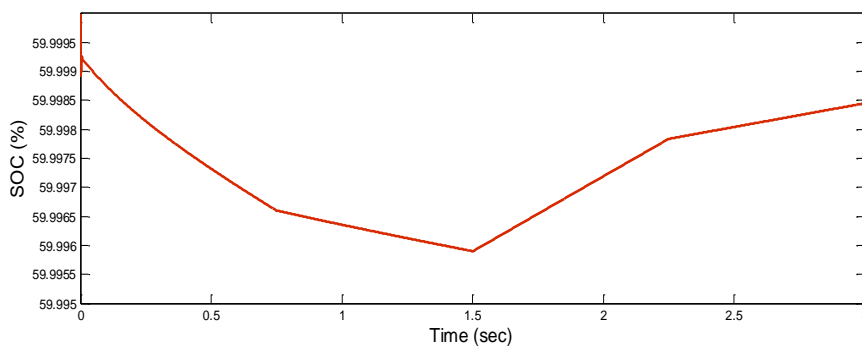


Figure 3.9 (a): State of Charge (%) of battery

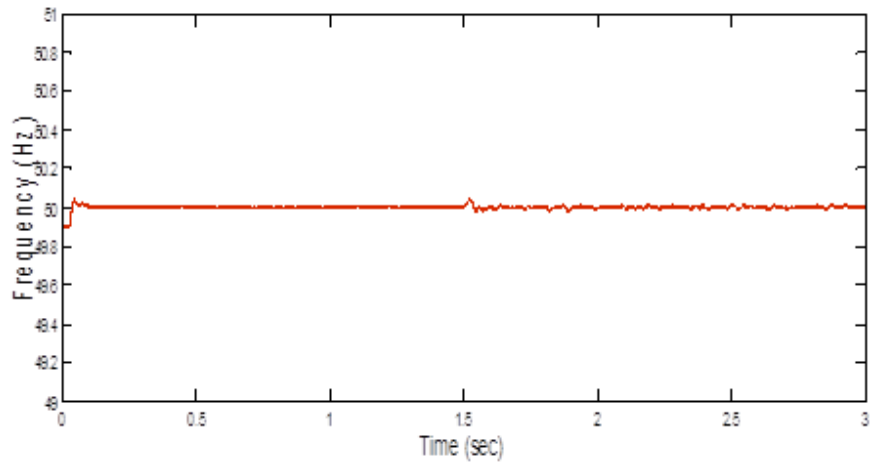


Figure 3.9 (b): System frequency

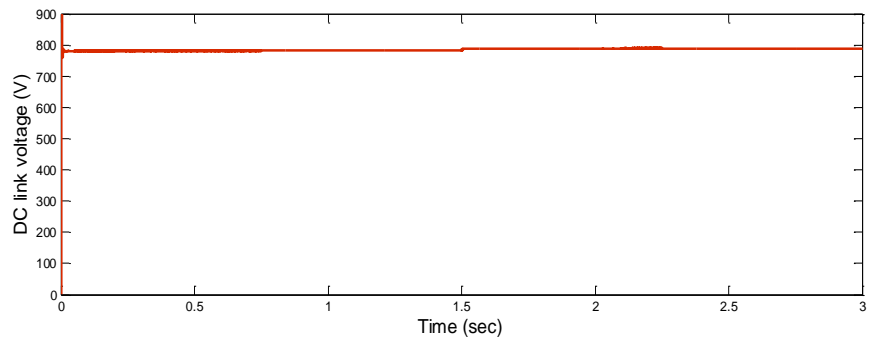


Figure 3.10: DC link voltage

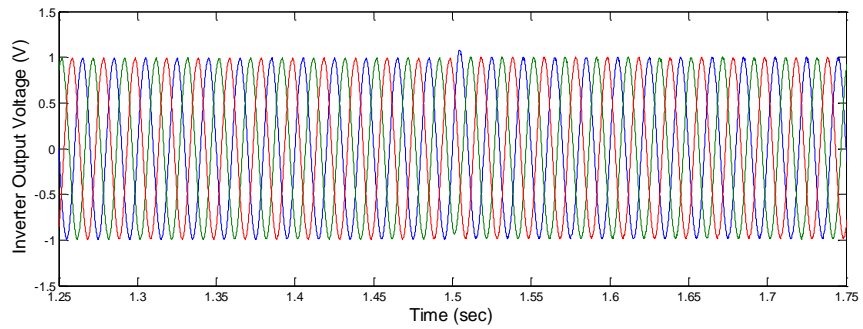


Figure 3.11 (a): Load voltage

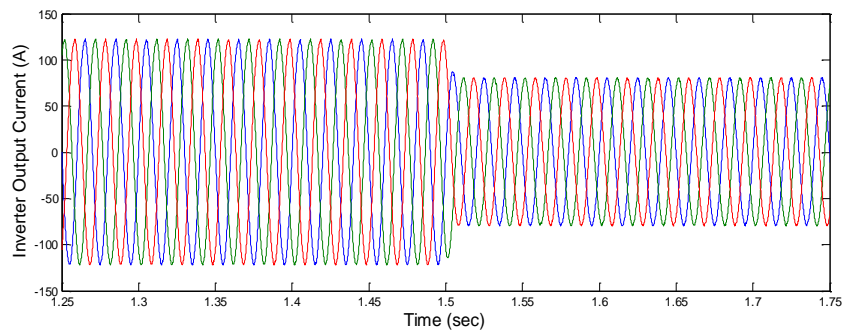
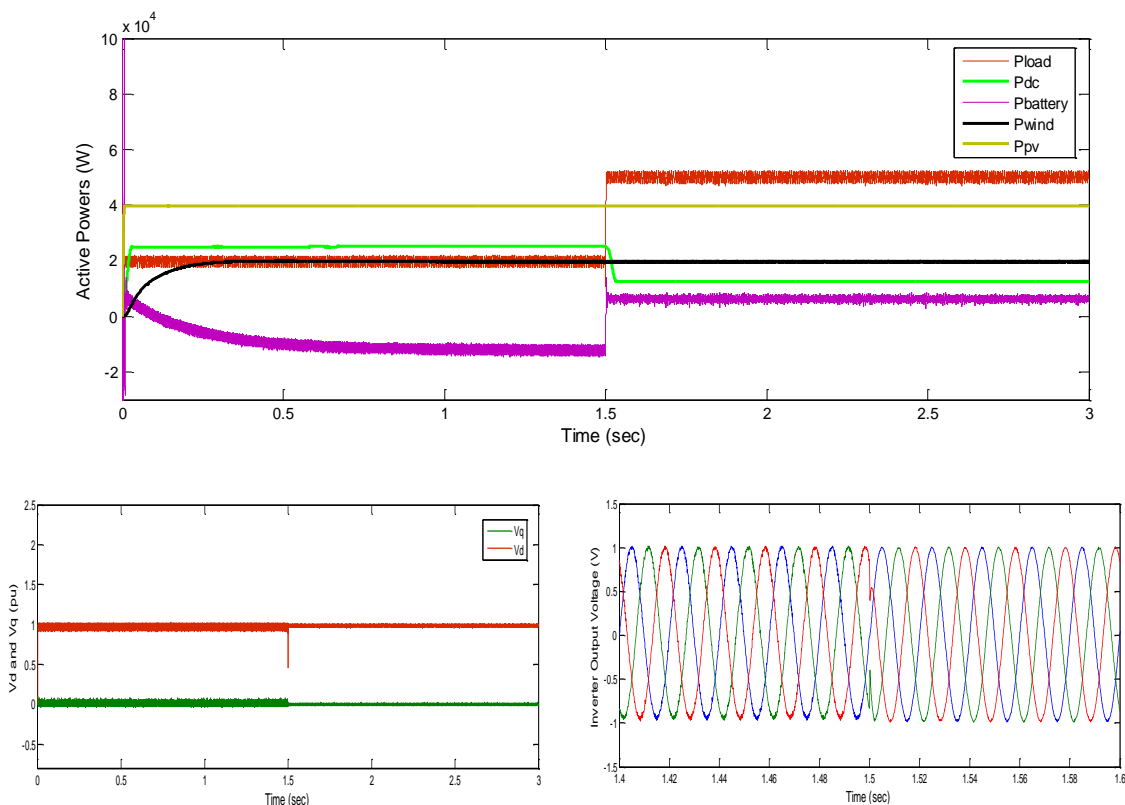


Figure 3.11 (b): Load current

3.3.3 Case Study with DC Load

The AC load demand changes from 20 kW to 50 kW at $t=1.5$ sec and DC load is varied from 25 kW to 12.5 kW. The wind speed (12 m/sec) and irradiation (1000 W/m^2) are constant and total generation is 60 kW. Figure 3.12 shows simulated results for the active power, d and q -axis components of voltage, inverter output voltage, percentage SOC of battery and system frequency. From the power responses it is found that upto 1.5 sec, the microgrid system produces more power than load requirement. As a result, the battery storage system stores excess power. After 1.5 sec it is found that, the power from wind and PV system is less than the load demand as a consequence of load increase. Hence, the battery storage system provides the required power temporarily. Figure 3.12 shows that the voltage and frequencies of the system are almost constant during the load changes. It can be clearly observed that the microgrid model has constant DC link voltage and a purely sinusoidal controlled ideal voltage at the inverter terminals.



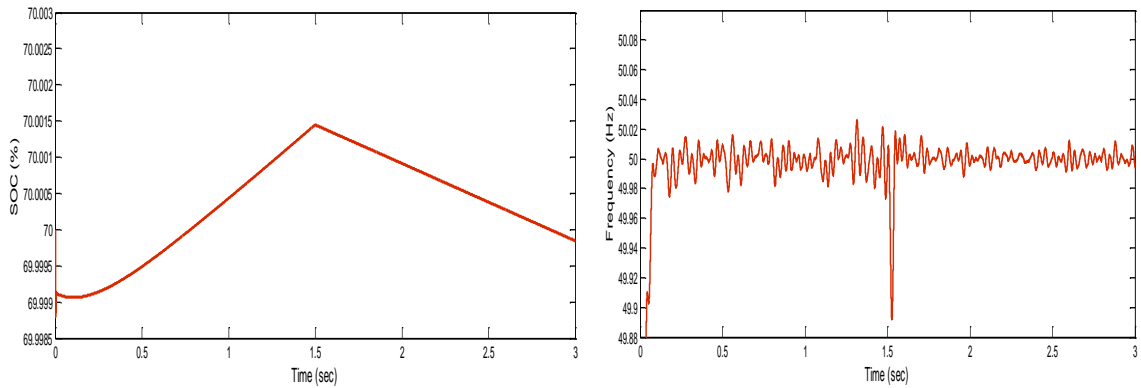


Figure 3.12: Active power of microgrid and load, d and q-axis components of voltage, load voltage, State of Charge (%) of battery and system frequency

3.3.4 Case Study with Nonlinear and Unbalanced Loads

In this case study, the effects of both unbalanced and nonlinear loads on the microgrid are considered. The unbalanced load represents an aggregate of unequal single phase loads which are connected between the phases and a neutral conductor. Three cases are considered to study the effectiveness of control strategies of the inverter and DC/DC converter of the battery. In the first case, microgrid system is supplying only unbalanced load. Figure 3.13 and Figure 3.14 show microgrid system responses with switching to an unbalanced load. Figure 3.13 illustrate the waveforms of the output powers of the microgrid system and loads. Initially, the total load on the microgrid is 30 kW and is increased to 60 kW at $t=1.5$ sec. It is observed that until $t = 1.5$ sec, the load demand is less than the generation and the extra power generated is stored in the battery. The simulated results for unbalanced load currents, inverter output voltage, system frequency and percentage THD variations in inverter output voltage are shown in Figure 3.14. Thus, the amplitude and frequency of the load voltage is well controlled under different load conditions. Also it is observed that, the percentage THD variations in inverter output voltage with respect to time is less than 2.5%.

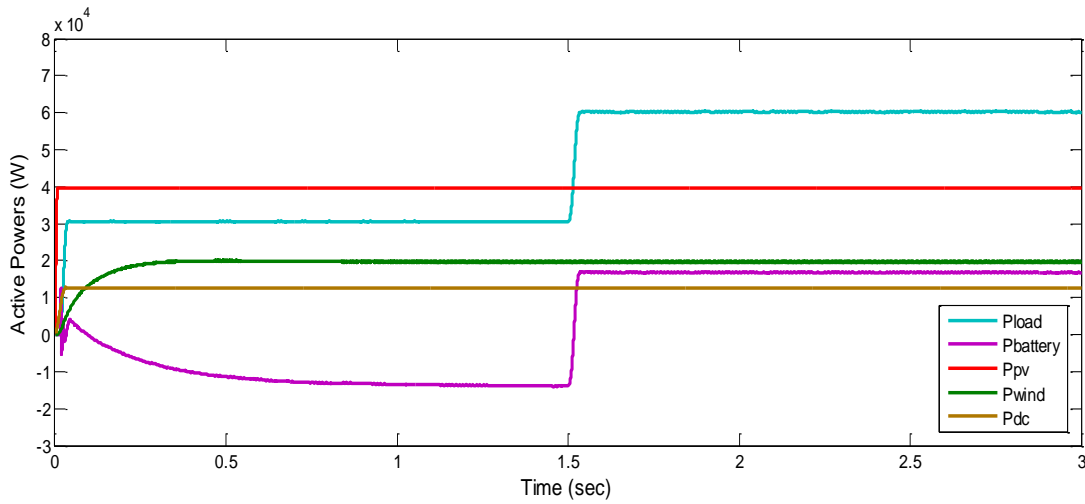


Figure 3.13: Active power of wind, PV system, battery, power consumed by DC load and total unbalanced power supplied to load

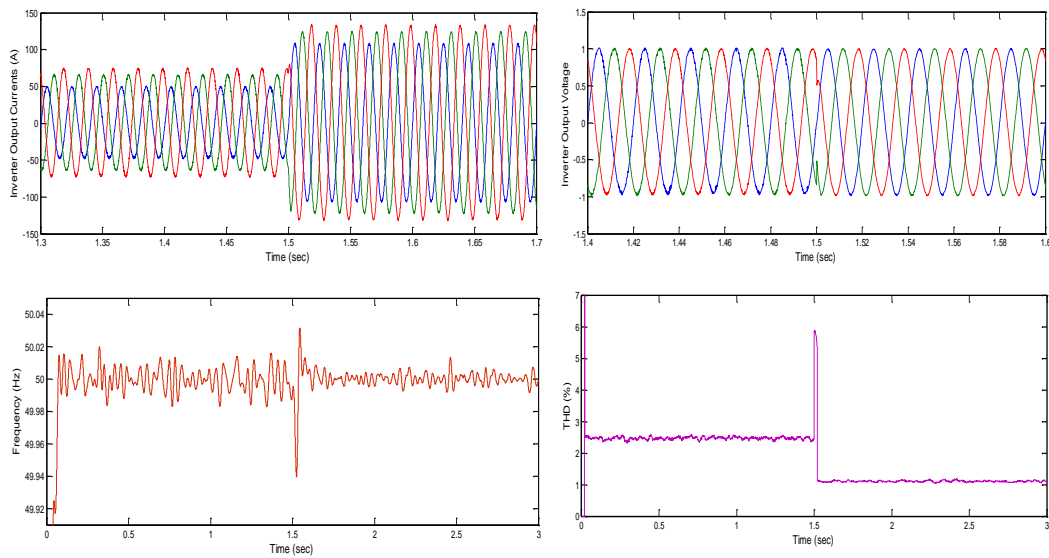


Figure 3.14: Unbalanced load currents, load voltage, system frequency and THD (%) variation in inverter output voltage

In the second case, initially the balanced load of 30 kW is considered and subsequently, at $t=1.5$ sec the unbalanced load in three phases (14 kW, 17 kW and 24 kW) is switched on. The waveforms for load current and percentage SOC of battery are shown in Figure 3.15 (a) and 3.15 (b). From Figures 3.16 (a) and 3.16 (b), it is observed that the voltage and frequency track their respective reference commands with stable and fast responses, although due to the unbalanced load switching from t

=1.5 sec. The percentage THD in voltage and current on load side are shown in Figure 3.17 and is about 1.8% and 1.9% respectively, which illustrates the good quality of voltage and current generated at the consumer side end.

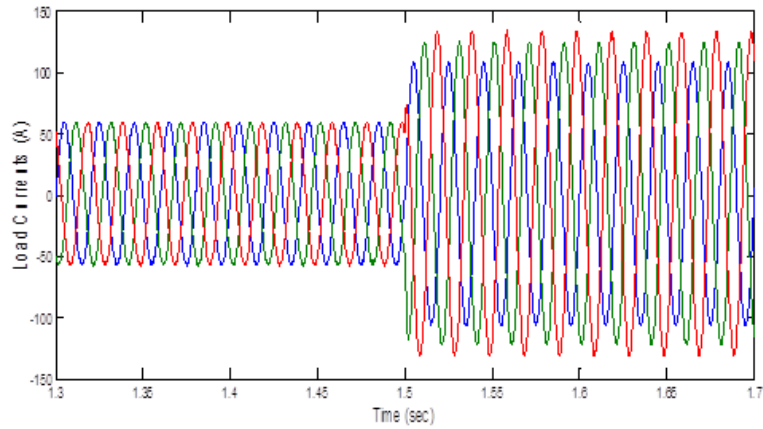


Figure 3.15 (a): The load current

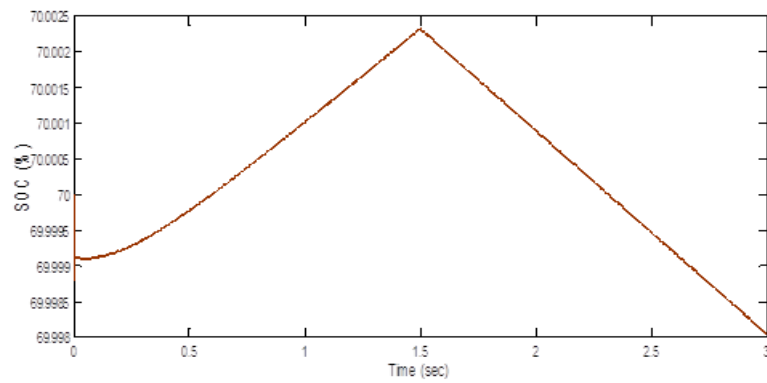


Figure 3.15 (b): State of Charge (%) of battery

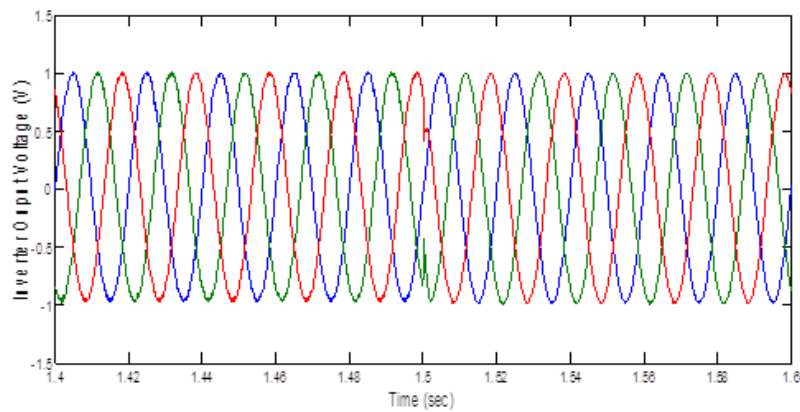


Figure 3.16 (a): Load voltage

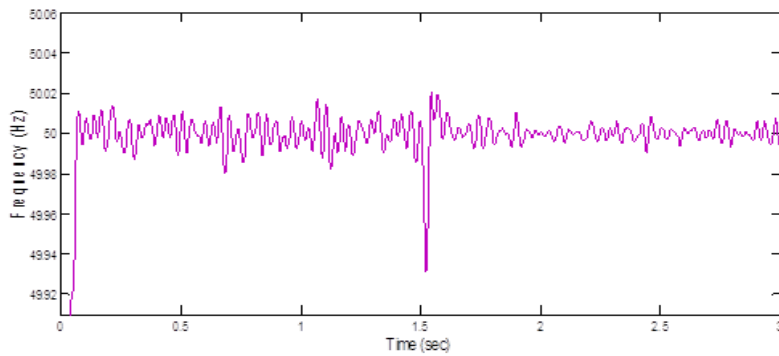


Figure 3.16 (b): System frequency

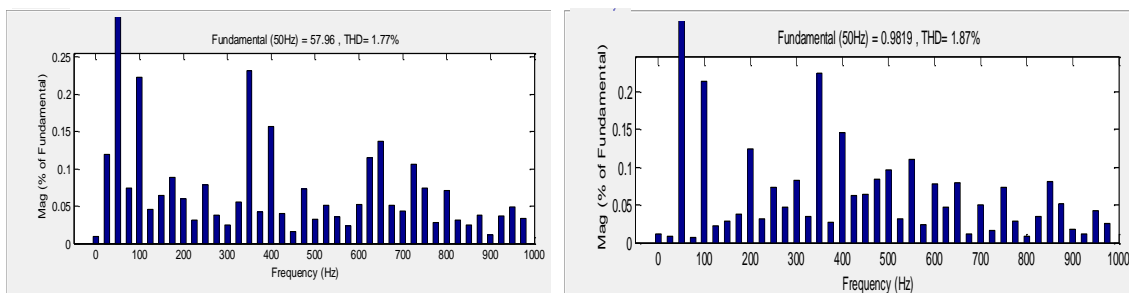


Figure 3.17: THD (%) in voltage and current on load side

In the third case, a nonlinear load (i.e., with uncontrolled rectifier supplying RL load with $R=75 \Omega$ and $L=50 \text{ mH}$) is connected to the microgrid. Initially total load connected to the microgrid is 34 kW (balanced) and is increased to 64 kW (unbalanced) at $t=1.5 \text{ sec}$ along with nonlinear load. Figure 3.18 and 3.19 show the simulated results for total power consumed by loads, battery power and load currents. The percentage THD in voltage and current on load side is about 2.6 % and 4.0 %, respectively as shown in Figure 3.20.

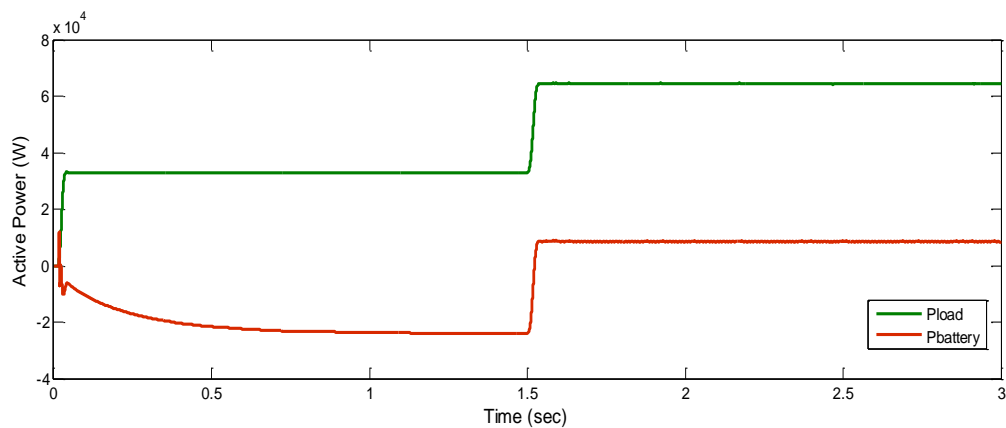


Figure 3.18: Total power consumed by loads and battery power

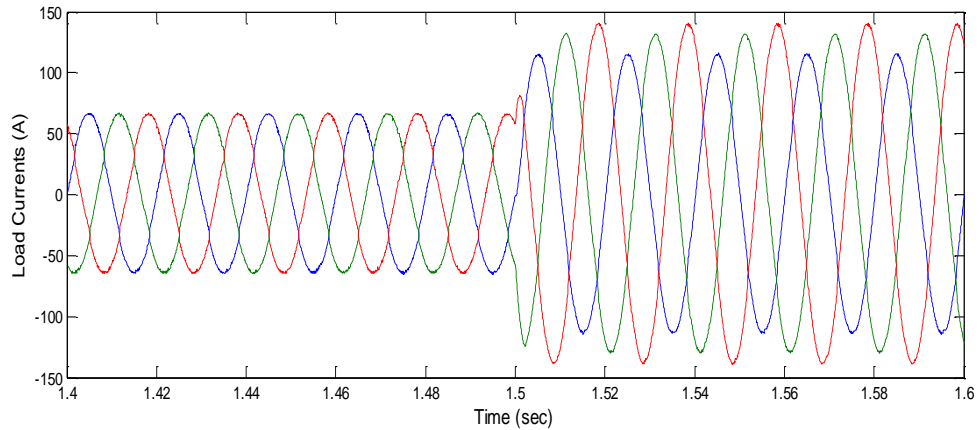


Figure 3.19: The waveforms for load currents

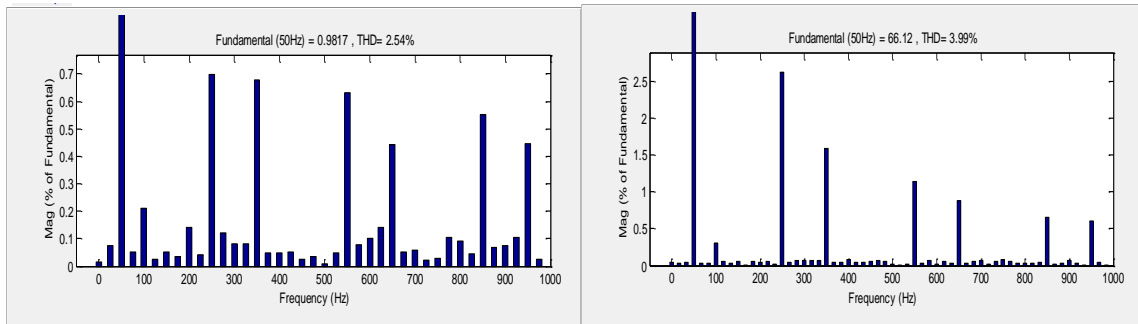


Figure 3.20: THD (%) in load voltage and current

3.3.5 Case Study with Wind or PV Generation Alone

In this case, the PV arrays or wind energy generator is excluded from the microgrid system and the load is varied. A DC load of 25 kW and AC load of 20 kW are connected to DC and AC buses respectively. To prove this condition, a simulation is carried out by disconnecting the PV arrays ($P_{PV} = 0$) as shown in Figure 3.21. This condition may happen during the night when the solar radiation is zero. The wind speed is initially 9 m/sec and increased to 12 m/sec at $t=1.5$ sec. Also the DC load is reduced to 12.5 kW and AC load is increased to 50 kW at $t=1.5$ sec. It is seen that, the power from wind energy system is less than the load demand. During this time the battery storage system provides required power demand.

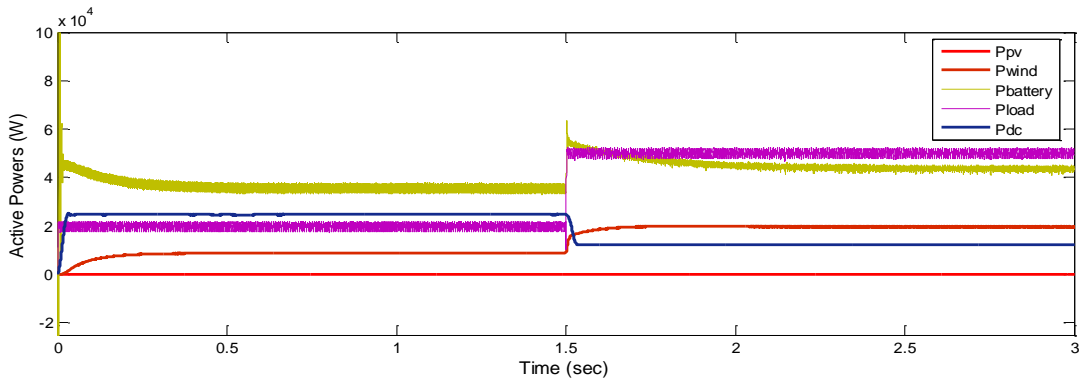


Figure 3.21: Active power with wind power generation alone

Figure 3.22 shows simulated active power if PV arrays are connected to the system while wind energy conversion system is disconnected ($P_{wind}=0$). The solar radiation increased from $700W/m^2$ to $1000W/m^2$. The DC and AC load changes considered is same as in Figure 3.21. As total power generated is less than the load requirement, the battery is capable of supplying the excess load demand and the battery is discharging as shown in Figure 3.23. From the results it is observed that the power balance between wind, PV power system, battery and load has been maintained while extracting maximum power from both sources.

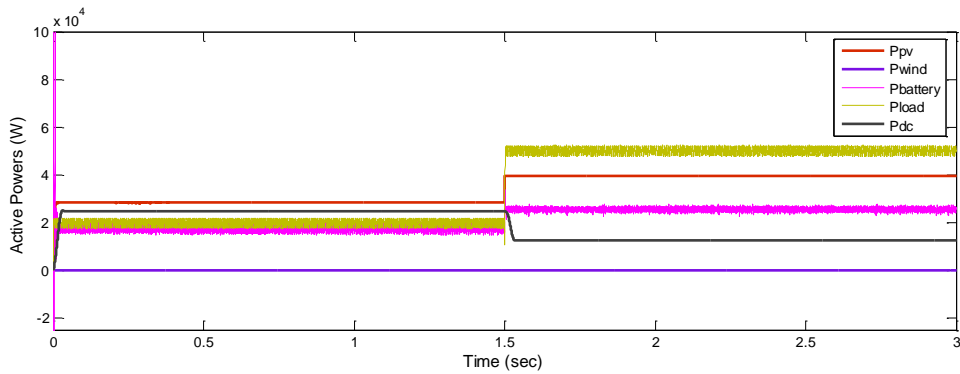


Figure 3.22: Active power with PV power generation alone

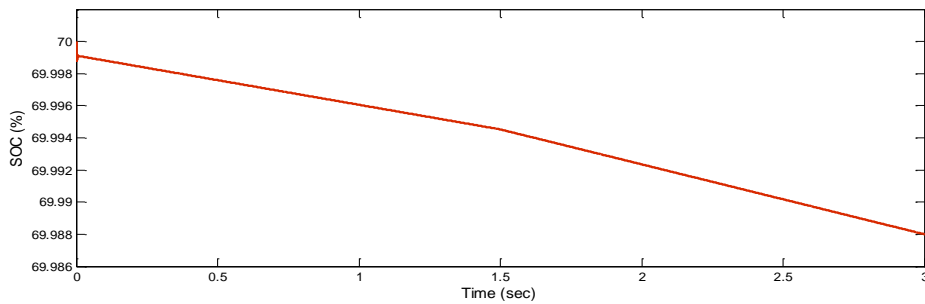


Figure 3.23: State of Charge (%) of battery

3.4 MICROGRID PERFORMANCE WITH INDUCTION MOTOR

In the case of a motor load, large oscillation in real and reactive power occurs due to a sudden change in applied terminal voltage. To investigate the microgrid performance with the motor load, a three phase induction motor load (dynamic load) is considered. The responses for connecting a three phase induction motor connected in parallel to the resistive load are studied. The power sharing between DGs and battery is observed.

A 3 phase resistive load and 10 HP (7.5 kW), 400 V, 50 Hz, 4 pole, 1440 RPM three phase squirrel-cage induction motor load is considered to study the dynamic behavior of the microgrid system. Initially, 3 phase resistive load of 40 kW and the load torque applied to the shaft of the 3 phase induction motor is 50 N-m. At $t=1.5$ sec resistive load and induction motor load torque is suddenly increased to 70 kW and 70 N-m respectively as shown below. The simulated results for load active and reactive powers, induction motor torques are shown in Figure 3.24 (a) and 3.24 (b). The corresponding waveforms for stator current, rotor speed, percentage THD variation in inverter output voltage and system frequency are shown in Figure 3.25. The total harmonic distortion variations throughout the whole simulation time in percentage of the system voltage under load conditions are observed to be well within IEEE Standards. As the load on the induction motor increases the electromagnetic torque also increases. When the applied torque is 50 N-m (i.e., rated value), the motor is running at rated speed of 1440 RPM. Suddenly when the torque is increased to 70 N-m, the motor speed reduced to 1420 RPM. Also from the simulated results it is observed that the stator current (peak value) is increased from 19 Amps to 27 Amps.

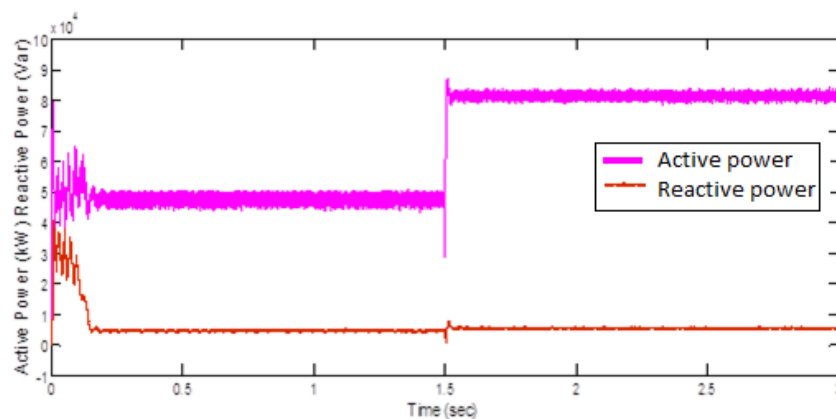


Figure 3.24 (a): Active and reactive power of load

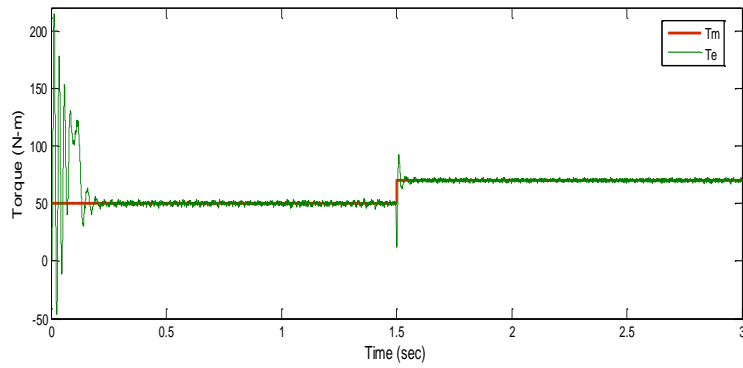


Figure 3.24 (b): Induction motor torques

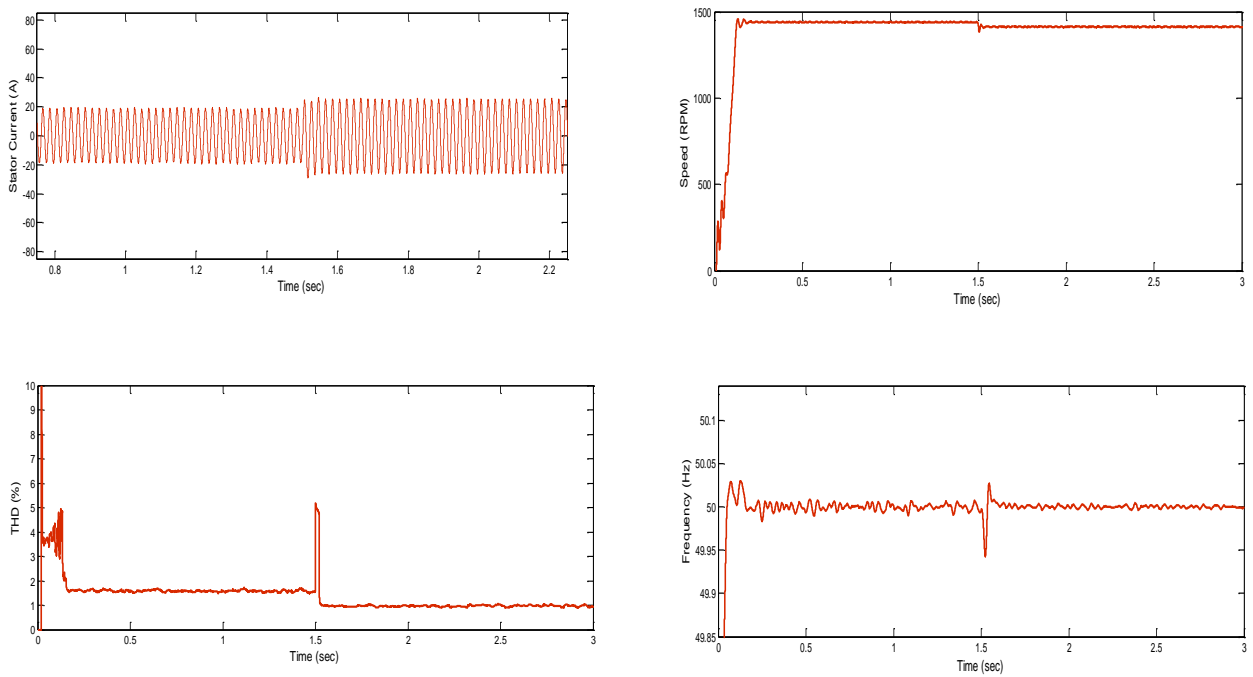


Figure 3.25: Waveforms for stator current, rotor speed, THD (%) variation in load voltage and system frequency

3.5 CONCLUSIONS

The dynamic performance analysis for different operating conditions of microgrid system implemented in Matlab/Simulink environment has been evaluated for isolated operation. The effectiveness of the control schemes was demonstrated through time-domain simulation studies with different case studies. In microgrid system, the battery bank plays very important role in the system. The power can be stored or consumed from the battery depending on generation and load conditions.

From the simulation results, it can be realized that the control strategies implemented for the microgrid system are able to achieve an acceptable level of voltage and frequency irrespective of the load variability and source power uncertainty. It is discussed that the terminal voltage across the load can be affected by unbalanced, nonlinear loads or induction motor load as well as by load switching incidents. The system voltage is well maintained at 415 V (1 p.u) under different loading conditions. The effects of a distorted load current appear as an undesirable harmonic distortion in the terminal voltage. The percentage THD of the system voltages and currents are within the permissible limits irrespective of the different types of loads connected to microgrid.

CHAPTER 4

PERFORMANCE ANALYSIS OF MICROGRID IN GRID CONNECTED MODE OF OPERATION

4.1 INTRODUCTION

Recently, much work has been focused on interfacing DG with the grid, mainly its control and operation. By integrating non-conventional energy sources like photovoltaic arrays, wind energy, fuel cells etc., which may suit a particular region and provide power at various load centers and also to the main power grid. Interconnection of these generators to distribution network will offer a number of benefits such as improved reliability, power quality, efficiency and alleviation of system constraints along with the environmental benefits [Barker and de Mello (2000)]. With these benefits and due to the growing momentum towards sustainable energy developments, it is expected that a large number of DG systems will be interconnected to the utility grid in the coming years [Juan Manuel Carrasco et al. (2006)]. Interconnecting large number of small DG systems with diverse characteristics to low voltage network causes many problems. The microgrid is a section of network functioning in a systematic way, comprising adequate generating resources in the autonomous or grid connected mode in an efficient and controlled technique [Lasseter et al. (2002)]. Thus the microgrid configuration with clean, efficient and sustainable energy technologies such as wind and PV will be dominant in the future power supply network.

The grid integration of hybrid DG systems is predicted to play an important role in the future electrical power system. Multi-source hybrid renewable energy sources to some extent overcome the uncertainty, intermittency and low availability of single-source renewable energy systems, which has made the power supply more reliable [Martinot and Sawin (2009)]. And because of this, hybrid power systems have caught worldwide research attention. To build a hybrid power system, there are

different combinations of renewable energy sources. The grid connected performance of fuel cell and photovoltaic based hybrid DG system is reported in [Gyu et al. (2010)]. An optimal design of a grid connected hybrid wind/photovoltaic/fuel cell system for distributed energy production is presented in [Das et al. (2005)]. The performance analysis of the PV/wind/wave hybrid power generation system is reported in [Wakao et al. (2003)]. The design and economic analysis of grid connected hybrid PV/wind systems for the intermittent production of hydrogen is presented in [Rodolfo et al. (2009)]. The controller for maximizing performance of a grid connected photovoltaic-fuel cell hybrid power plant is presented in [Ro and Rahman (1998)]. From these listed hybrid power systems, it is observed that the main renewable power sources employed are wind power and photovoltaic power.

This study is orientated towards small-scale grid connected wind/PV microgrid system. The wind and photovoltaic are chosen as the primary power sources for the system to take full advantages of renewable energy available around us. For a grid connected application, the alternative energy sources in the microgrid can supply power both to the local loads and the utility grid. The utility grid behaves as backup energy source for grid connected operation of microgrid system. The suitable power electronic converters are required to operate microgrid in grid connected mode of operation. The more power converter usage produces more losses. Some of the loads like battery, electronic equipment, DC drives require DC power which can be supplied from DC voltage directly from DC bus with proper DC/DC converter. A grid connected microgrid with wind and PV as the energy resources which can reduce the multiple conversion stages is implemented. The microgrid can supply both DC and three phase AC loads.

In this chapter, the utility interactive performance analysis of microgrid system is presented. The microgrid system model developed in Chapter 2 is used for this study. The performance of the grid connected microgrid system is studied for changes in the DG capacities and also for changes in the load conditions. In this mode of operation of microgrid, each DG will generate its maximum power and the grid will supply extra load demand requirements. The DC link voltage (V_{dc}) is regulated

through inverter controller. The performance study of microgrid system includes the load sharing of the DGs with utility and induction motor and the power quality assessment with non-linear loads. The performance study of microgrid system is presented by considering the transition from grid connected to islanding mode of operation. The performance of the microgrid model is also evaluated through simulation study under grid disturbance conditions and results are reported. In this study, the balanced voltage dip, polluted grid voltages and unbalanced grid voltages are considered as the grid perturbation conditions.

4.2 GRID INTEGRATION OF MICROGRID

The schematic diagram of the microgrid system implemented in Matlab/Simulink for studying its grid connected performance is shown in Figure 4.1. The complete model of microgrid system developed in Chapter 2 is used for this study. The PV arrays are connected to DC bus through a DC/DC boost converter. A wind turbine generator (WTG) with PMSG is connected to a DC bus through uncontrolled rectifier and DC/DC boost converter. The wind and photovoltaic generators are controlled locally to obtain the maximum power extraction. Both DC and three phase AC loads are connected to the grid connected microgrid system. The DC load is connected to the DC bus through a DC/DC buck converter. The rated voltages for DC load and AC load are 500 V and 415 V RMS respectively. The grid is represented by a balanced three-phase source, 415 V line to line (RMS) with 50 Hz frequency. In grid tied mode, the grid side inverter is to provide stable DC bus voltage and injects only active power to the grid with zero reactive power. When the total power generation is greater than the total load in the microgrid system, it will inject power to the utility grid. Otherwise, the load will receive power from microgrid and utility grid. The parameters of load and microgrid system are given in Appendix A.

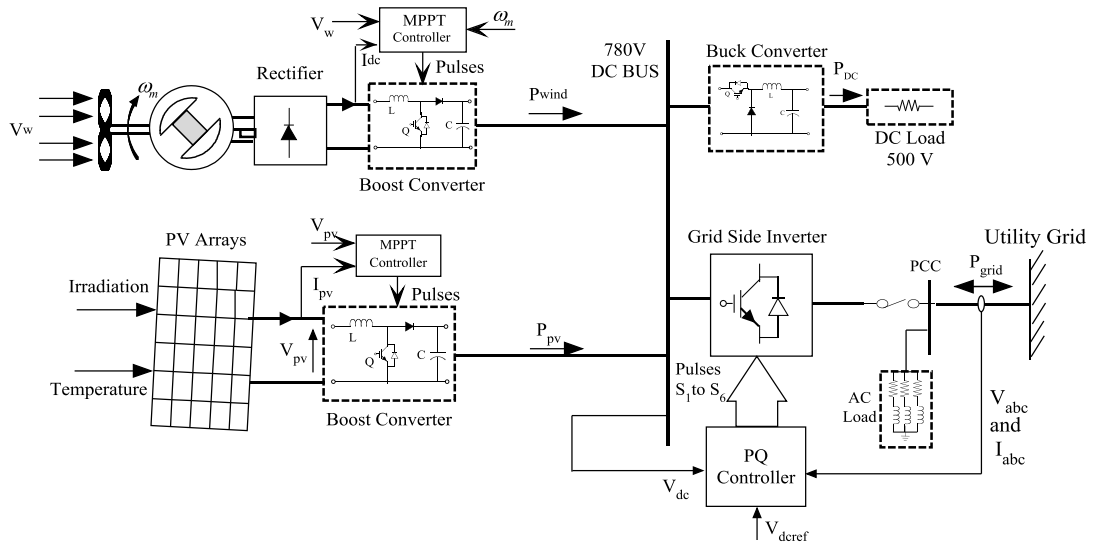


Figure 4.1: Schematic diagram of grid connected microgrid system

4.3 RESULTS AND DISCUSSION

In this section, the utility interactive performance analysis of microgrid system is presented. The sharing of the local loads by the microgrid among different DGs and utility grid are reported. The performance studies include different types of loads on the microgrid like DC loads, induction motor and non-linear loads. Also, to evaluate the effectiveness of the control scheme of the grid side inverter of the microgrid system for different grid perturbations originating from the utility grid is considered. The programmable three phase voltage source is used to study the microgrid system performance for grid perturbation conditions.

4.3.1 Load Sharing

In this section, the sharing of the local load by the microgrid with DGs and utility grid are presented. To analyze the dynamic response of the grid connected microgrid system step changes in wind speed, solar irradiation and load are considered. The following two different cases are considered for the analysis with variations in source power and load conditions.

Case I: With constant source power and variable load

In this case the wind speed (12 m/sec) and the irradiation (1000 W/m²) are constant and the total generation is 60 kW. The DC load and three phase AC load are

connected to the DC and AC buses respectively. The initial value of DC load is 25 kW and is reduced to 12.5 kW at $t=1.5$ sec. Initially the three phase AC load connected is 20 kW and at $t=1.5$ sec it is increased to 50 kW with 0.9 power factor lagging. Since the power consumed by the DC load is 25 kW from $t=0$ to 1.5 sec, the inverter injects only difference between generated and DC power. Since the load demand is lower than the total power generation upto 1.5 sec, the extra power generated (negative) is injected to the utility grid. After 1.5 sec the load demand is higher than the total power generation, the deficit power (positive) is consumed by the grid as shown in Figure 4.2. From the response of q -axis component of grid current as shown in Figure 4.3 (a), it is evident that the i_q component of the injected grid current is approximately zero. Hence no reactive power is injected to the grid by the microgrid system. The inverter is controlled in such a way that it operates at unity power factor. The grid will supply the reactive power demand of the connected load as shown in Figure 4.3 (b). From Figure 4.4 (a) it is observed that the DC bus voltage remains constant under different load conditions. One of the important aspects of microgrid system operation is to maintain the harmonic distortion level as low as possible. As per IEEE Standards [IEEE Standard 1547 (2003); Thomas S. Basso and Richard (2004)], it should be less than 5%. It can be observed from Figure 4.4 (b) that the total harmonic distortion (THD) factor of the grid current is around 2.2% for grid connected mode which satisfies the grid current regulation.

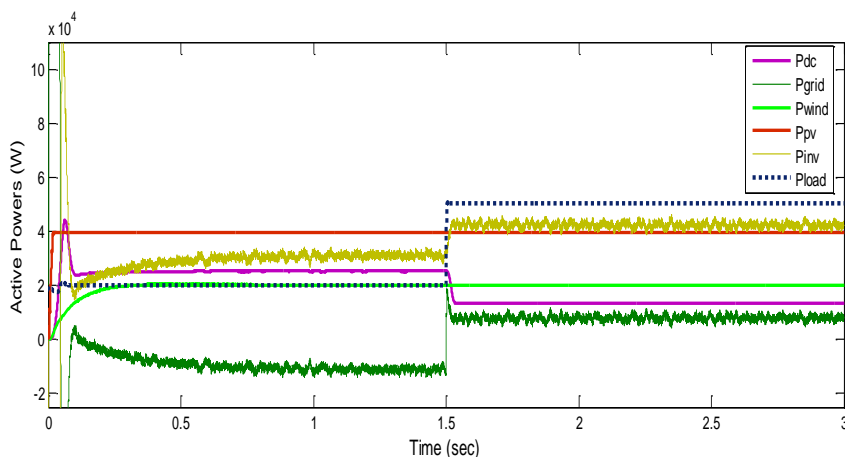


Figure 4.2: Active power of microgrid and load

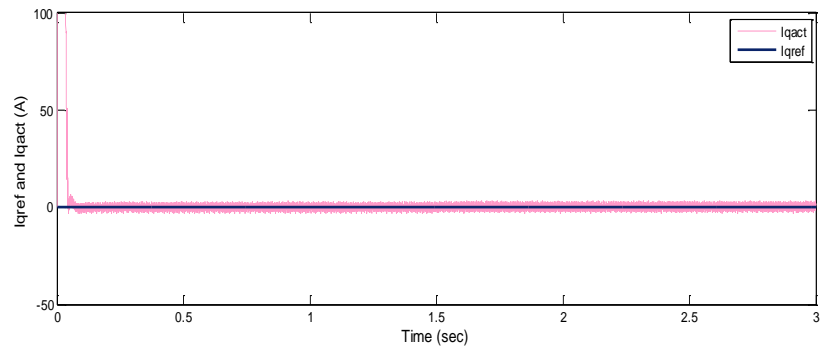


Figure 4.3 (a): q -axis currents

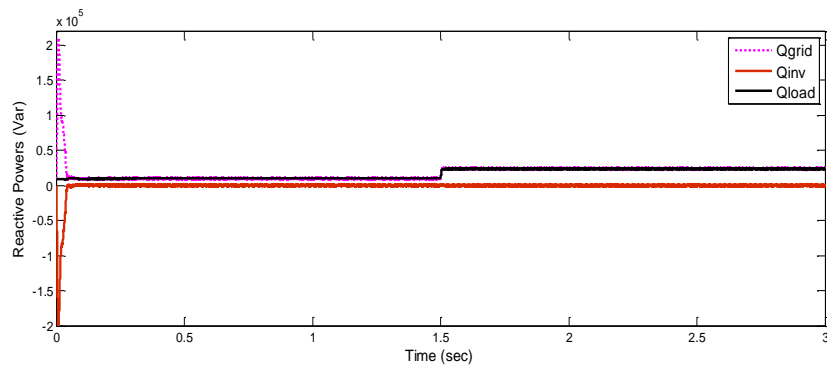


Figure 4.3 (b): Reactive power

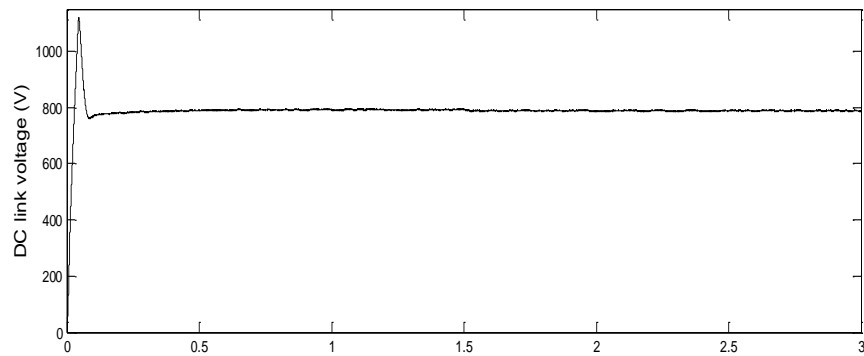


Figure 4.4 (a): DC link voltage

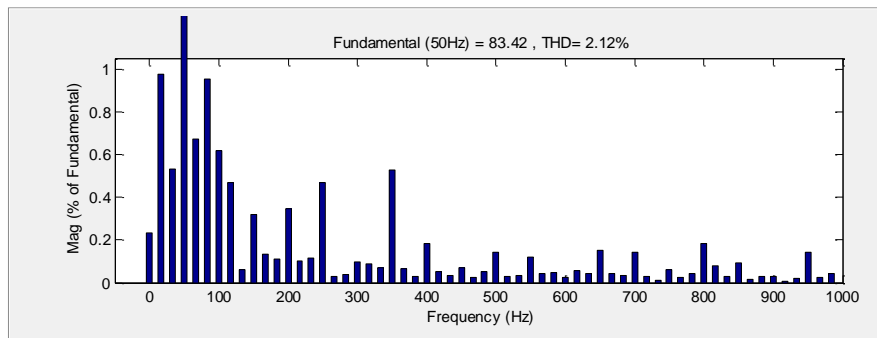


Figure 4.4 (b): THD (%) of inverter output current

Case II: With variable source powers and constant load

In this case, the load demand is kept constant and the wind speed or irradiation are varied. A fixed DC load of 25 kW and AC load of 35 kW with 0.9 power factor lagging are connected to the DC and AC buses respectively. The wind speed is kept constant at 12 m/sec and initially solar radiation is 700 W/m^2 and is increased to 1000 W/m^2 at 1.5 sec as shown in Figure 4.5 (a). As the total generated power is less than the load requirement, deficit power is consumed from the grid. But at $t=1.5$ sec, due to increase in PV power output (10 kW) the power consumed from the grid is reduced (10 kW) as shown. From Figure 4.5 (b), it is seen that the reactive power injected to the grid by the microgrid is zero. And the utility grid will supply the reactive power requirement of the three phase inductive load.

The simulated results for active power with variable wind speed condition are shown in Figure 4.6 (a). The wind speed is increased from 9 m/sec to 12 m/sec at $t=1.5$ sec and solar radiation is kept constant at 1000 W/m^2 . Since the generated power is less than the user power demand, the grid will supply the deficit power. The power coefficient has been maintained at the maximum value of 0.47 as shown in Figure 4.6 (b), which shows that the turbine speed is well controlled to capture the maximum energy from wind generation system.

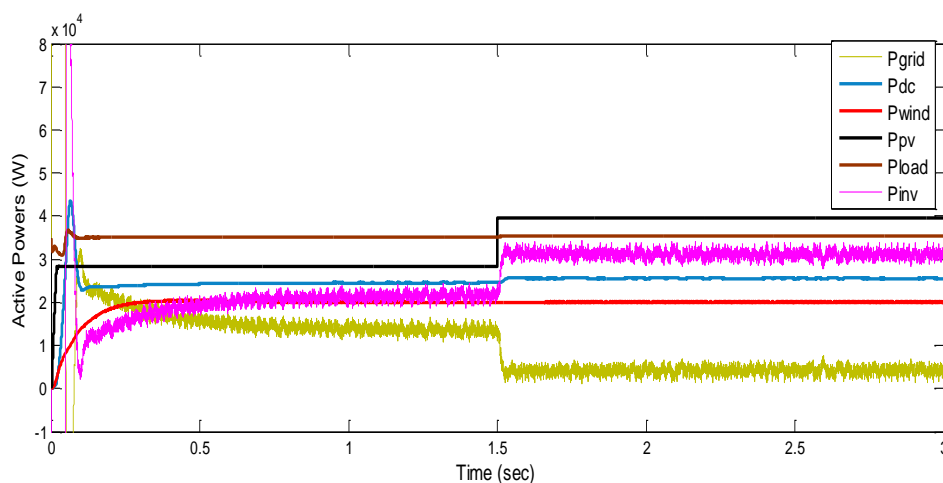


Figure 4.5 (a): Active power of microgrid and load with variable irradiation

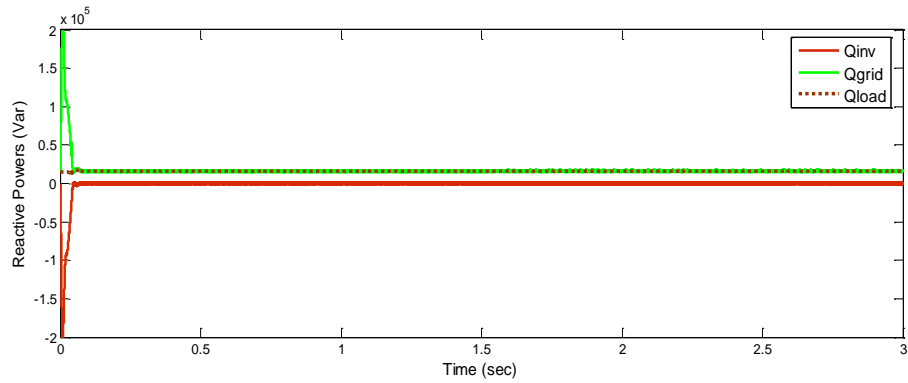


Figure 4.5 (b): Reactive power

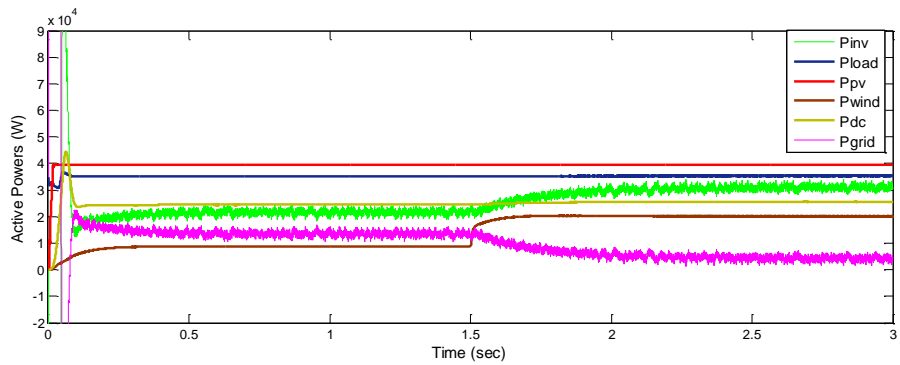


Figure 4.6 (a): Active power of microgrid and load with variable wind speed

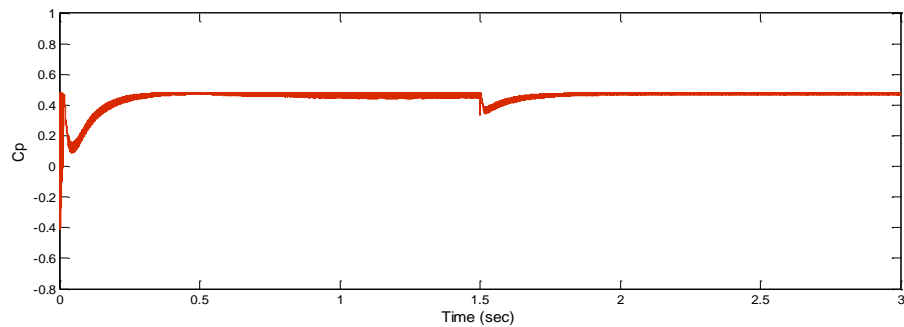


Figure 4.6 (b): Power coefficient C_p of wind turbine

4.3.2 Case Study with Induction Motor Load

Due to a sudden change in applied terminal voltage, large oscillation in real and reactive power occurs in case of a motor load. To study the dynamic behavior of the system, a DC load of 25 kW, 3 phase AC load of 10 kW at 0.9 p.f. lagging and a 20 HP, 50 Hz, 4 pole, 1460 RPM three phase squirrel-cage induction motor load are connected to the microgrid. Initially the wind speed is 9 m/sec and is increased to 12 m/sec at $t = 1.5$ sec. The solar irradiation is varied from 700 W/m^2 to 1000 W/m^2 .

Figure 4.7 illustrates the time domain simulated results for solar irradiation and dI_{pv}/dV_{pv} and $-I_{pv}/V_{pv}$ curves for PV System. As solar irradiation changes, the active power generation from PV systems also varies. From the results from PV systems we can observe that incremental conductance MPPT works in such a way that for every instant $\frac{dI_{pv}}{dV_{pv}} = -\frac{I_{pv}}{V_{pv}}$ i.e. PV array is operating at its maximum power point. So the

MPPT is able to track the maximum power point.

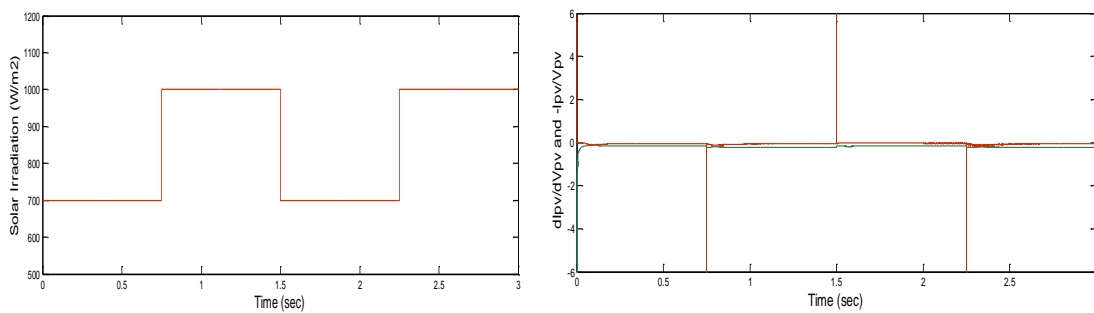


Figure 4.7: Solar irradiation, dI_{pv}/dV_{pv} and $-I_{pv}/V_{pv}$ curves for PV System

Figure 4.8 illustrates the time domain simulated results for Active power of microgrid system, load demand and power supplied by utility grid. Due to sudden variations in wind speed, the turbine reference speed ω_{ref} changes. Accordingly the active power output of the wind generation system changes. The generator output tracks the corresponding maximum power very successfully with just small delays in the dynamic response. During the lower power demand in the microgrid, the extra generated power will be supplied to the utility grid. When power demand is more, in order to meet the load demand, the deficit power will be supplied from the utility grid.

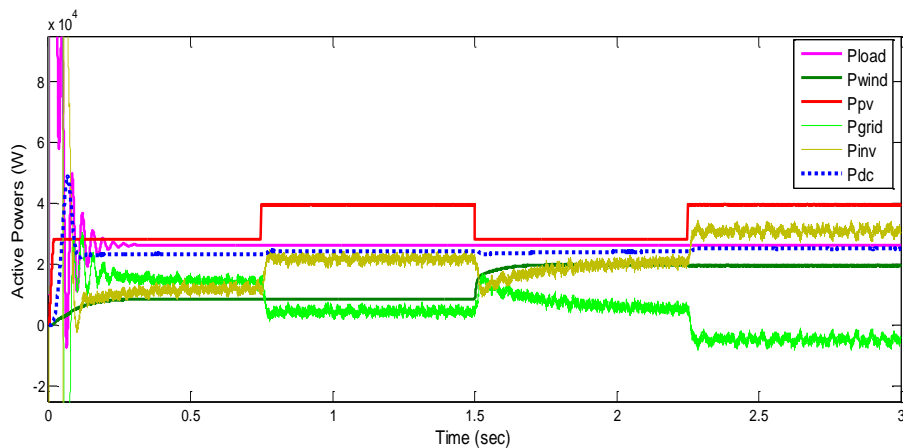


Figure 4.8: Active power of microgrid system, load and power supplied by grid

To study the performance of the microgrid system, a step change in load torque on the induction motor is considered. The DC load connected is 25 kW and 3 phase AC load is suddenly increased from 20 kW to 50 kW (0.9 p.f.) at $t=1.5$ sec. Also the load torque applied to the shaft of the 3 phase 20 HP induction motor is 80 N-m and is suddenly increased to 120 N-m at $t=1$ sec. Figure 4.9 (a) and 4.9 (b) illustrates the time domain simulated results for active and reactive powers. From the power response it is evident that no reactive power is injected by microgrid system. The grid will supply the reactive power demand of the induction motor load. The corresponding variations in load current are shown in Figure 4.10. As the load on the induction motor increases the electromagnetic torque also increases as reported in Figure 4.11. The rotor speed reduces due to increase in load on the motor. The results for rotor speed and stator current for step change in torque T_m are shown in Figure 4.12 below.

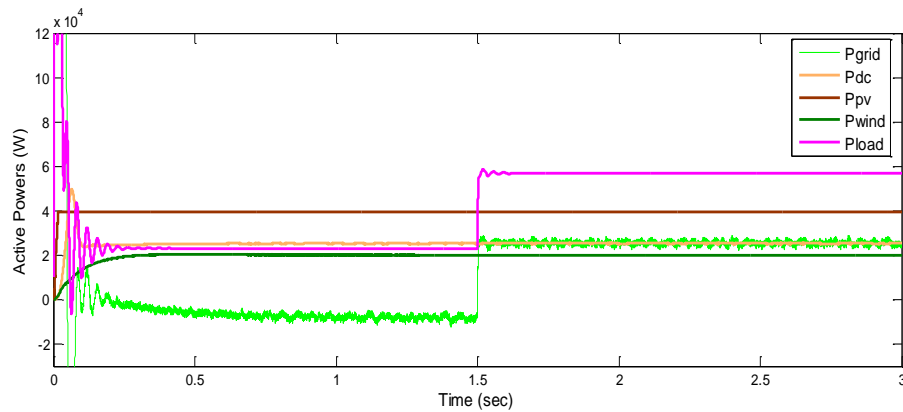


Figure 4.9 (a): Active power of microgrid and load

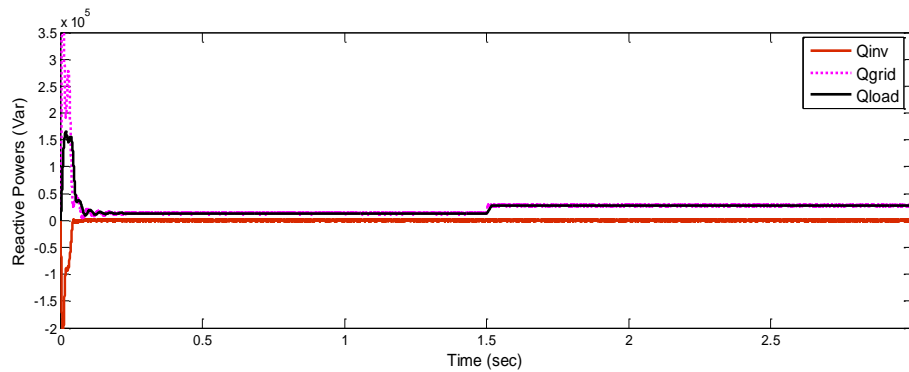


Figure 4.9 (b): Reactive power

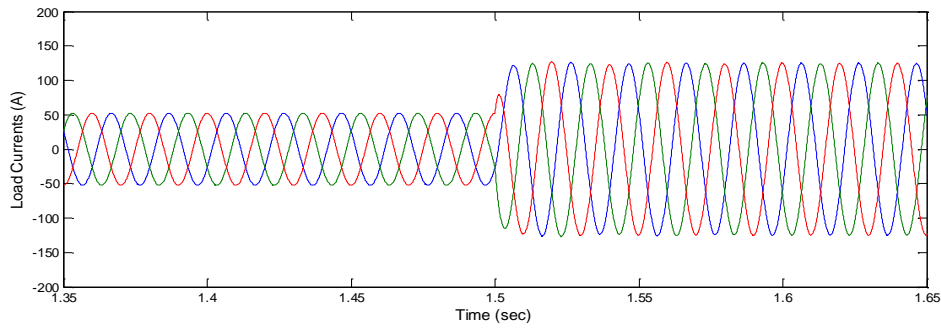


Figure 4.10: Load current

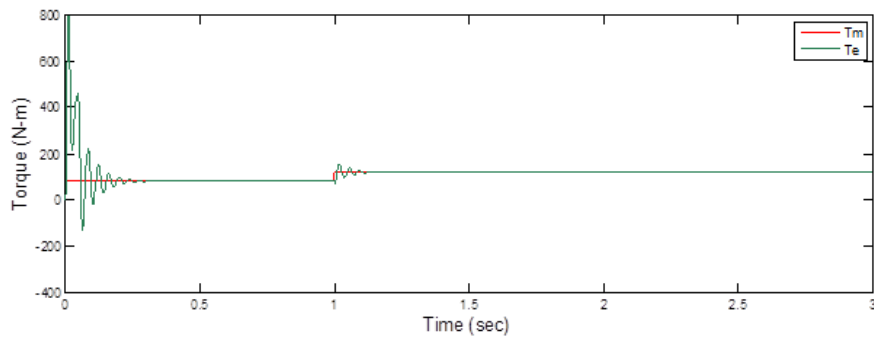


Figure 4.11: Induction motor torques

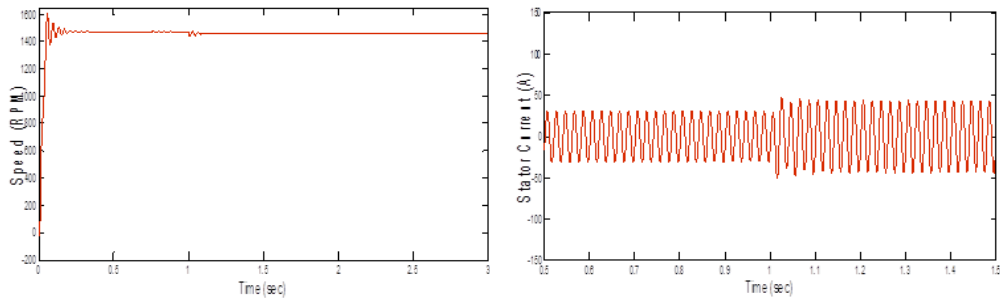


Figure 4.12: Rotor speed and stator current for step change in torque T_m

4.3.3 Case Study with Nonlinear Loads

A microgrid may contain nonlinear loads. To investigate the performance of the microgrid system, a three phase uncontrolled rectifier supplying RL load with $R=75 \Omega$ and $L=50 \text{ mH}$ is considered. The DC power drawn is $P_{dc}=25 \text{ kW}$, initially a three phase AC load connected is 20 kW and at $t=1.5 \text{ sec}$ is suddenly increased to 50 kW with 0.9 p.f. lagging. Figure 4.13 illustrates the time domain simulated results for Active power microgrid system, load and power supplied by utility grid. Figure 4.14 shows the waveforms for injected grid currents. It is seen from the waveforms that the harmonics in grid currents is increased in presence of nonlinear loads. It can be

observed from Figure 4.15 that the total harmonic distortion factor of the grid current is 3.86% for grid connected mode which satisfies the grid current regulation (THD less than 5%). Thus the grid connected microgrid system is capable of supplying nonlinear loads satisfactorily.

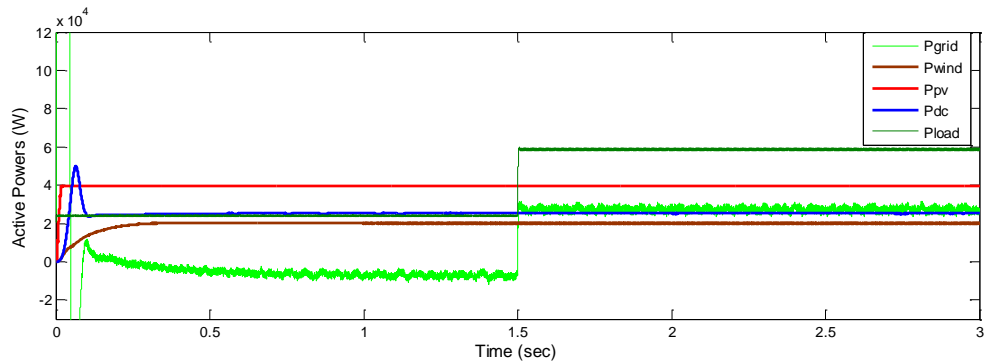


Figure 4.13: Active power of microgrid system, load and power supplied by grid

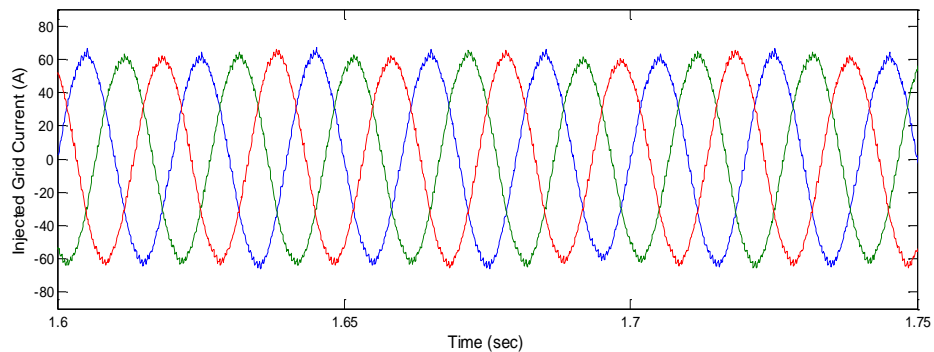


Figure 4.14: Waveforms for currents injected to grid

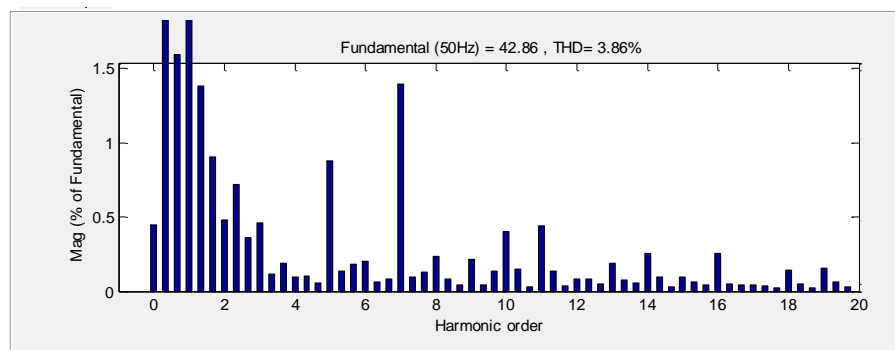


Figure 4.15: THD (%) of currents injected to grid

4.3.4 Intentional Islanding Operation

In this section, the performance study of microgrid system is presented by considering the transition from grid connected to islanding mode of operation. In this study, the microgrid system uses PQ and VF control schemes for grid connected and

islanded mode of operation respectively. The utility connection to the microgrid is disconnected by opening the circuit breaker and this may take place due to the existence of faults at the grid side. Islanding is a condition in which microgrid is electrically separated from the utility system, but continues to provide power to the local loads. The voltage and frequency control scheme presented in Chapter 2 is used for the islanding operation of microgrid.

The simulated results for Active power of wind, PV system, battery, power supplied by grid and power supplied to load are shown in Figure 4.16. Initially, the microgrid is operating in grid connected mode and supplying 72 kW to a three phase resistive load. At $t=1$ sec, utility connection to the microgrid is disconnected and load demand is reduced to 62 kW. Also at $t=2$ sec a step load change from 62 kW to 48 kW is applied to check whether the microgrid operates for local load switching. Up to 1 sec, the power supplied by battery is zero and grid will supply the excess load demand. At $t = 1$ sec, the microgrid gets islanded from the grid, thus the connected load demand is shared by both microgrid and battery. From Figure 4.16 it is observed that the grid power is zero after 1 sec. The simulated result for reactive power of microgrid is shown in Figure 4.17 and it is seen that the reactive power generated by the microgrid is zero during entire simulation period. This is because of the reactive power injected to the grid is zero upto 1 sec due to PQ control scheme of the grid connected inverter and after 1 sec, the reactive power requirement of load is zero.

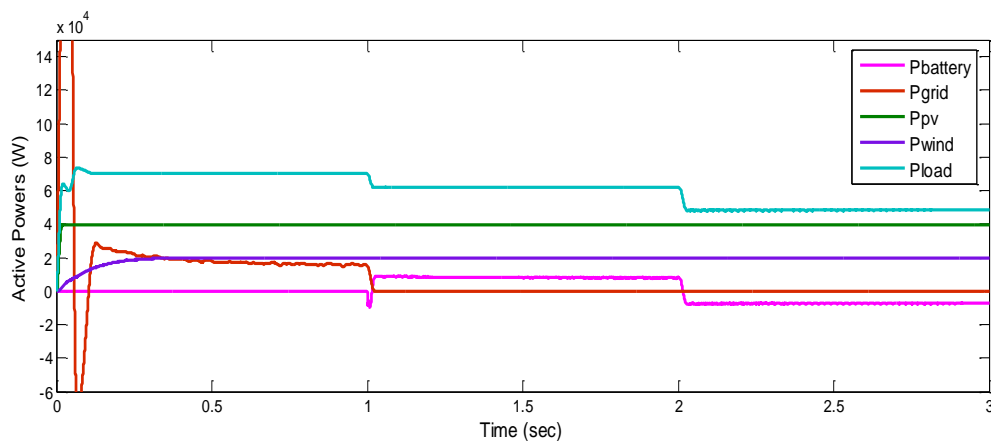


Figure 4.16: Active power of microgrid, power supplied by grid and load power

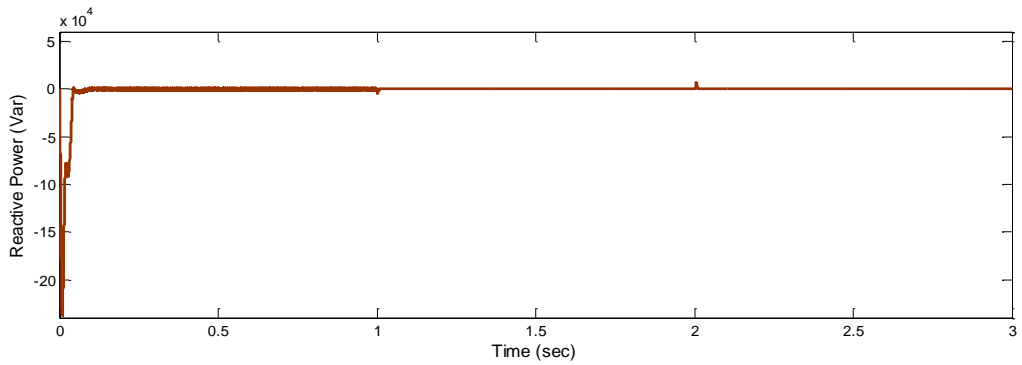


Figure 4.17: Reactive power of microgrid

Figure 4.18 shows the variations of percentage SOC of the battery and it is seen that the battery SOC is zero upto 1 sec. The battery is discharging from 1 to 2 sec and is charging after 2 sec as shown. The variations of output terminal voltage across the inverter and system frequency during entire simulation period are shown in Figure 4.19 and Figure 4.20 respectively. Thus, the amplitude and frequency of the load voltage is well regulated during transition between grid connected to islanding mode of operation under different load conditions.

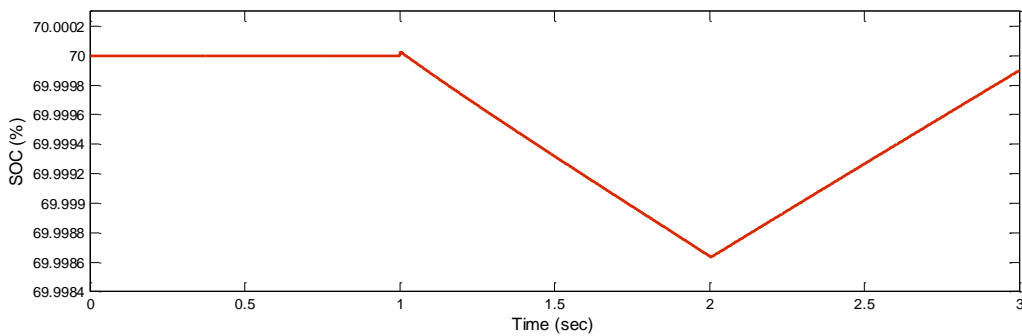


Figure 4.18: State of Charge (%) of battery

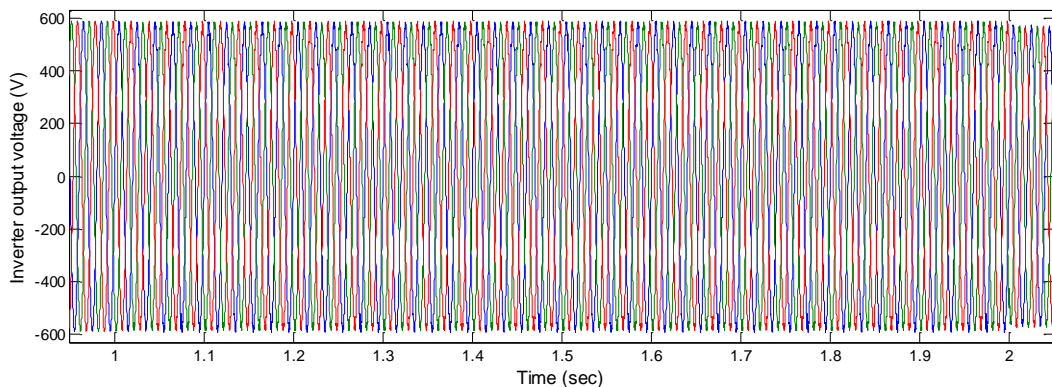


Figure 4.19: Inverter output voltage

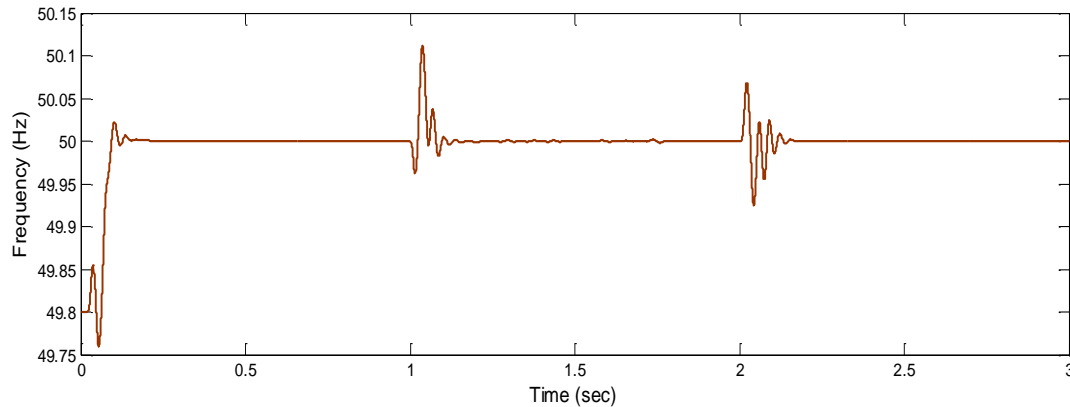


Figure 4.20: Frequency variation

4.4 PERFORMANCE OF MICRGRID SYSTEM WITH GRID PERTURBATIONS

In order to test the ability of the inverter controller in presence of different perturbations originating from the grid, simulation tests were carried out for three typical perturbations. The first case deals with microgrid operation under balanced dip in grid voltages. The second case with heavy distorted grid voltages and the third is microgrid system operation under unbalanced grid voltages. The wind speed (12 m/sec) and irradiation (1000 W/m^2) are constant and total generation is 60 kW. A DC load of 25 kW is connected to DC bus and the active power injected to the grid is only 35 kW. Three phase AC load is drawing a power of 20 kW at 0.9 p.f. lagging.

4.4.1 Balanced Voltage Dip

The performance of microgrid system with balanced voltage dip is shown in Figure 4.21 (a). By using a three-phase programmable voltage source available in the Matlab/Simulink, 20% balanced voltage dip is introduced in the grid voltages at $t = 1.4$ to 1.6 sec, as shown Figure 4.21 (a). The waveform for DC link voltage is shown in Figure 4.21 (b) and DC link voltage due to the grid balanced voltage dip is constant. The variations of active and reactive power injected to the grid are shown in Figure 4.21 (c). It is observed that the values of active and reactive power injected into the utility grid remains the same with regards to the perturbation. This is due to the constant current control scheme used for the grid side inverter operation.

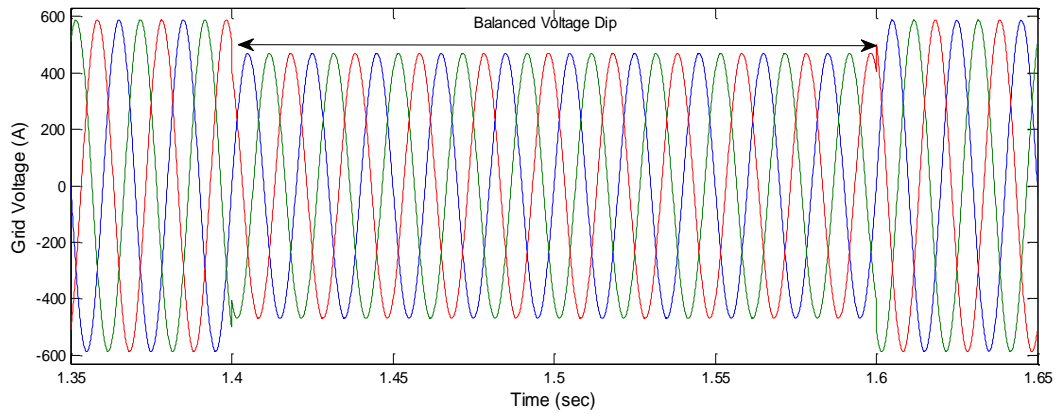


Figure 4.21 (a): Balanced voltage dip in grid voltages

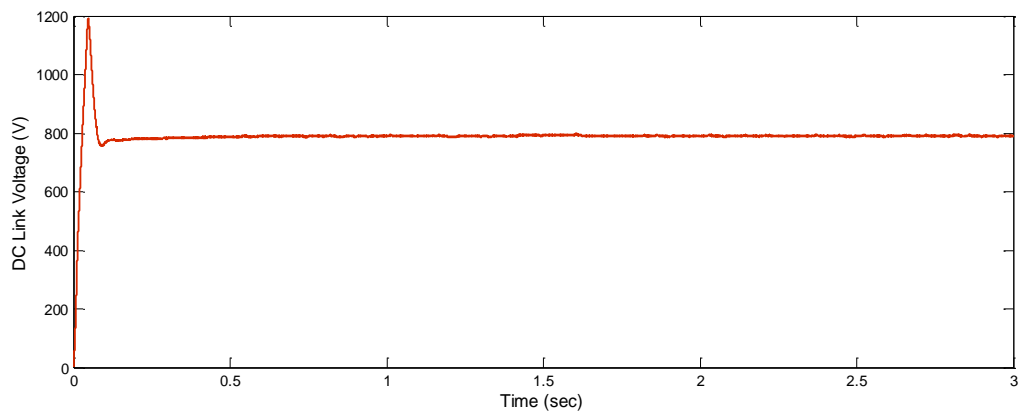


Figure 4.21 (b): DC link voltage

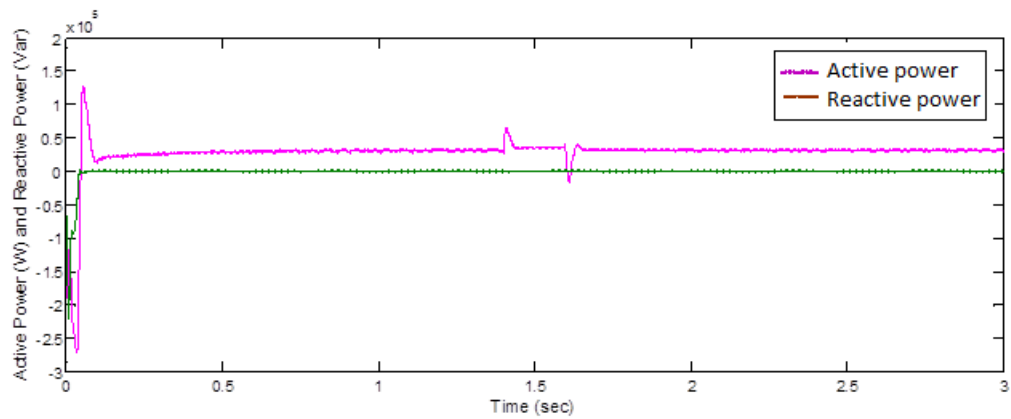


Figure 4.21 (c): Active and reactive power injected to the grid

4.4.2 Polluted Grid Voltages

According to the standard prescribed [IEEE Std. 1547 (2003)], the utility voltage total harmonic distortion is kept lower than 5 % at the point of common coupling. But in industrial plants and factories it can however exceed this prescribed value because of both line impedances and transformers in presence of nonlinear load

currents. In order to represent this situation, utility voltage total harmonic distortion considered is 10 % (6 % of 7th harmonic and 8 % of the 11th harmonic) as shown in Figure 4.22 (a). The waveforms of polluted three-phase grid voltages are shown in Figure 4.22 (b). The corresponding variations in d and q -axis components of injected current by microgrid system are reported in Figure 4.22 (c). Figure 4.23 shows the variations of the injected active and reactive powers to the utility grid. Figure 4.24 shows % THD for injected grid currents. We note a significant increase in % THD line current injected to the grid to 4.57 % when the grid voltage is strongly polluted.

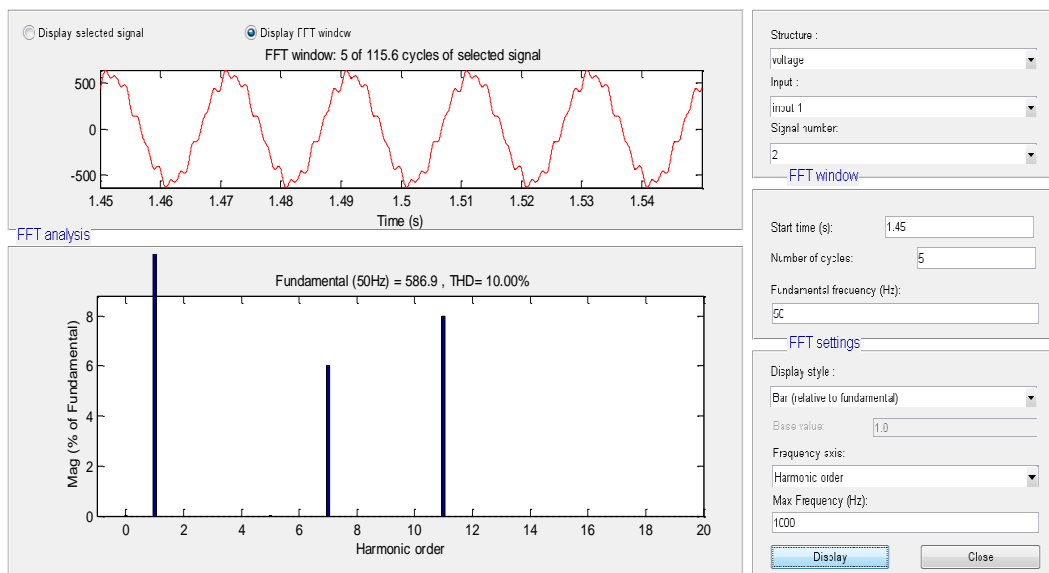


Figure 4.22 (a): THD (%) in polluted grid voltages

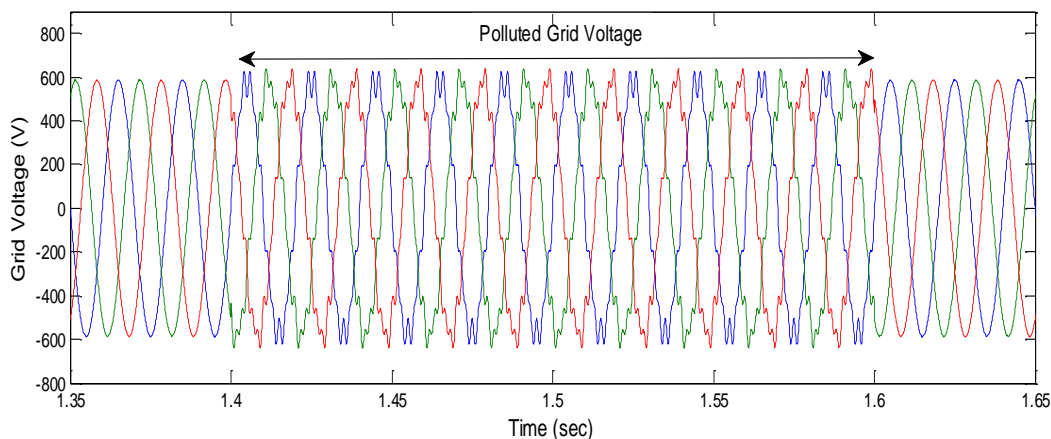


Figure 4.22 (b): Polluted three phase grid voltages

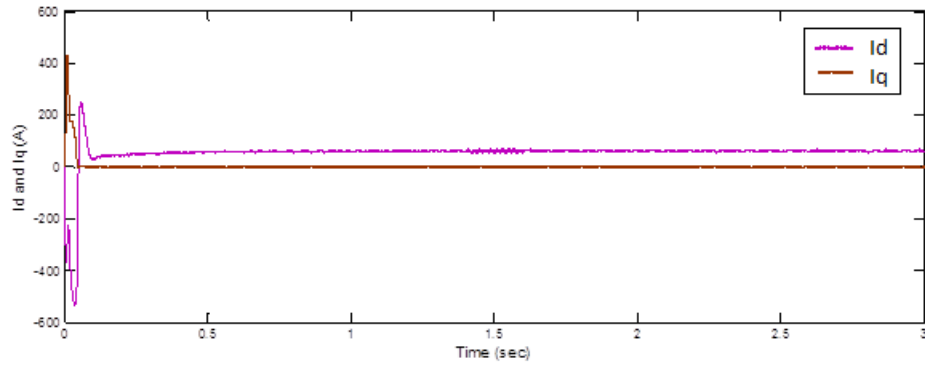


Figure 4.22 (c): d and q -axis components of current injected to the grid

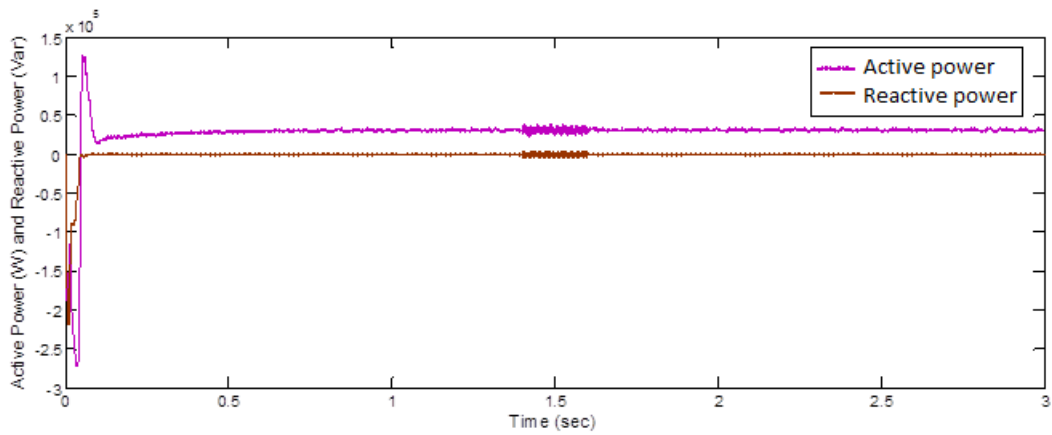


Figure 4.23: Active and reactive power injected to the grid

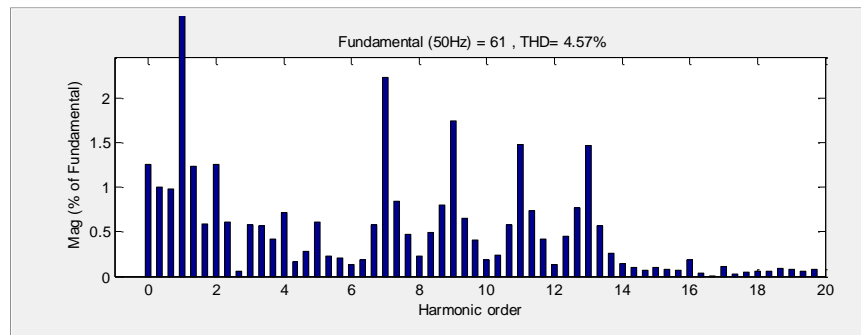


Figure 4.24: THD (%) for injected grid currents

4.4.3 Unbalanced Grid Voltages

The grid voltage unbalance condition represents single phase to ground short-circuits. To simulate unbalanced condition, the voltage of phase ‘B’ is varied by 15 % of its nominal value and maintaining other phase voltages at normal values. The voltage of phase ‘B’ is reduced to 15 % of its normal value from 1.4 to 1.5 sec and is

increased to 15 % of its normal value from 1.5 to 1.6 sec. The simulated grid voltages are shown in Figure 4.25 (a). Figure 4.25 (b) shows the variation in the of i_d and i_q currents due to the unbalanced voltage effect between $t=1.4$ and 1.6 sec. The variation in the injected active and reactive power due to the unbalanced grid voltages is shown in Figure 4.25 (c). It is seen that the values of active and reactive power injected into the utility grid remains the same with regards to the unbalanced grid voltages.

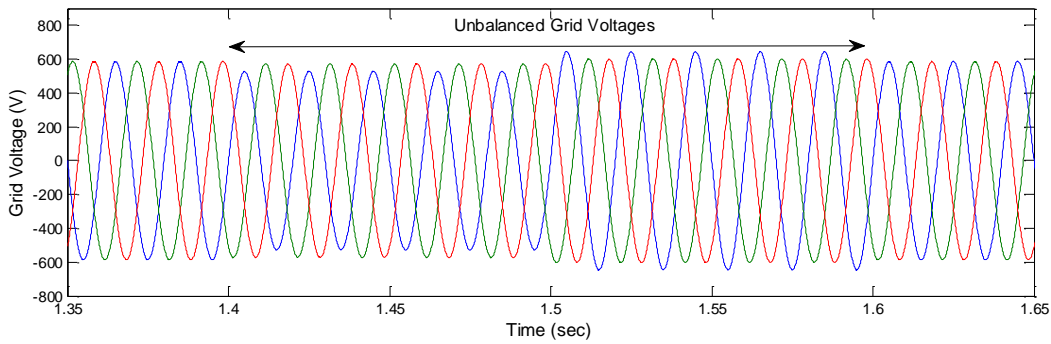


Figure 4.25 (a): Grid unbalanced three phase voltages

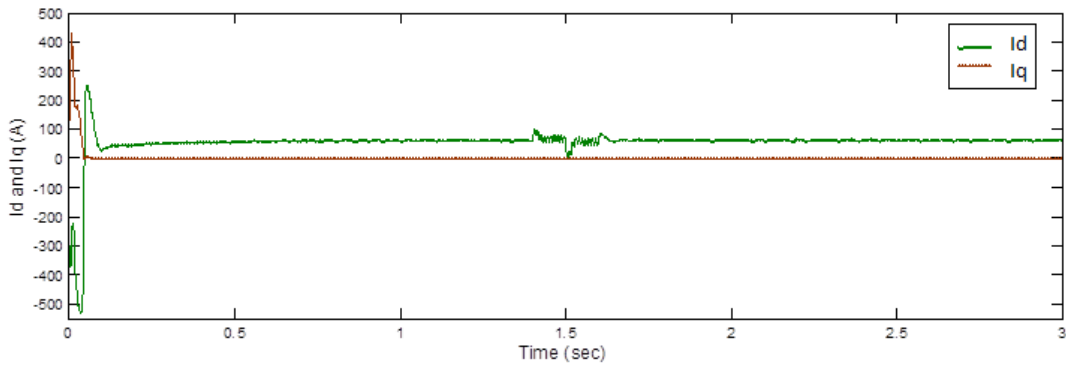


Figure 4.25 (b): d and q -axis components of current injected to the grid

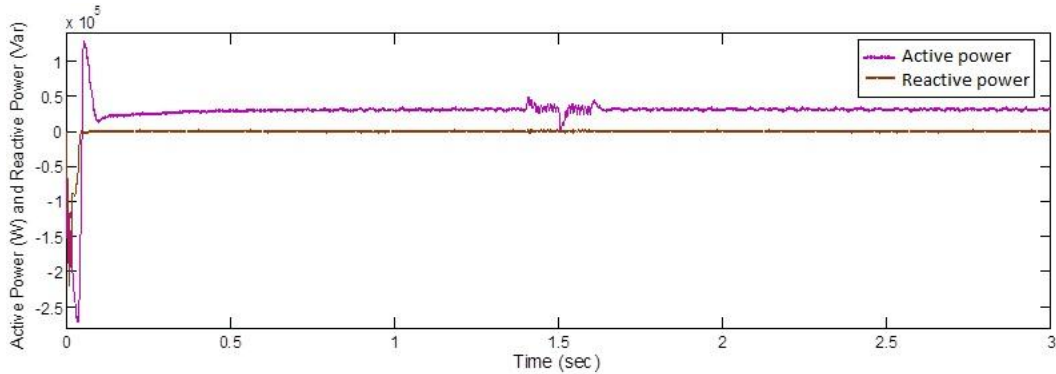


Figure 4.25 (c): Active and reactive power injected to the grid

4.5 CONCLUSIONS

In this chapter, the performance study of grid connected microgrid system with wind and PV generation system has been evaluated. For performance studies, the different types of loads considered on the microgrid are DC loads, induction motor loads and non-linear loads. The simulation results show that, the presented microgrid model has ability to supply the power as per the load demand along with the utility grid. It is seen that the percentage total harmonic distortion factor of the grid current with normal operation of the microgrid for grid connected mode of operation is around 2.2%, which is well within the standard prescribed by IEEE standards [IEEE Std.1547 (2003)]. Also, it can be observed that the total harmonic distortion factor of the grid current is 3.86% even with nonlinear loads, which satisfies the grid current regulation. The performance study of microgrid system is presented by considering the transition from grid connected to islanding mode of operation. Also, the performance of microgrid system has been analyzed for different grid perturbation conditions. It is observed that the values of active and reactive power injected into the utility grid remains the same with regards to the perturbation. The simulation results demonstrate the capability of the current control scheme of the grid side inverter in regulating the active and reactive power injected by the microgrid system during grid perturbation conditions.

CHAPTER 5

POWER SMOOTHING OF GRID INTEGRATED MICROGRID SYSTEM

5.1 INTRODUCTION

In the recent years considerable attention has been given to generate electricity using wind/solar hybrid system worldwide. The output power of wind and solar system depends upon the weather conditions and fluctuates continuously with variations in wind speed and solar irradiation respectively. These power fluctuations cause adverse effects on the voltage, frequency and transient stability of the utility grid. The large integration of these intermittent renewable energy (RE) generation sources into the utility grid, may introduce adverse effects on the utility grid [Muhamad Zalani Daud, et al. (2013)]. Thus mitigation of output power fluctuations is one of the major challenges in large integration of wind and solar based generation systems to the utility network. Hence, before delivering power to the utility grid it is essential to smoothen the power fluctuations.

Conventionally battery based energy storage systems are used to compensate the output power fluctuations in wind and solar based power generation systems [Tao Zhou and Bruno Francois (2011)]. To compensate or absorb the difference between the generated wind power and the required grid power energy storage systems are used. Conventionally battery based ESSs are used to compensate the output power fluctuations in wind and solar based power generations [Fakham et al. (2011)]. The battery ESS can be used to improve the power quality and the transient stability of wind farm can be improved [Jie Zeng et al. (2006)]. A smoothing control method for reducing microgrid output power fluctuations using battery and regulating battery SOC is proposed in [Xiangjun Li et al. (2013)]. To improve the power quality and stability of the power system, vanadium redox flow battery based energy storage system (ESS) is used for power control of a grid connected wind power system [Baoming Ge et al. (2013)]. The use of an energy storage system embedded in the

direct current link of a wind turbine with a fully rated converter for smoothing output power and contributing to DC link voltage control is presented in [Guoyi Xu et al. (2013)]. In [Xu et al. (2011)] the energy storage system embedded into a wind turbine in order to enhance fault ride-through ability, power quality improvement and dampen short-term power oscillations.

Recently ultracapacitors based energy storage systems are used in many literatures for renewable energy applications in addition to other ESSs. The ultracapacitors have high power and energy densities, large life expectancy and high efficiency. Therefore, ultracapacitors are ideal for short-term (i.e., seconds to minutes) energy storage that enables wind turbine generators to compensate for fast changes in the power output [Chad Abbey and Geza Joos (2007); Liyan Qu and Wei Qiao (2011)]. The ultracapacitor energy storage device is used in a doubly fed induction generator based wind power system in order to smoothen the wind power output [Muyeen et al. (2008)]. A hybrid generator with a PV energy conversion system is proposed in [Fakham et al. (2011)] with ultracapacitors and lead acid batteries in a DC coupled structure. Integration of ultracapacitor with the flexible AC transmission systems is one of the good solutions to smoothen the wind power fluctuations [Muyeen et al. (2007)]. The power management strategy for control of the power exchange among different sources and to provide some services to the grid, power management strategies are implemented [Zhou et al. (2008); Ipsakis et al. (2009)].

Most of the technical literature discusses the control performance of battery storage devices or ultracapacitors used for power smoothening of individual renewable power sources such as either PV or wind power system. In this research work, a control method is presented for power smoothening of grid integrated microgrid system using energy storage devices in a DC coupled structure. The power smoothening control utilizes energy storage systems in order to absorb power fluctuations, so that a smoother version of power is delivered to the load or utility grid. The microgrid system is integrated to the utility grid through single three phase inverter. The grid side inverter control strategy presented in Chapter 2 is used to maintain DC link voltage constant while injecting power to the grid at unity power factor considering different operating conditions. Actual wind speed and solar irradiation data are used in this study to evaluate the performance of the developed system using

MATLAB/Simulink software. The simulation results show that output power fluctuations of microgrid system can be significantly mitigated using the storage devices.

In this work, both battery and ultracapacitors have been proposed to mitigate the output power fluctuations of a grid connected wind/PV microgrid system. In the first case, ultracapacitor banks are integrated at the common DC link through DC/DC bidirectional converter of the microgrid system. A simple control scheme for power smoothing of the grid integrated microgrid system using ultracapacitor has been proposed. In order to observe the real-time performance of ultracapacitor energy system in smoothing the output power fluctuations, the practical site data for wind speed and solar irradiation (sampled at each second) are considered for 10 minutes duration. The final result of proposed control strategy is a smooth and ramp controlled power output that can be injected to the grid.

In the second case, both battery and ultracapacitors are considered for mitigating output power fluctuations for grid connected microgrid system. In this case, practical site data for wind speed and solar irradiation for one day are considered. To reduce the battery stress and to promise an increased lifetime of the battery, ultracapacitors are used. The battery provides power during long term power variations and the ultracapacitor supports during the power fluctuations for a very short time. The battery and ultracapacitor storage devices are embedded in the DC link with the use of bidirectional DC/DC converters. A control strategy is developed for DC/DC converters for power smoothing of the grid integrated microgrid system. The fluctuating power is absorbed by both battery and ultracapacitors during wide variations in solar and wind power, so that the power injected to the grid is smoothed. This makes higher penetration and integration of distributed energy resources to the grid possible.

5.2 SYSTEM CONFIGURATION

Figure 5.1 shows schematic diagram of the grid integrated DC coupled wind/PV microgrid system with energy storage devices. Both sources and storage devices are connected to a common DC bus. The system is connected to the utility

grid through a 3 phase inverter. Both wind and PV system consists of MPPT controllers which are used to extract the maximum power at any operating conditions thereby increasing the efficiency of the available energy. The controller designed for the inverter is able to maintain constant DC link voltage and the smoothed power is injected to the grid at unity power factor for different operating conditions.

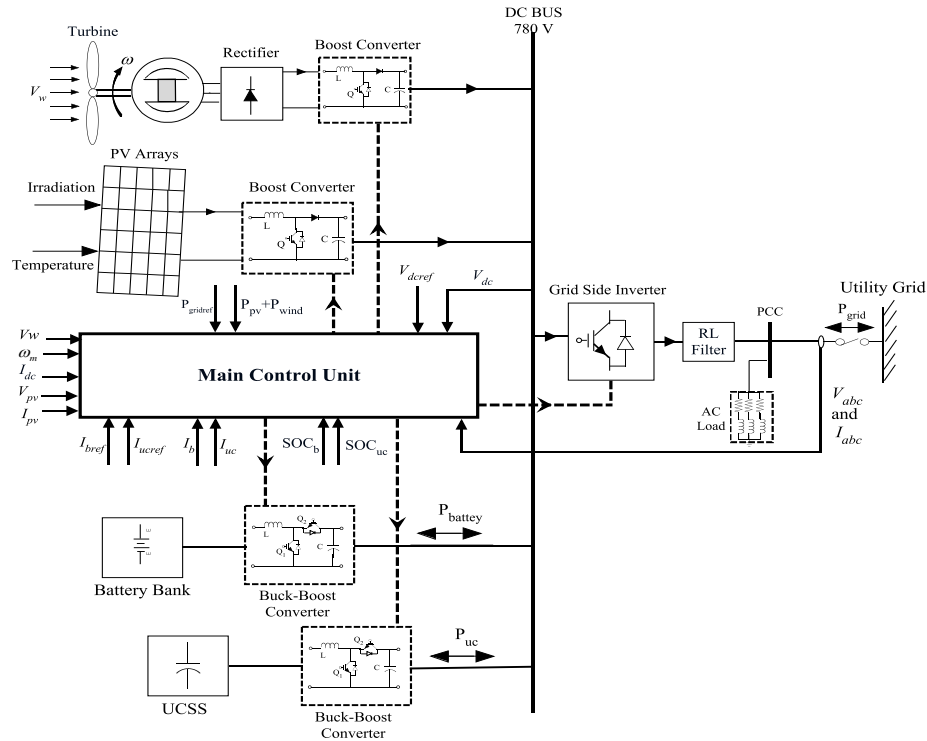


Figure 5.1: Schematic diagram of grid integrated wind/PV microgrid system with storage devices

5.3 CONTROL STRATEGIES FOR POWER SMOOTHING

The purpose of power smoothing of the renewable energy sources is to improve the quality of power delivered to the grid and transfer more stable power into the grid. This research work presents two different power control strategies for power smoothing of a grid connected microgrid system. The output power of wind/PV microgrid is smoothed using ultracapacitors for the short duration of time and 10 minutes data for wind speed and solar irradianations are taken for simulation study. And for the long duration of time, both battery bank and ultracapacitors are used for power smoothing and one day data for wind speed and solar irradianations are considered. To

evaluate the dynamic performance of the microgrid system, the simulation results were presented for these developed control strategies.

5.3.1 Ultracapacitors

The output power produced from wind/PV microgrid system fluctuates due to changes in weather conditions. Ultracapacitors are used to mitigate these short term power fluctuations and the ultracapacitor energy is managed by using a bidirectional DC/DC converter. For the proposed system the ramp up and down rate is limited at 10% per 60 sec for a 60 sec average. That is if the average power for the last minute is at 60 kW, the power output can ramp up or down for more than 6 kW per 60 sec. For obtaining smooth output power reference the overall power output is passed through a rate limiter first and then moving average is taken for a suitable duration of time. The combined power from wind and PV is subtracted from the reference power and the difference in power is then passed and multiplied with the multiplication factor obtained from the look-up table as shown in Figure 5.2. The rating of the ultracapacitors can be reduced by utilizing the energy stored in an efficient way. When the stored energy goes below or more than a pre-defined value (25% to 75%), by multiplying a proper factor the reference power can be modified. This resulting power for the ultracapacitor is divided by the voltage across the ultracapacitor bank this gives the current that has to be supplied by the ultracapacitor and it is the reference current. The difference between the actual and reference current is controlled using the PI controller and is then compared with a saw tooth waveform which produces pulses for the switches Q_1 or Q_2 of UC controller for charging or discharging. The control strategy of the DC/DC bidirectional converter to manage ultracapacitor energy is given in Figure 5.3.

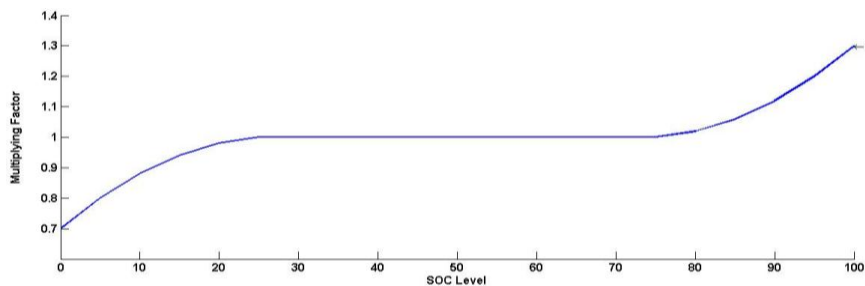


Figure 5.2 (a): SOC vs. multiplying factor in boost mode

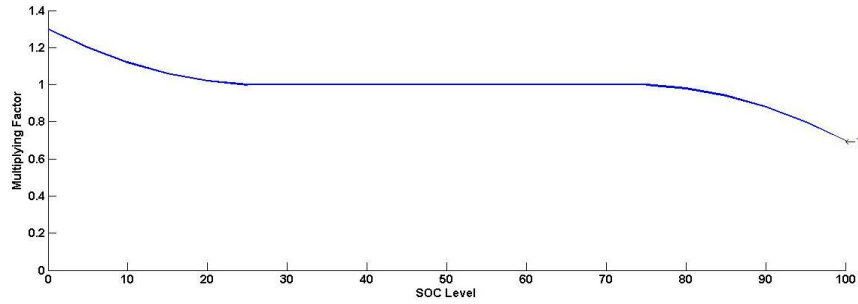


Figure 5.2 (b): SOC vs. multiplying factor in buck mode

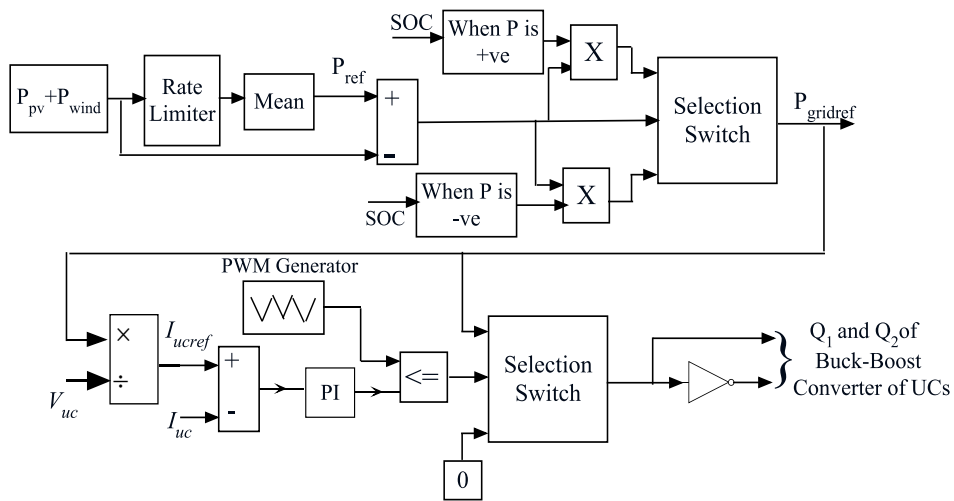


Figure 5.3: Control strategy for reference grid power generation

5.3.2 Combination of Battery and Ultracapacitors

By combining UCs with batteries, which are typically low power devices, the battery performance can be improved in terms of the power density. Figure 5.4 shows control strategy for battery and ultracapacitors in detail. Two DC/DC bidirectional converters are considered for connecting the battery energy storage systems and ultracapacitors to the DC bus of the microgrid system. Since the DC bus voltage is controlled by the grid side converter, the bidirectional converters control strategy is to control the power flow of storage devices. The bidirectional converters consist of two insulated gate bipolar transistor switches Q_1 and Q_2 . By controlling their duty ratios the charging and discharging of storage devices can be regulated. The DC/DC converter configuration can operate either in buck or boost mode depending on the state of the switches. The duty ratio D_1 of switch Q_2 in buck mode can be given as

$$D_1 = \frac{V_b \text{ or } V_{sc}}{V_{dc}} \quad (5.1)$$

And the duty ratio D_2 of switch Q_1 in boost mode is $D_2=1-D_1$. The control strategy has two control loops. The outer loop regulates power fluctuations of the microgrid system. And inner current loops which controls battery and ultracapacitors currents. If power generation is more, the converters act in buck mode and storage devices absorbing the power difference which results an increase in voltage of storage devices. If generation is less, the converters act in boost mode the difference power is supplied by storage devices so that the voltage of storage devices decreases. However for achieving equal load sharing a gain factor K is multiplied in the feedback path and the factor is $K=0.5$. Thus two reference currents and I_{bref} and I_{ucref} are obtained. In the Figure 5.4, I_b and I_{uc} are battery and ultracapacitor currents respectively. Hence by proper controlling of duty cycles and the storage devices will act as either sink or source of power. The transfer functions of DC/DC converters of battery and ultracapacitor bank are

$$\frac{\hat{i}_b}{\hat{d}} = \frac{3.39 \times 10^5 (s + 20)}{s^2 + 10s + 5.14 \times 10^4} \quad (5.2)$$

$$\frac{\hat{i}_{uc}}{\hat{d}} = \frac{86667 (s + 20)}{s^2 + 10s + 1.31 \times 10^4} \quad (5.3)$$

The Bode diagrams for DC/DC converters of battery and ultracapacitor bank are shown in Figure 5.5 and Figure 5.6 respectively. The PI controller of inner current loop of battery constants (K_p and K_i) are $K_p = 0.015$, $K_i = 1.5$; Similarly, The PI controller constants for ultracapacitor bank are $K_p = 0.045$, $K_i = 1.5$.

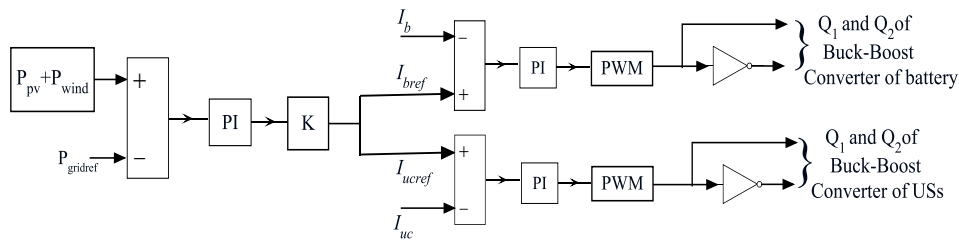


Figure 5.4: Control strategy for battery and ultracapacitors

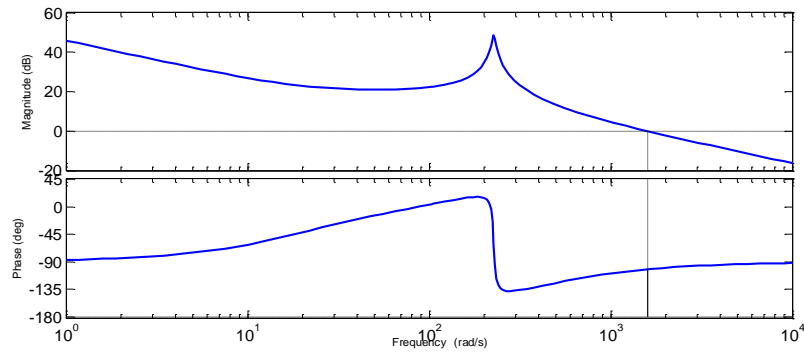


Figure 5.5: The Bode diagrams for DC/DC converter of battery bank

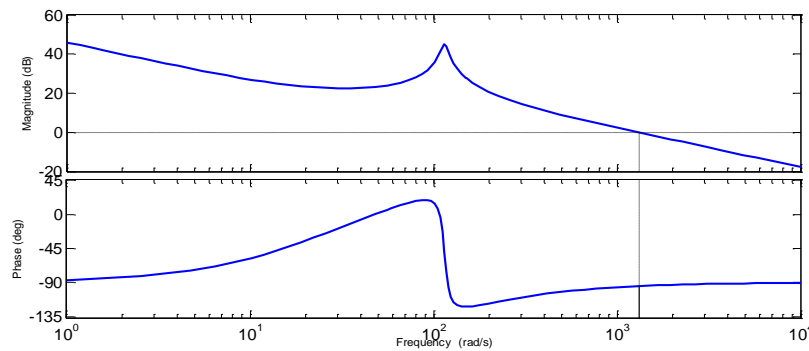


Figure 5.6: The Bode diagrams for DC/DC converter ultracapacitor bank

5.4 RESULT ANALYSIS AND DISCUSSION

5.4.1 Case Study with Ultracapacitors

The main objective of this section is to evaluate the performance of the developed grid connected wind/PV microgrid system and to demonstrate power smoothing with and without considering local loads using UC bank. The parameters of the ultracapacitor (Maxwell ultracapacitor) module are given in Appendix A. The microgrid system is connected to the utility grid through a 0.415/3.3 kV step-up transformer. In order to observe the real-time performance of developed system, the practical site data for wind speed and solar irradiation [Google_heliostat_wind_data_collection.pdf and Data source from the NREL] are sampled at each second for 600 sec during the simulation. The DC bus voltage is maintained constant by the three phase inverter controller. To test the performance of the system following two different cases were analyzed. The simulation results were presented to evaluate the dynamic performance of the microgrid system under the

proposed methods of control strategies. The parameters of the PI controllers for different controllers are listed in Appendix B.

5.4.1.1 Microgrid without Local Loads

In this case the performance of the grid connected wind/PV microgrid system to demonstrate power smoothing without local loads is evaluated. Figure 5.7 and Figure 5.8 shows wind speed and solar irradiation profile respectively. Figure 5.9 represents the corresponding variation in wind power output and solar power output. The responses of combined wind and PV output power fluctuations, grid power reference of the system and output power of the ultracapacitors are shown in Figure 5.10 and Figure 5.11. The grid power reference and smooth power output from the microgrid system supplied to the grid are shown in Figure 5.12. These results enable to conclude that the major part of the fluctuating power produced by the wind/PV power system is absorbed by ultracapacitors. Also the real power output of microgrid system is following the grid power reference and this smooth power output is delivered to the grid. By incorporating an ultracapacitors storage system into the system, the final result of proposed control strategy is a smooth and ramp controlled power output that can be injected to the grid.

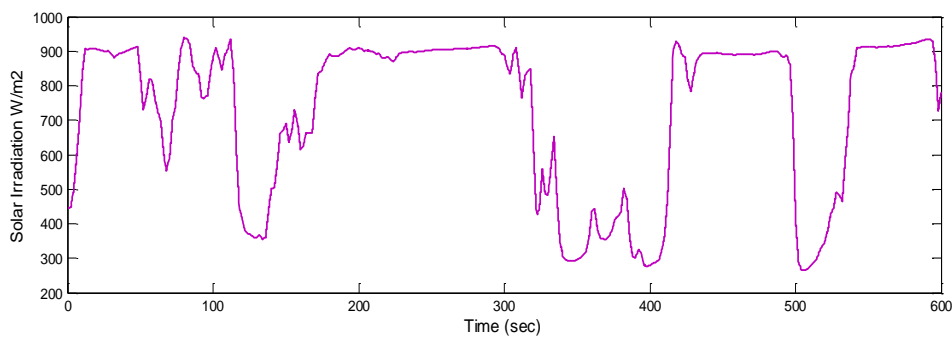


Figure 5.7: Solar irradiation profile

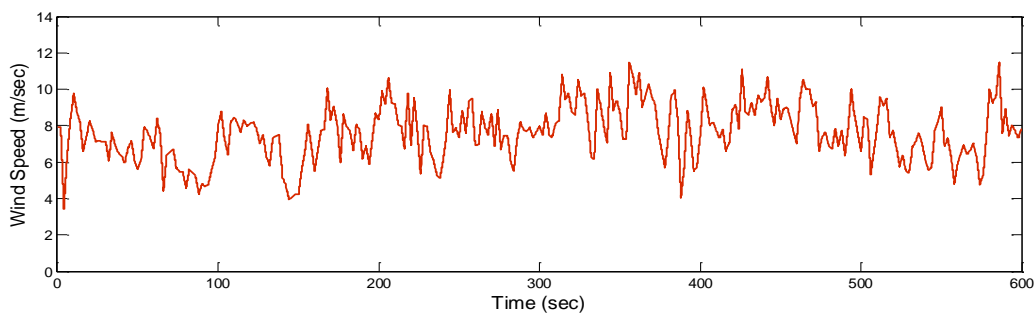


Figure 5.8: Wind speed profile

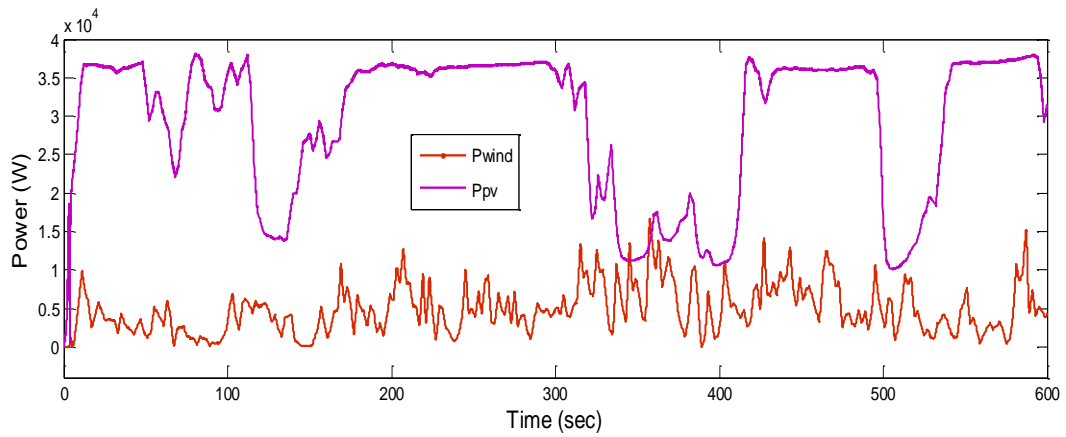


Figure 5.9: Wind and solar power output corresponding to wind speed data and solar irradiation

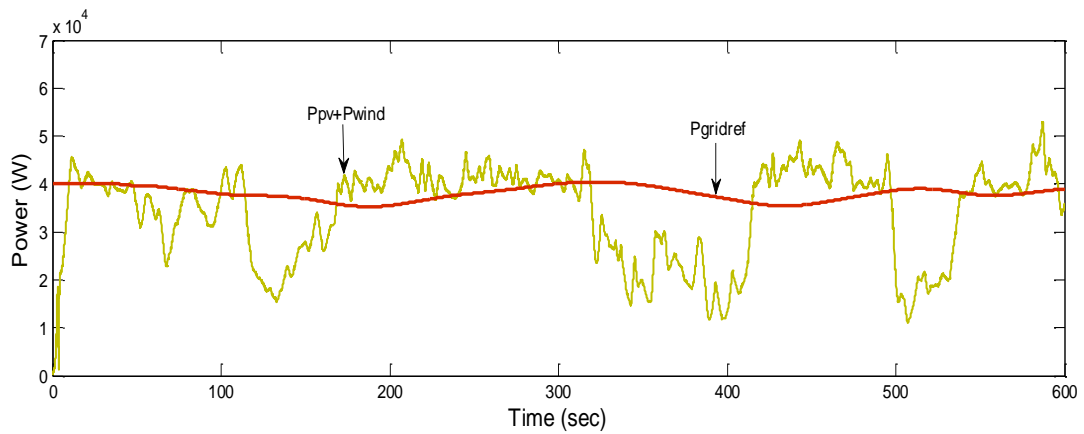


Figure 5.10: Total power generated from microgrid and grid power reference of the system

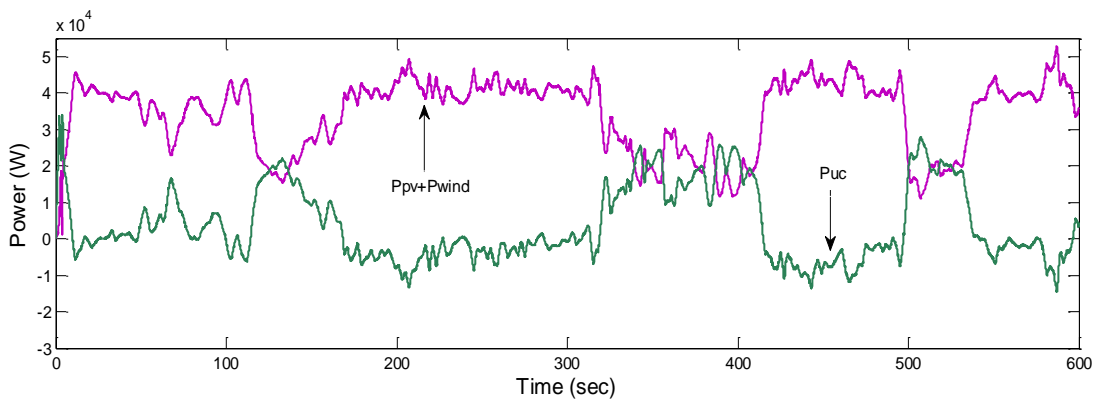


Figure 5.11: Total power generated from microgrid and power output of ultracapacitors

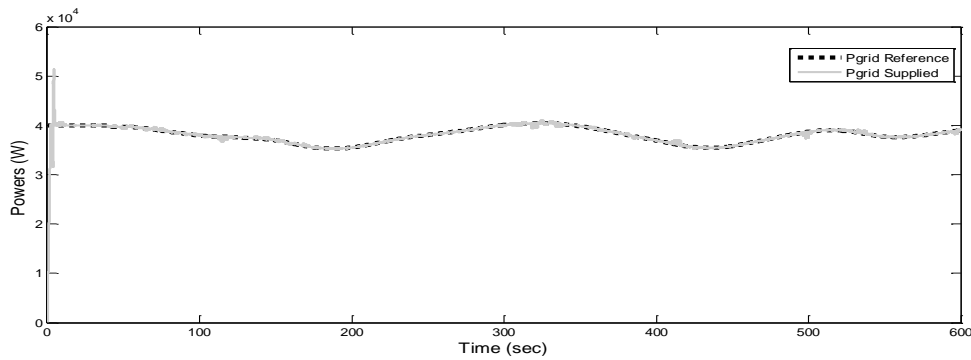


Figure 5.12: Grid power reference and microgrid power supplied to the grid

The DC link voltage is maintained at 780 V through the closed loop voltage control of the inverter as shown Figure 5.13. The variation of percentage SOC with time of ultracapacitors storage system is shown in Figure 5.14. The reference and actual quadrature component of injected grid current are reported in Figure 5.15. From the response it is evident that the quadrature component of injected grid current injected to the utility grid is zero. Hence, according to power equations reported in Chapter 2 the reactive power is injected to the utility grid by microgrid system is zero.

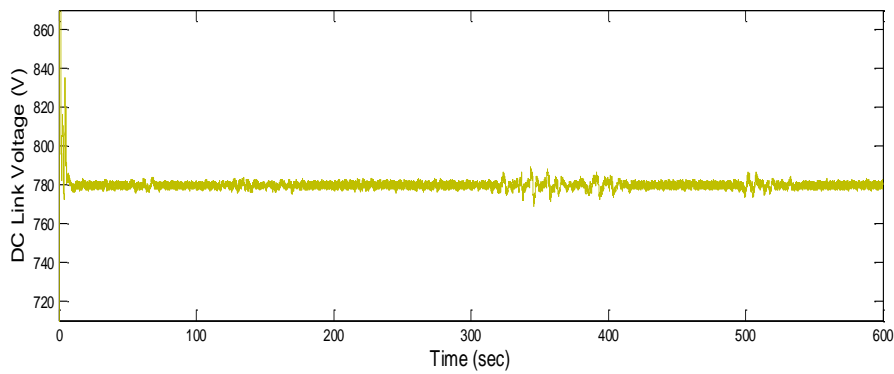


Figure 5.13: DC link voltage

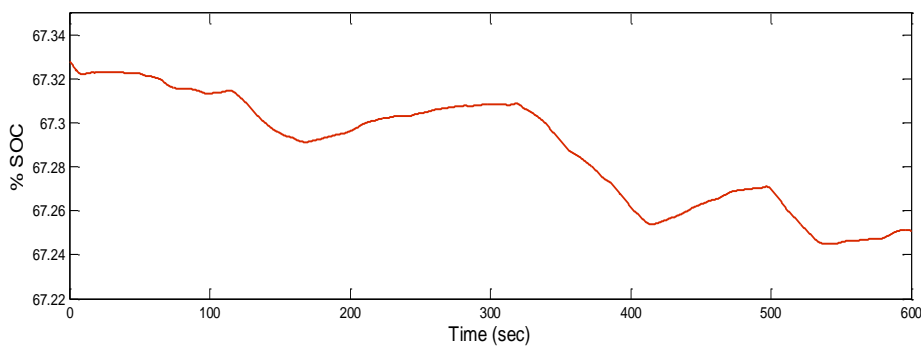


Figure 5.14: State of Charge (%) of ultracapacitors

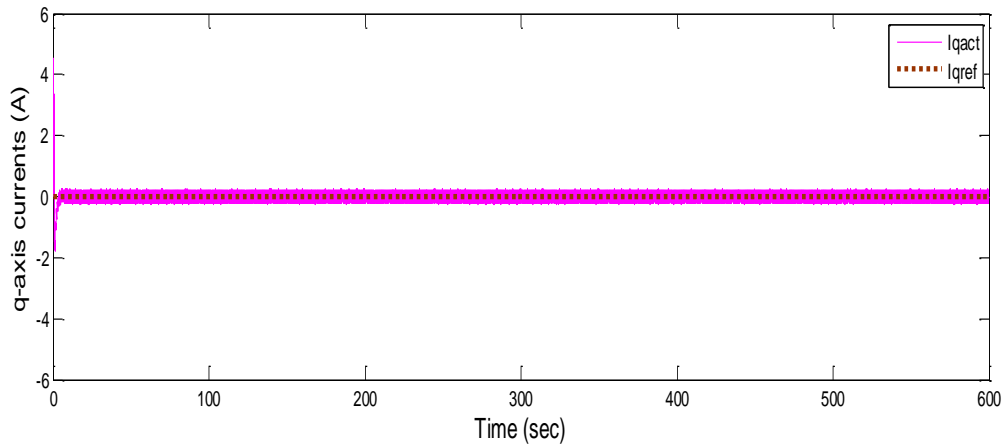


Figure 5.15: q -axis component of current supplied to the grid

5.4.1.2 Microgrid Supplying Local Load

Three phase local load at 0.8 p.f. lagging is connected to secondary side of three phase transformer of the microgrid system. For this case, initially a 40 kW load is considered, during $200 < t < 400$ sec the load power is increased to 60 kW and is reduced to 20 kW at $t = 400$ sec. Figure 5.16 shows simulated results of active power consumed by load, microgrid system power injected and active power supplied by the grid. In order to meet the load demand, the deficit active power will be supplied from the utility grid. The simulated results of reactive power consumed by load, wind/PV microgrid system power injected and reactive power supplied by the grid is given in Figure 5.17. From the reactive power response it is seen that no reactive power is injected by microgrid system. The inverter controller is designed in such a way that it operates at unity power factor. The utility grid will supply the reactive power demand of the three phase inductive load. The DC link capacitor voltage is shown in Figure 5.18. It can be clearly observed that the proposed microgrid system has constant DC link voltage (780 V) during changes in load conditions. With these simulation results it was confirmed that the proposed topology with ultracapacitor storage system can successfully reduce the output power fluctuations and ease the integration of the renewable resources to the grid. Also we can have increased penetration of the renewable resources into the grid without affecting the grid reliability.

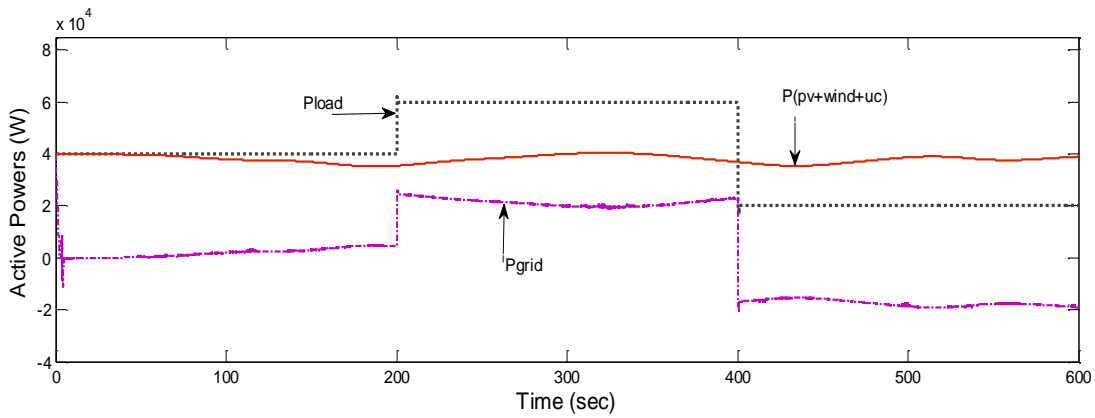


Figure 5.16: Active power of microgrid, load and utility grid

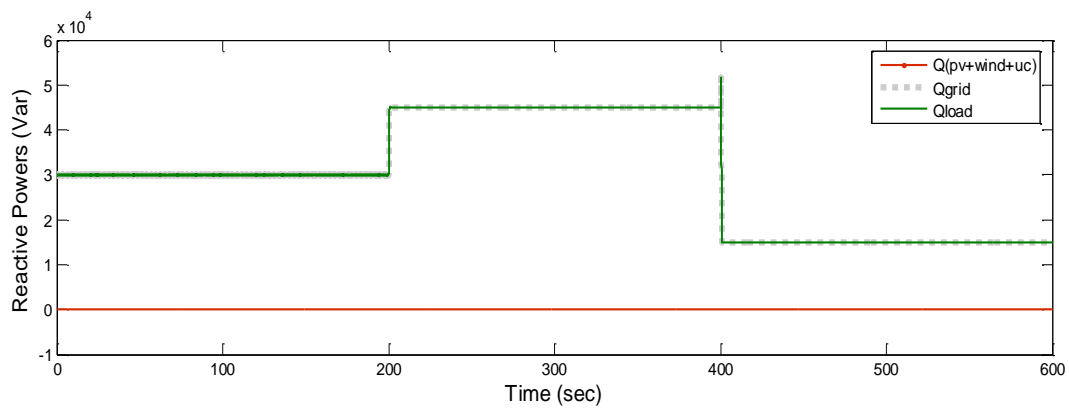


Figure 5.17: Reactive power of microgrid, load and utility grid

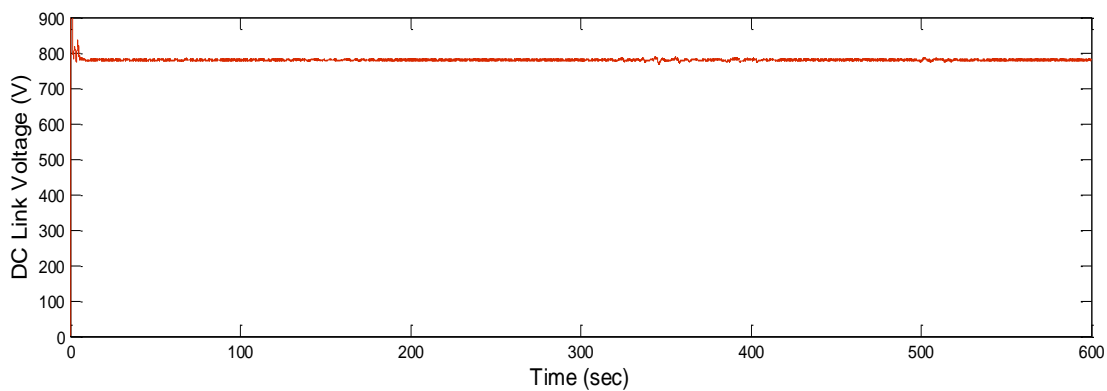


Figure 5.18 DC link voltage

5.4.2 Case Study with Battery and Ultracapacitors Combination

The 420 Ah lead acid battery bank is used for the study. For simulation model, Maxwell Boostcap PC2500 ultracapacitor unit [Electric Double Layer Capacitor: Available: <http://www.maxwell.com/pdf/uc/datasheets/PC2500.pdf>] is chosen. Each

unit has nominal voltage of 2.5V, corresponding to 2700F. The initial and maximum voltages are 400V and 600V respectively. The ultracapacitor bank having a string of 240 units connected in series. The simulation is done by considering the practical site data for wind speed and solar irradiation for one day [Google_heliostat_wind_data_collection.pdf and Data source from the NREL] and scaling it down to 4.8 sec. The parameters of the PI controllers for different controllers are listed in Appendix B. Figure 5.19 (a) and Figure 5.19 (b) shows wind speed and solar irradiation profile for one day respectively. Figure 5.20 represents the total wind and PV power fluctuation rate during the one-day period. The wind power generation is high during night time. Also, the PV arrays provide electrical power only during the day around the midday with a peak power with huge variations may occur in output power as shown. These variations in the power fluctuations will affect the stability of the grid. Hence power injected to the grid should be smoothed.

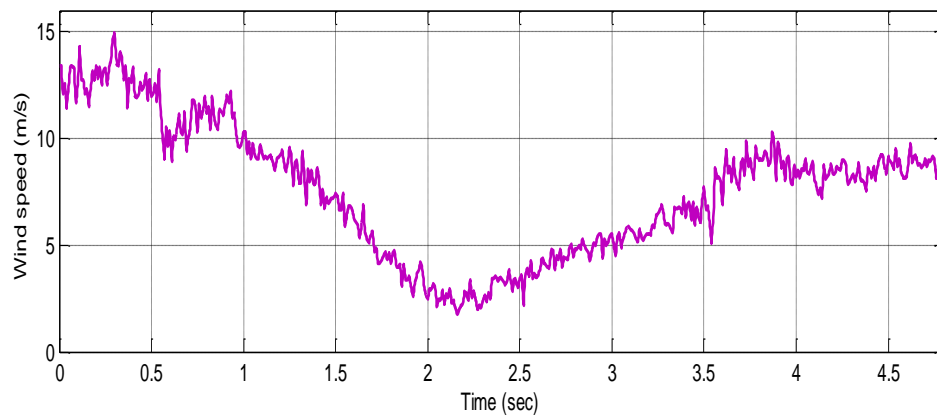


Figure 5.19 (a): Wind speed profile for one day

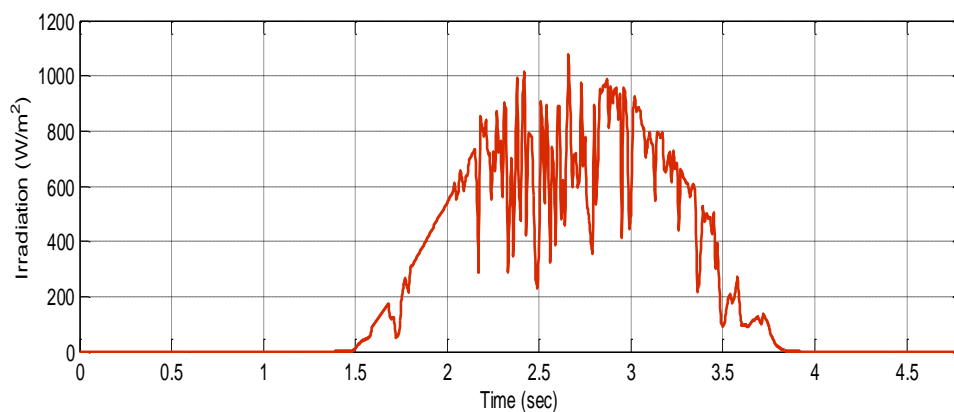


Figure 5.19 (b): Solar irradiation profile for one day

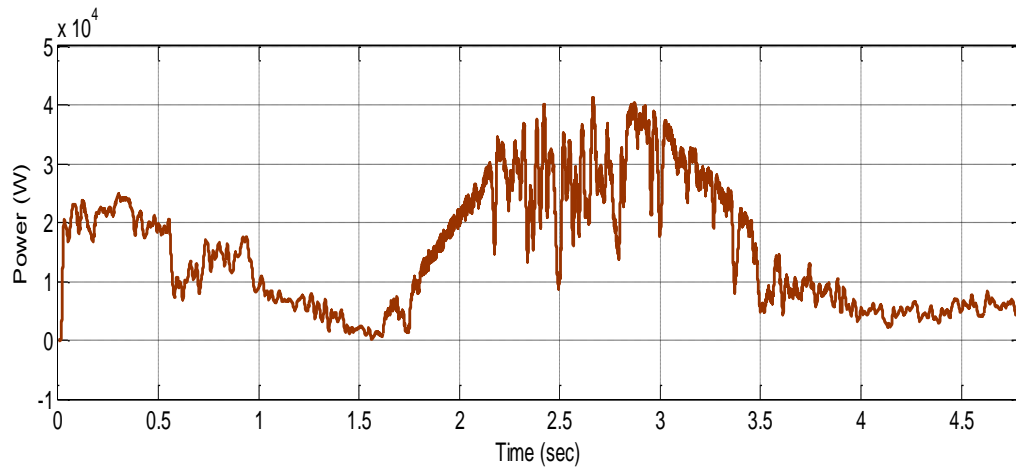


Figure 5.20: Total wind and solar power generation

The power supplied by battery and percentage SOC of battery during the one-day period are shown in Figure 5.21 (a) and Figure 5.21 (b) respectively. Initially, the state of charge of the battery storage is set to 80%. The battery supplies maximum power of 11 kW during lowest power generation period. And battery is absorbing a maximum of 8 kW during period of peak power generation. The voltage across the battery bank is shown in Figure 5.22. The ultracapacitor power and percentage SOC of ultracapacitor are reported respectively in Figure 5.23 (a) and Figure 5.23 (b). Most of the transient power is supplied by ultracapacitors in the beginning and it will supply maximum power of 11 kW and absorbs a maximum of 8 kW. Therefore, it is observed from the simulated results that both battery and ultracapacitors supply or absorb the power difference. The voltage across the ultracapacitor bank is shown in Figure 5.24.

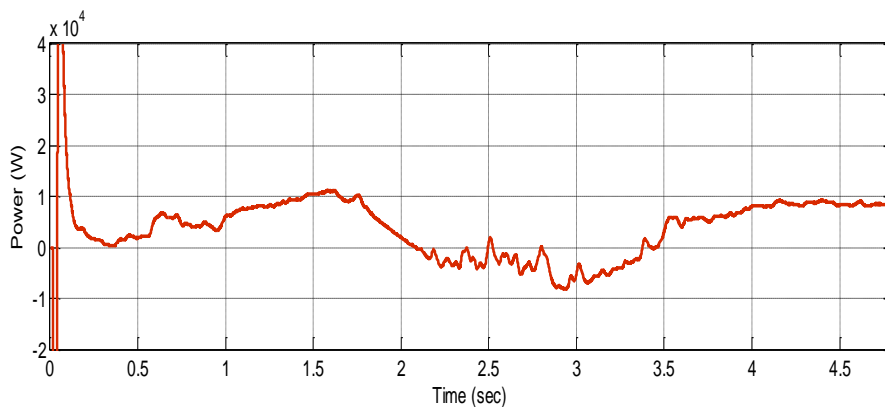


Figure 5.21 (a): Battery power

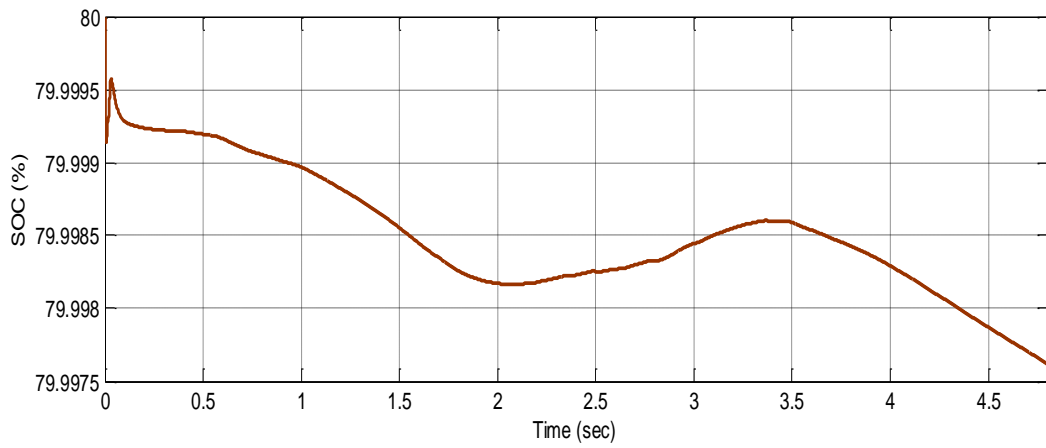


Figure 5.21 (b): State of charge (%) of battery

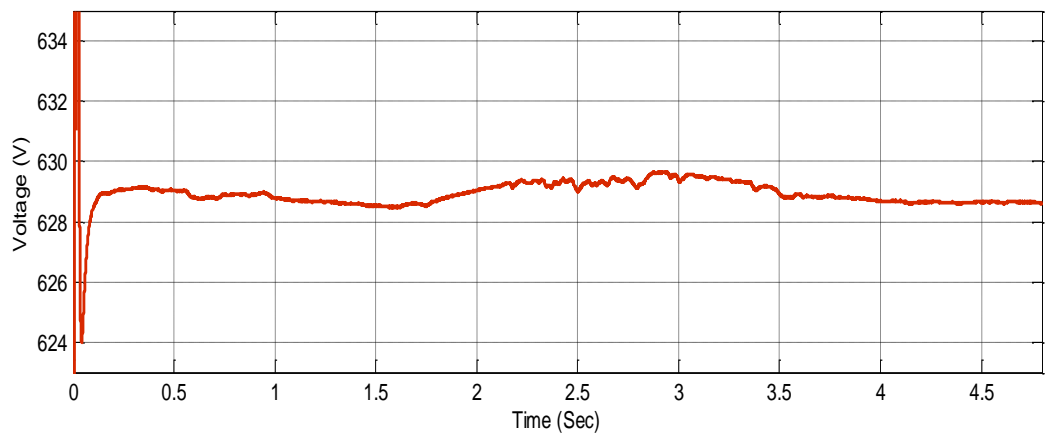


Figure 5.22: Voltage of battery

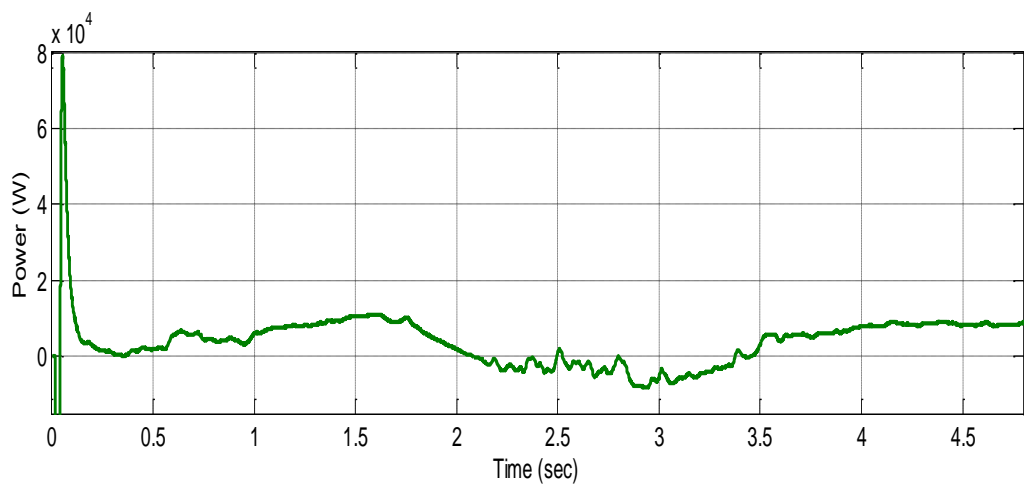


Figure 5.23 (a): Ultracapacitor power

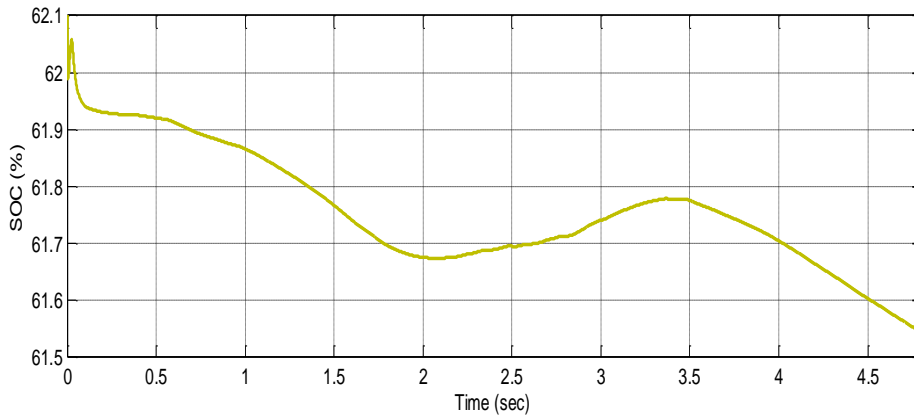


Figure 5.23 (b): State of charge (%) of Ultracapacitor

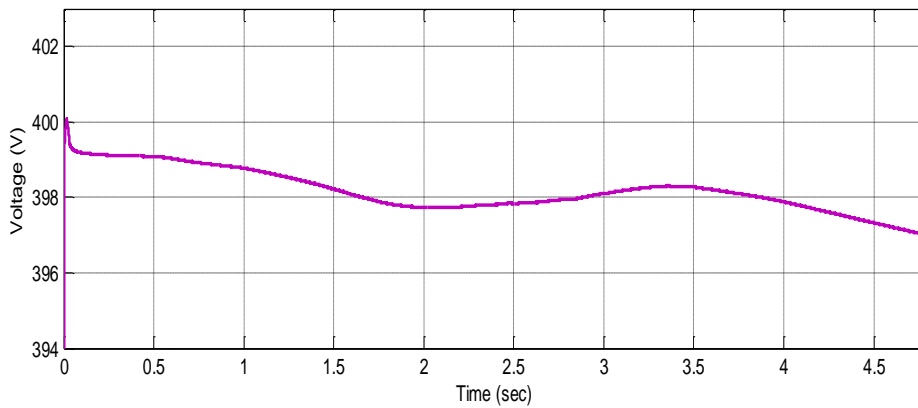


Figure 5.24: Voltage of Ultracapacitor

Figure 5.25 represents total wind and PV power generations and smoothed power injected to the grid. Most of the fluctuating powers are supplied or absorbed by storage devices. It can be observed from Figure 5.25 that, the proposed control strategy was effectively used to control the total wind and PV power fluctuations. Figure 5.26 (a) and Figure 5.26 (b) shows variation in DC link voltage and reactive power injected by the microgrid system to the grid respectively. The reference value of V_{dc} chosen is 780 V. The DC bus voltage is well controlled around 780 V by the grid side converter controller even during huge variations in power output. The reactive power injected by the microgrid system to the grid is zero during variations in the wind and PV power generations. The DC bus voltage and the injected grid power can be well regulated using the proposed combined battery-ultracapacitor storage devices.

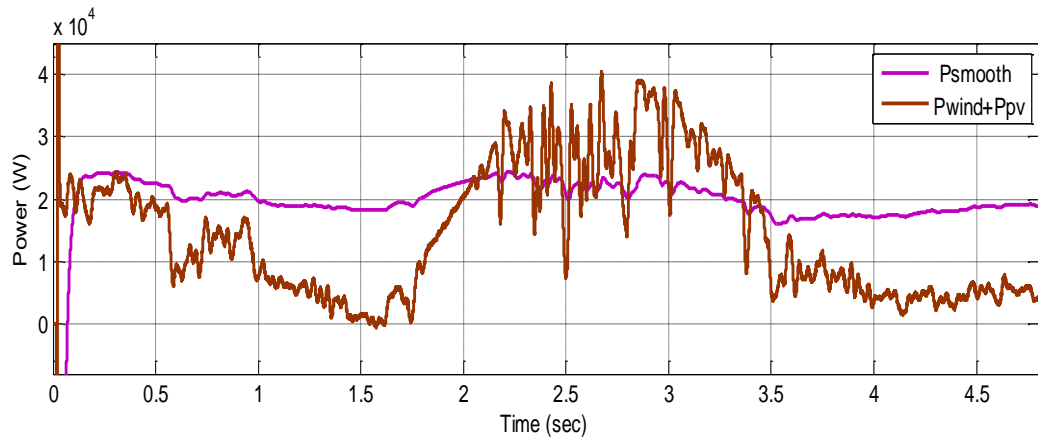


Figure 5.25: Total wind/PV power generations and smoothed power injected to the grid

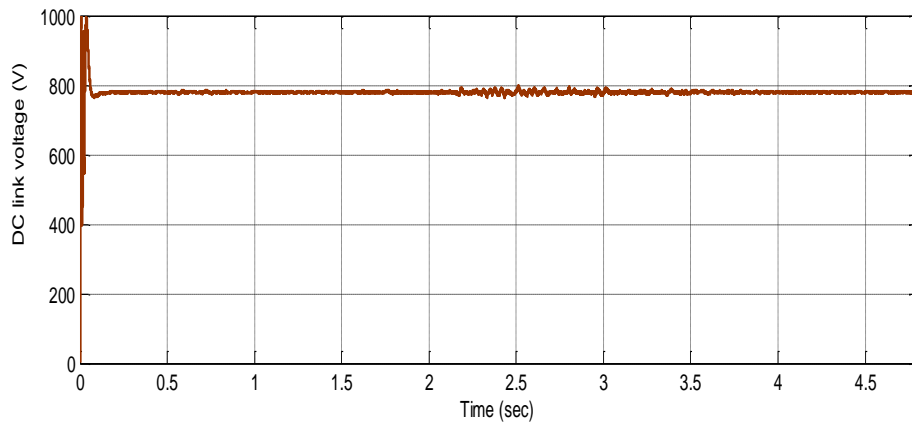


Figure 5.26 (a): DC link voltage

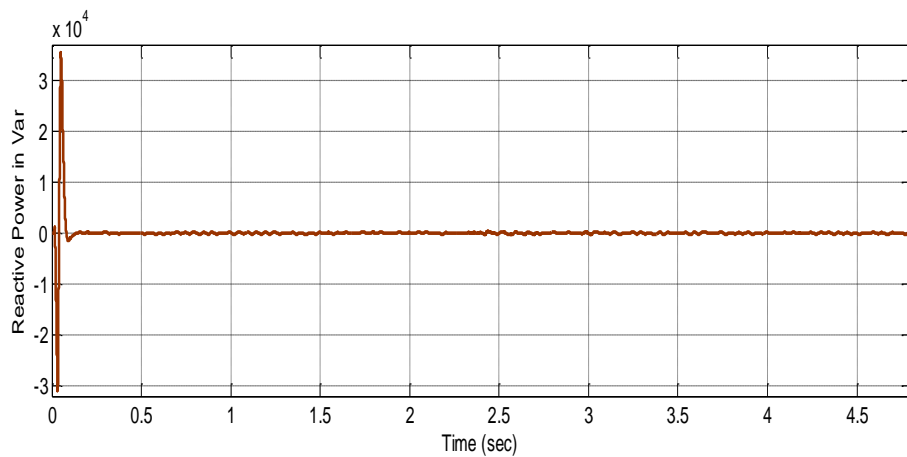


Figure 5.26 (b): Reactive power injected by the microgrid system to the grid

5.5 CONCLUSIONS

In this chapter, output power smoothing of a DC coupled wind/PV microgrid system has been studied with energy storage devices in Matlab/Simulink environment. The fluctuating power output of wind and solar power generation systems create adverse effects on utility grid operations. The control strategies of the microgrid system with ultracapacitors alone and combination of battery and ultracapacitors are developed for power smoothing of microgrid which is injected to the utility grid. The control system and the power management of the entire microgrid system have been detailed. The performance of the system is studied with considering three phase RL load with 0.8 power factor lagging. The requirement of maintaining constant DC voltage is realized considering different operating conditions while injecting demanded power to the grid. It is observed that the output power of microgrid system can be smoothed using energy storage devices through the developed controllers with power electronic interfaces. And the simulation results verify the excellent dynamic response of the energy storage devices and can respond very fast to level the active power output supplied to the utility grid.

CHAPTER 6

CONCLUSIONS AND SCOPE FOR FUTURE WORK

6.1 CONCLUSIONS

The wind and PV based DG system has more potential to improve the distribution system performance. Thus, the use of presented microgrid system can strongly contribute for reliable, clean and cost effective energy source for distribution network in the near future. However, the distribution system designs and operating practices are normally based on radial power flow and this creates a significant challenge for the successful integration of microgrid system. As the issues are new and are the key for sustainable future power supply, lot of research is required to study their impacts and exploit DGs to the full extent. This thesis has presented modeling and performance study of wind and PV based microgrid system both in grid connected and isolated mode of operation. A control strategy is developed for power smoothing of the microgrid system which is injected to the utility grid. In order to observe the real-time performance of ultracapacitor energy system in smoothing the output power fluctuations, the practical site data for wind speed and solar irradiation are considered. This section summarizes the study conducted by the author in this thesis.

- The dynamic model of wind and PV based microgrid model in grid connected and isolated modes of operation has been implemented successfully in Matlab/Simulink environment. The components of the model are built from the dynamics of each part and with their interconnections. The individual component modeling of wind and PV based DG system and power electronics interfacing circuits along with the necessary control schemes are presented. The given model can be useful tool to study the performance of microgrid system in grid connected and isolated mode of operation.
- In this research work, both wind generator and photovoltaic panels are controlled to operate at their maximum power point using MPPT controllers.

- The wind power system presented in this work uses the PMSG, because of its property of self-excitation, which allows an operation at a high efficiency and power factor. It also results in smaller size, minimum weight and higher torque to size ratio. The wind generation system uses PMSG with passive rectifier and boost converter combination. This will reduce the switching losses of the system, since there is only one switching device in the boost converter.
- The wind and PV power system are integrated at common DC link in the microgrid system and it is interfaced to the grid or isolated load using single three phase inverter. This is the salient feature of the presented which avoids use of two separate inverters. The controller of grid side converter is used to control the DC link voltage.
- For performance studies, the different types of loads considered on the microgrid are DC loads, induction motor and non-linear loads. The model of microgrid system is suitable to study the performance of most electrical phenomena that occur when it is connected to grid.
- The voltage and frequency control scheme used in this thesis is maintained both voltage and frequency within the standard permissible levels during isolated mode of operation of the microgrid system. The different types of loads on the microgrid such as DC loads, induction motor and non-linear loads are considered for performance studies.
- The dynamic performance of microgrid system is studied in grid connected mode of operation. The load sharing property of wind and PV power system in microgrid configuration along with the grid has been studied through simulation results.
- It is seen that the percentage THD when the presented microgrid system is connected to distribution network is around 2.2%, which is well within the standard prescribed by IEEE Std.1547 (2003).
- The performance of microgrid model in grid connected mode along with grid perturbations is also carried out through simulation. The grid perturbation conditions like balanced voltage dip, polluted and unbalanced grid voltage conditions are considered. Simulation results show that, the microgrid system can

able to supply the power even during the grid perturbations without affecting the overall performance of the system.

- The simulation results show that significant improvement can be achieved to smoothen the output power of the microgrid system injected to the grid using the ultracapacitors alone and combination of battery and ultracapacitors.

6.2 SCOPE FOR FUTURE WORK

The research work presented in this thesis can be further focused on:

- The control scheme for power electronic interface for microgrid DG system using neural network and fuzzy logic can be implemented for utility interactive operation.
- The microgrid system with wind and PV based DG system can be considered along with fuel cells or micro turbine generator based DG system to study the operational interaction among the DG sources in utility interactive and isolated mode of operation.
- The investigation on stability of microgrid with diverse DG systems can be carried out as future work. The protection aspects of microgrid system can be considered in detail.
- The passive or active techniques may be developed for detection of islanding to further enhance the effectiveness of the microgrid system.
- Different control strategies can be implemented considering the economic benefits of ESSs. Also the power smoothing of grid connected microgrid using other storage technologies with comparisons may be carried out.

APPENDIX A

SIMULATION PARAMETERS OF THE MICROGRID SYSTEM

Wind Turbine Parameters

Number of Blades	3
Blade Radius	3.7 m
Air density	1.225 Kg/m ²
C _{pmax}	0.47
Rated Wind Speed	12m/sec

PMSG Parameters

Output power	20 kW
Stator Phase Resistance	0.1764 Ω
Inertia	0.205 Kg-m ²
L _d and L _q	4.35 mH
Torque constant	13.91 N-m/A peak
Pole pairs	18
V _{w(rated)}	12 m/sec

PV Arrays Parameters

Output power (P _{out})	40 kW
Maximum power of PV module (P _m)	60 W
Voltage at MPP (V _m)	17.1 V
Current at MPP (I _m)	3.5 A
G _{ref}	1000 W/m ²
I _{sc}	3.8 A
V _{oc}	21.1 V
N _S	32
N _P	21
V _g	1.12eV
k	1.38e ⁻²³
q	1.6e ⁻¹⁹
n	1.2

Maxwell Boostcap PC2500 UC Characteristics

UC Parameters	Value
Capacitance	2700±20% F
Internal Resistance (DC)	0.001±25% ohm
Leakage Current	0.006 A, 72 hours, 25°C
Operating Temperature	-40°C to 65°C
Rated Current	100 A
Voltage	2.5 V
Weight	0.725 kg

Control System Parameters

PV Arrays MPPT Controller	$K_p = 500; K_i = 0.0001$
PMSG MPPT Controller	$K_p = 0.8; K_i = 0.001$
Battery Controller:	
Voltage loop controller	$K_p = 100, K_i = 0.01$
Current loop controller	$K_p = 0.1, K_i = 0.0001$
DC link voltage loop	$K_p = 7, K_i = 800$
Inverter <i>d</i> -axis current loop controller	$K_p = 0.3, K_i = 20$
Inverter <i>q</i> -axis current loop controller	$K_p = 0.3, K_i = 20$
Inverter <i>d</i> -axis voltage loop controller	$K_p = 500, K_i = 0.1$
Inverter <i>q</i> -axis voltage loop controller	$K_p = 50, K_i = 1000$

Electrical Parameters

DC link Voltage	780 V
DC link Capacitor	5000 μ F
Filter Parameters	$R_f = 0.5 \Omega; L_f = 5 \text{ mH}$
Grid Parameters	415 V; 50 Hz; X/R ratio=7
Type of Battery	Lead Acid
Rated Capacity of Battery	600 V, 200 Ah

APPENDIX B

Parameters of PI Controllers with Ultracapacitors

Ultracapacitor current loop	$K_p = 10; K_i = 0.1$
DC link voltage loop	$K_p = 0.8; K_i = 10$
Inverter d -axis current loop controller	$K_p = 0.1; K_i = 0.1$
Inverter q -axis current loop controller	$K_p = 0.01; K_i = 0.001$

Parameters of PI Controllers with Combination of BESS and UCs

Ultracapacitor current loop	$K_p = 0.045, K_i = 1.5$
Battery current loop	$K_p = 0.015, K_i = 1.5$
DC link voltage loop	$K_p = 7, K_i = 800$
Inverter d -axis current loop controller	$K_p = 0.3, K_i = 20$
Inverter q -axis current loop controller	$K_p = 0.3, K_i = 20$

REFERENCES

- Abedini, A. and Nikkhajoei, H. (2011). "Dynamic model and control of a wind-turbine generator with energy storage." *IET Renewable Power Generation*, 5(1), 67-78.
- Ackermann, T., Andersson, G. and Soder, L. (2001). "Distributed generation: a definition." *Electric Power Systems Research*, 57, 195-204.
- Agustoni, A., Brenna, M. and Tironi, E., (2003). "Proposal for a high quality DC network with distributed generation." *In: Proceedings of 17-th International Conference on Electricity Distribution*, Barcelona, 1-6.
- Ahmad, M. Eid (2013). "Standalone DC microgrids: analysis and control." *In: Proceedings of the 2nd International Conference on Engineering and Applied Science*, Tokyo, Japan, 2191-2198.
- Akie Uehara, Alok Pratap, Tomonori Goya, Tomonobu Senjyu, Atsushi Yona, Naomitsu Urasaki and Toshihisa Funabashi (2011). "A coordinated control method to smooth wind power fluctuations of a PMSG-based WECS" *IEEE Transactions on Energy Conversion*, 26(2), 550-558.
- Appelbaum, J. and Weiss, R. (1982). "An Electrical Model of the Lead Acid Battery." *In: Proceedings of International Telecommunications Energy Conference*, Washington, DC, USA 304-307.
- Arifujjaman, M., Iqbal, M. and Quaicoe, J. E. (2006). "Maximum power extraction from a small wind turbine emulator using a DC/DC converter controlled by a microcontroller." *In: Proceedings of International Conference on Electrical and Computer Engineering*, Dhaka, 213-216.
- Arul Daniel, S. and Ammasai Gounden N. (2004). "A novel hybrid isolated generating system based on PV fed inverter-assisted wind-driven induction generators." *IEEE Transactions on Energy Conversion*, 19(2), 416-422.
- Assano, H., Iravani, R. and Marnay, C. (2007). "Microgrids." *IEEE Power and Energy Magazine*, 5(4), 78-94.

- Bae, I. and Kim, J. (2007). "Reliability evaluation of distributed generation based on operation mode." *IEEE Transactions on Power Systems*, 22(2), 785-790.
- Balamurugan, K., Dipti Srinivasan and Thomas Reind (2012). "Impact of distributed generation on power distribution systems." *In: Proceedings of PV Asia Pacific Conference 2011, Energy Procedia*, 25, 93-100.
- Bullard, G. L., Sierra-Alcatraz, H. B., Lee, H. L. and, Morris, J. L. (1989). "Operating principles of the ultracapacitor." *IEEE Trans. on Magnetics*, 25(1), 102-106.
- Baoming Ge, Wenliang Wang, Daqiang Bi, Craig B. Rogers, Fang Zheng Peng, Anibal T. de Almeida and Haitham Abu-Rub (2013). "Energy storage system-based power control for grid connected wind power farm." *International Journal of Electrical Power and Energy Systems*, 44(1), 115-122.
- Barker, P. P. and de Mello, R. W. (2000). "Determining the impact of distributed generation on power systems: part 1 - radial distribution systems." *In: Proceedings of the IEEE/PES Summer Meeting*, 3, 1645-1656.
- Hammons, T. J. (2003). "Geothermal power generation worldwide." *In: Proceedings of IEEE power Tech. Conference, Bologna, Italy*, 1-8.
- Bhende, C. N., Mishraand, S. and Siva Ganesh Malla (2011). "Permanent magnet synchronous generator-based standalone wind energy supply system." *IEEE Transactions on Sustainable Energy*, 2(4), 361-373.
- Bloomquist, R. G. (2002). "Direct use geothermal resources." *In: Proceedings of IEEE Power Engineering Society Summer Meeting, Chicago, IL, USA*, 1, 15-16.
- Borbely, A. and Kreider, J.F. (2001). "Distributed generation: a new paradigm for the new millenium." CRC Press.
- Borges, C. L. and Pinto, R. J. (2008). "Small hydro power plants energy availability modeling for generation reliability evaluation." *IEEE Trans. on power system*, 23(3), 1125-1135.
- Bose Bimal, K. (2002). "Modern power electronics and AC drives." Prentice Hall PTR.

- Burke, A. (2000). "Ultracapacitors: why, how, and where is the technology." *Journal of Power Sources*, 91, 37-50.
- Caisheng Wang, (2006). "Modeling and control of hybrid wind/photovoltaic/fuel cell distributed generation systems." *Ph. D. Dissertation*, Montana State University, Bozeman, Montana.
- Caldon, R., Rossetto, F. and Turri, R. (2003). "Analysis of dynamic performance of dispersed generation connected through inverter to distribution networks." *In: Proceedings of 17th International Conference on Electricity Distribution, CIRED*, Barcelona, 12-15.
- Cetin, E. (2010). "A micro-DC power distribution system for a residential application energized by photovoltaic-wind/fuel cell hybrid energy systems." *Journal of Energy and Buildings*, 42(8), 1344-1352.
- Chad Abbey and Geza Joos (2007). "Supercapacitor energy storage for wind energy applications." *IEEE Transactions on Industry Applications*, 43(3), 769-776.
- Chen, Z. and Spooner, E. (1998). "Grid interface options for variable-speed, permanent magnet generators." *In: Proceedings of Inst. Elect. Eng., Elect. Power Applications*, 145(4), 273-283.
- Chiang, S. J., Shieh, H. J. and Chen, M. C. (2009). "Modeling and control of PV charger system with sepic converter." *Industrial Electronics, IEEE Transactions*, 56(11), 4344-4353.
- Chinchilla, M., Arnaltes, S. and Burgos, J. C. (2006). "Control of permanent magnet generators applied to variable speed wind energy systems connected to the grid." *IEEE Transaction on Energy Conversion*, 21(1), 130-135.
- Chung, I. Y., Liu, W., Cartes, D. A., Collins, E. G. and Moon, S. I. (2010). "Control methods of inverter interfaced distributed generators in a microgrid system." *IEEE Trans. Ind. Appl.*, 46(3), 1078-1088.
- Chunhua Liu, Chau, K. T. and Xiaodong Zhang (2010). "An efficient wind-photovoltaic hybrid generation system using doubly excited permanent-magnet brushless machine" *IEEE Transactions on Industrial Electronics*, 57(3), 831-839.

- Cramer, G., Reekers, J., Rothert, M. and Wollny, M. (2003). "The future of village electrification-more than two years of experiences with AC-coupled hybrid systems." *In: Proceedings of 2nd European PV-Hybrid and Mini-Grid Conference*, Kassel, Germany, 1-6.
- Daniel, S. A. and Ammasai Gounden, N. (2004). "A novel hybrid isolated generating system based on PV fed inverter-assisted wind-driven induction generations." *IEEE Trans. Energy Converters*, 19(2), 416-422.
- Das, D., Esmaili, R., Xu, L. and Nichols, D. (2005). "An optimal design of a grid connected hybrid wind/photovoltaic/fuel cell system for distributed energy production." *In: Proceedings of 31st Annual Conference of the IEEE Ind. Electr. Society, IECON'05*, Raliegh, NC, USA, 1223-1228.
- Data source from the National Renewable Energy Laboratory http://www.nrel.gov/midc/oahu_archive/ downloaded on 13, March 2014.
- Diaf, S., Notton, G., Belhamel, M., Haddadi, M., and Louche, A. (2008). "Design and techno-economical optimization for hybrid PV/wind system under various meteorological conditions." *Applied Energy*, 85(10), 968-987.
- Djamel, L. and Abdallah, B. (2013). "Power quality control strategy for grid connected renewable energy sources using PV array, wind turbine and battery." *In: Proceedings of 2013 Fourth International Conference on Power Engineering, Energy and Electrical Drives (POWERENG)*, Istanbul, 1671-1675.
- Doolla, S. and Banerjee, R. (2010). "Diffusion of grid connected PV in India: an analysis of variations in capacity factor." *In: Proceedings of IEEE Photovoltaic Specialist Conference*, Honolulu, HI, 2349-2352.
- Durr, M., Cruden, A., Gair, S. and McDonald, J. R. (2006). "Dynamic model of a lead acid battery for use in a domestic fuel cell system." *Journal of Power Sources*, 161(2), 1400-1411.
- Eghtedarpour, N. and Farjah, E. (2012). "Control strategy for distributed integration of photovoltaic and energy storage systems in DC microgrids." *Renewable Energy*, 45, 96-110.

- Electric Double Layer Capacitor: Boostcap Ultracapacitor, Available: <http://www.maxwell.com/pdf/uc/datasheets/PC2500.pdf>, downloaded on 20, March 2014.
- Ellis, M. W., Spakovsky, M. R. V. and Nelson, D. J. (2001). "Fuel cell systems: efficient, flexible energy conversion for the 21st century." *Proceedings of the IEEE*, 89(12), 1808-1818.
- Esmaili, R., Xu, L. and Nichols, D. K. (2005). "A new control method of permanent magnet generator for maximum power tracking in wind turbine application." *In: Proceedings of Power Engineering Society General Meeting*, 3. 1-6.
- Esrarn, T. and Chapman, P. L. (2007). "Comparison of photovoltaic array maximum power point tracking technique." *IEEE Transactions on Energy Conversion*, 22(2), 439-449.
- Fakham, H., Di L. and Francois, B. (2011). "Power control design of a battery charger in a hybrid active PV generator for load-following applications." *IEEE Trans. Ind. Electronics*, 58(1), 85-94.
- Fei Ding, Peng Li, Bibin Huang, Fei Gao, Chengdi Ding and Chengshan Wang (2010). "Modeling and simulation of grid connected hybrid photovoltaic/battery distributed generation system." *In: Proceedings of China International Conference on Electricity Distribution*, Nanjing, 1-10.
- Fernando Valencaga, Pablo F. Puleston and Pedro E. Battaiotto (2003). "Power control of a solar/wind generation system without wind measurement: a passivity/sliding mode approach." *IEEE Trans. Energy Conversion*, 18(4), 501-507.
- Francisco M. Gonzalez-Longatt, (2005). "Model of photovoltaic module in matlab™", *II CIBELEC 2005*, 1-5.
- Frede Blaabjerg, Zhe Chen and Soeren Baekhoej Kjaer (2004). "Power electronics as efficient interface in dispersed power generation systems." *IEEE Transactions on Power Electronics*, 19(5), 1184-1194

- Gaonkar, D. N., Pillai, G. N., and Patel, R. N. (2008). "Seamless transfer of microturbine generation system operation between grid connected and islanding modes." *Journal of Electric Power Systems and Components*, (37), 174-188.
- Gaonkar, D.N. and Pillai, G.N. (2011). "Operation and control of multiple Distributed Generation systems in the microgrid." *Int. Journal Energy Technology and Policy*, 7(4), 325-341.
- Georgakisl, D., Papathanassiou, S., Hatziaargyriod, N., Engle, A. and Hardt, Ch. (2004). "Operation of a prototype microgrid system based on micro-sources equipped with fast-acting power electronics interfaces." *In: Proceedings of 35th Annual IEEE Power Electronics Specialists Conference, Aachen, Germany*, 2521-2526.
- Giraud, F. and Salameh, Z. M. (2001). "Steady state performance of a grid connected rooftop hybrid wind-photovoltaic power system with battery storage." *IEEE Transactions on Energy Conversion*, 16(1), 1-7.
- Google_heliostat_wind_data_collection.pdf,<http://google.org/pdfs/>,downloaded on 13, March 2014.
- Grauers, A. (1996). "Efficiency of three wind energy generator system." *IEEE Trans. Energy Conversion*, 11, 650-656.
- Guoyi Xu, Lie Xu and Liangzhong Yao, (2013). "Wind turbines output power smoothing using embedded energy storage systems." *Journal of Mod. Power Syst. Clean Energy* 1(1), 49-57.
- Gyu, Y. C., Jong-S.K., Byong-K. L., Chung-Y. Won, J.-Wook K., Ji-Won J. and Jae-S. S. (2010). "Comparative study of power sharing algorithm for Fuel cell and Photovoltaic's hybrid generation system." *In: Proceedings of IEEE International Power Electronics Conference, Sapporo*, 2615-2620.
- Haque, M. E., Negnevitsky, M. and Muttaqi, K. M. (2010). "A novel control strategy for a variable-speed wind turbine with a permanent-magnet synchronous generator." *IEEE Trans. Ind. Appl.*, 46(1), 331-339.

- Hatziargyriou, N., Asano, H., Iravani, R. and Marnay, C. (2007). "Microgrids." *IEEE Power Energy Mag.*, 5(4), 78-94.
- Higuchi, Y., Yamamura, N., Ishida, M. and Hori, T. (2000). "An improvement of performance for small scaled wind power generating system with permanent magnet type synchronous generator." *In: Proceedings of IEEE Industrial Electronics Society Conference*, 2, Nagoya, 1037-1043.
- Hiroaki Nakayama, Eiji Hiraki, Toshihiko Tanaka, Noriaki Koda, Nobuo Takahashi and Shuji Noda (2008). "Standalone photovoltaic generation system with combined storage using lead battery and EDLC." *In: Proceedings of Power Electronics and Motion Control Conference, EPE-PEMC, Poznan*, 1877-1883.
- Hohm, D. P. and Ropp, M. E. (2000). "Comparative study of maximum power point tracking algorithms using an experimental, programmable, maximum power point tracking test bed." *In: Proceedings of 28th IEEE Photovoltaic Specialists Conf.*, Anchorage, AK, 1699-1702.
- Honorati, O., Bianco, G. L., Mezzetti, F. and Solero, L. (1996). "Power electronic interface for combined wind/PV isolated generating system." *In: Proceedings of the European Union Wind Energy Conf.*, Goteborg, Sweden, 321-324.
- Huang, K., Zhang, Y., Huang, S., Lu, J., Gao, J. and Luoqian (2009). "Some practical consideration of a 2mw direct-drive permanent-magnet wind-power generation system." *In: Proceedings of International Conference on Energy and Environment Technology*, Guilin, China, 824-828.
- Hussein, K.H., Murta, I., Hoshino, T., Osakada, M. (1995). "Maximum photovoltaic power tracking: an algorithm for rapidly changing atmospheric conditions." *In: Proceedings of IEEE Proceedings of Generation, Transmission and Distribution*, 142(1), 59-64.
- IEEE Standard 1547, (2003). "IEEE standard for interconnecting distributed resources with electric power systems." New York, NY, USA, 1-28.

- Illindala, M. (2012). "Flexible distribution of energy and storage resources." *In: Proceedings of IEEE Energy Conversion Congress and Exposition (ECCE)*, Raleigh, NC, 4069-4076.
- Ipsakis, D., Voutetakis, S., Seferlis, P., Stergiopoulos, F. and Elmasides, C. (2009). "Power management strategies for a standalone power system using renewable energy sources and hydrogen storage." *International Journal of Hydrogen Energy*, (16), 7081-7095.
- Jhunjunwala, A., Lakshminarasamma, N. and Vasudevan, K. (2013). "Solar DC powered commercial buildings." *In: Proceedings of IEEE 39th Photovoltaic Specialists Conference (PVSC)*, Tampa, FL 1500-1505.
- Jie Zeng, Buhan Zhang, Chengxiong Mao and Yunling Wang, (2006). "Use of battery energy storage system to improve the power quality and stability of wind farms." *In: Proceedings of 2006 International Conference on Power System Technology*, Chongqing, 1-6.
- Joseph, E., Lasseter, R., Schenkman, B., Stevens, J., Volkommer, H., Klapp, D. (2008). "CERTS microgrid laboratory testbed. Consortium for electric reliability technology solutions (CERTS)." *In: Proceedings of Public Interest Energy Research Program*, CEC-500-2008.
- Juan Manuel Carrasco, Leopoldo Garcia Franquelo, Jan T. Bialasiewicz, Eduardo Galvan, Ramon C. Portillo Guisado, Ma. Angeles Martin Prats, Jose Ignacio Leon, and Narciso Moreno-Alfonso (2006). "Power-electronic systems for the grid integration of renewable energy sources: a survey." *IEEE Transactions on Industrial Electronics*, 53(4), 1002-1016.
- Kai Strunz, Ehsan Abbasi, and Duc Nguyen Huu (2014). "DC microgrid for wind and solar power integration." *IEEE Journal of Emerging and Selected Topics in Power Electronics*, 2(1), 115-126.
- Kakigano, H., Miura, Y., Ise T. and Uchida, R. (2007). "DC voltage control of the DC microgrid for super high quality distribution." *In: Proceedings of the Power Conversion Conference*, Nagoya, Japan, 518-525.

- Kalantar, M., S. M. Mousavi G. (2010). "Dynamic behavior of a standalone hybrid power generation system of wind turbine, microturbine, solar array and battery storage." *Applied Energy* 87, 3051-3064.
- Kaldellisa, J. K., Kavadiasa K. A., Koronakis, P. S. (2007). "Comparing wind and photovoltaic standalone power systems used for the electrification of remote consumers." *Renewable and Sustainable Energy Reviews*, 11(1), 57-77.
- Kanellos, F. D., Tsouchnikas A. I. and Hatziaargyriou, N. D. (2005). "Microgrid simulation during grid connected and islanded modes of operation." *In: Proceedings of Int. Conf. on Power Systems Transients (IPST'05)*, Montreal, Canada, 1-6.
- Katiraei, F., Iravani, M. R. and Lehn, P. W. (2005). "Microgrid autonomous operation during and subsequent to islanding process." *IEEE Transactions Power Delivery*, 20(1), 248-257.
- Kazmi, M. R., Goto, H., Guo, H. J. and Ichinokura, O. (2011). "A novel algorithm for fast and efficient speed sensor-less maximum power point tracking in wind energy conversion systems," *IEEE Trans. Ind. Electron.*, 58(1), 29-36.
- Kurozumi, K., Takeru Tawara, Toshikazu Tan, Yuji Kawagoe, Takashi Yaman, Hiroaki Ikebe, Kazuhiko Shindou, and Tetsuo Miyazato (1998). "A hybrid system composed of a wind power and a photovoltaic system at NTT kume-jima radio relay station," *In: Proceedings of the 20th Int. Telecommun. Energy Conf.*, San Francisco, CA, 785-789.
- Kellogg, W. Nehrir, M. H., Venkataramanan, G., and Gerez, V. (1996). "Optimal unit sizing for a hybrid wind/photovoltaic generating system." *Electric Power Systems Research* 39(1), 35-38.
- Kelvin Tan and Sayed Islam, (2004). "Optimum control strategies in energy conversion of PMSG wind turbine system without mechanical sensors." *IEEE Trans on Energy Conversion*, 19(2), 392-399.

- Kim, S. Kim, C., Song, J., Yu, G. and Jung, Y. (1997). "Load sharing operation of a 14 kW photovoltaic/wind hybrid power system." *In: Proceedings of 26th IEEE Photovoltaic Specialists Conf.*, Anaheim, CA, 1325-1328.
- Kim, S., Jeon, J., Cho, C. Ahn, J. and Kwon, S. (2008). "Dynamic modeling and control of a grid connected hybrid generation system with versatile power transfer." *IEEE Transactions on Industrial Electronics*, 55(4), 1677-1688.
- Kinjo, T., Senjyu, T., Urasaki, N. and Fujita, H. (2006). "Output leveling of renewable energy by electric double-layer capacitor applied for energy storage system." *IEEE Tran. Energy Conversion*, 21(1), 221-227.
- Kjaer, S. B. (2005). "Design and control of an inverter for photovoltaic applications." *Ph. D. Dissertation*, Aalborg University, Institute of Energy Technology, Denmark.
- Krishnan, R. (2001). "*Electric motor drives modeling, analysis and control.*" Prentice-Hall, NJ.
- Lasseter, R. H. (2002). "Microgrids." *In: Proceedings of 2002 IEEE PES Winter Meeting*, 1, 305-308.
- Lasseter, R. H. and Paigi, P. (2004). "Microgrid: A conceptual solution." *In: Proceedings of 35th Annual IEEE Power Electronics Specialists Conference*, Aachen, 4285-4290.
- Li, W., Joos, G. and Belanger, J. (2010). "Real-time simulation of a wind turbine generator coupled with a battery supercapacitor energy storage system." *IEEE Tran. Industrial Electronics*, 57(4), 1137-1145.
- Liyan Qu and Wei Qiao, (2011). "Constant power control of DFIG wind turbines with supercapacitor energy storage." *IEEE Transactions on Industry Applications*, Vol. 47(1), 359-367.
- Majid A. Abdullah, Yatim, A. H. M., Chee Wei and Tan, (2011). "A study of maximum power point tracking algorithms for wind energy system." *In: Proceedings of 2011 IEEE First Conference on Clean Energy and Technology CET*, Kuala Lumpur 321-326.

- Molina, M. G. and Luis E. Juanico (2010). "Dynamic modeling and control design of advanced photovoltaic solar system for distributed generation applications." *Journal of Electrical Engineering: Theory and Application*, 1(3), 141-150.
- Martinot, E. and Sawin, J. L. (2009). "Renewables global status report 2009 update." Renewable Energy Policy Network for the 21st Century, REN21, 1-32.
- Md. Arifujjaman, (2010). "Modeling, simulation and control of grid connected permanent magnet generator (PMSG) based small wind energy conversion system." *IEEE Electrical Power & Energy Conference, EPEC*, Halifax, NS 1-6.
- Md. Enamul Haque, Michael Negnevitsky, and Kashem M. Muttaqi (2010). "A novel control strategy for a variable speed wind turbine with a permanent magnet synchronous generator." *IEEE Transactions on Industry Applications*, 46(1), 331-339.
- Meghdad Fazeli (2010). "Wind generator energy storage control schemes for autonomous grid." *Ph. D. Dissertation*, University of Nottingham.
- Meinhardt, M., Rothert, M., Wollny, M. and Engler, A. (2004). "Pure AC-coupling – the concept for simplified design of scalable PV-hybrid systems using voltage/frequency statics controlled battery inverters." *In: Proceedings of PVSEC-14*, 1-4.
- Mohamed Ibrahim, Amr Khairy, Hani Hagrass, Mina Zaher, Abdellatif El Shafei, Adel Shaltout, and Naser Abdel Rehim, (2010). "Studying the effect of decentralized battery storage to smooth the generated power of a grid integrated wind energy conversion system." *In: Proceedings of 14th International Middle East Power Systems Conference (MEPCON'10)*, Cairo University, Egypt, 641-645.
- Mohammad Bagher Delghavi, (2011). "Advanced islanded mode control of microgrids." *Ph.D. Dissertation*, the School of Graduate and Postdoctoral Studies, The University of Western Ontario London, Ontario, Canada.
- Mohan, N., Undeland T. M. and Robbins, W. P. (2010). "*Power electronics-converters, applications and design.*" John Wiley and Sons, Third Edition.

- Molina, M. G. and Mercado, P. E. (2008). "Modeling and control of grid connected photovoltaic energy conversion system used as a dispersed generator." *In: Proceedings of Transmission and Distribution Conference and Exposition, Latin America*, 1-8.
- Monica Chinchilla, Santiago Arnaltes and Juan Carlos Burgos (2006). "Control of permanent-magnet generators applied to variable-speed wind-energy systems connected to the grid." *IEEE Transactions on Energy Conversion*, 21(1), 130-135.
- Moutawakkil, M. and Elster, S. (2006). "RE hybrid systems - coupling of renewable energy sources on the AC and DC side of the inverter." *Refocus*, 7(5), 46-48.
- Muhamad Zalani Daud, Azah Mohamed and Hannan, M. H. (2013). "An optimal state of charge feedback control strategy for battery energy storage in hourly dispatch of PV sources." *In: Proceedings of 4th International Conference on Electrical Engineering and Informatics (ICEEI 2013), Procedia Technology*, 11, 24-31.
- Mustapha, R. and Moulay, T. L. (2004). "Average current mode control of a voltage source inverter connected to the grid: application to different filter cells." *Journal of Electrical Engineering*, 55(3), 77-82.
- Mutoh, N., Ohno, M. and Inoue, T. (2006). "A method for MPPT control while searching for parameters corresponding to weather conditions for PV generation systems." *IEEE Transactions on Industrial Electronics*, 53(4), 1055-1065.
- Muyeen, S. M., Mohd. Hasan Ali, Takahashi, R., Murata, T. and Tamura, J. (2007). "Wind generator output power smoothing and terminal voltage regulation by using STATCOM/ESS." *In: Proceedings of IEEE Power Tech 2007 conference, Lausanne, Switzerland*, 1232-1237.
- Muyeen, S. M., Shishido, S., Mohd. Hasan Ali, Takahashi, R., Murata, T. and Tamura, J. (2008). "Application of energy capacitor system (ECS) to wind power generation." *Wind Energy*, 11(4), 335-350.
- Najafi, M., Siah, M., Ebrahimi R. and Hoseynpoor, M. (2011). "A new method to control of variable speed wind generation system connected to permanent magnet

- synchronous generator.” *Australian Journal of Basic and Applied Sciences*, 5(5), 433-440.
- Narasimharaju B. L., Dubey, S. P. and S. P. Singh (2012). “Design and analysis of coupled inductor bidirectional DC-DC convertor for high voltage diversity applications.” *IET Power Electronics*, 5(7), 998-1007.
- Nelms, R. M., Cahela, D. R. and Tatarcuk, B. J. (2003). “Modeling of double layer capacitor behavior using ladder circuits.” *IEEE Trans. Aerosp. Electron. Syst.*, 39(2), 430-438.
- Nishad Mendis, Kashem M. Muttaqi, Saad Sayeef and Sarath Perera, (2012). “Standalone operation of wind turbine-based variable speed generators with maximum power extraction capability.” *IEEE Transactions on Energy Conversion*, 27(4), 822-834.
- Oystein Ulleberg, (1998). “Standalone power systems for the future: optimal design, operation and control of solar-hydrogen energy systems.” *Ph. D. Dissertation*, Norwegian University of Science and Technology, Trondheim.
- Pandiaral, K. and Fox, B. (2000). “Novel voltage control for embedded generators in rural distribution networks”, *In: Proceedings of Int. Conf. on power system technology*”, Perth, WA, 1, 457-462.
- Patel, M. R. (1999). “*Wind and solar power systems*.” CRC Press, Technology and Engineering.
- Piagi, P. and Lasseter, R. H. (2006). “Autonomous control of microgrids.” *IEEE PES Meeting*, Montreal, 1-8.
- Prasad, A. R. and Natarajan, E. (2006). “Optimization of integrated photovoltaic-wind power generation systems with battery storage.” *The international Journal of Energy*, 31(12), 1943-1954.
- Previsic, M. (2005). “Wave power technologies.” *In: Proceedings of IEEE Power Engineering Society General Meeting*, 2, 2011-2016.
- Raza Kazmi, S. M., Goto, H., Hai-Jiao, G. and Ichinokura, O. (2010). “Review and critical analysis of the research papers published till date on maximum power

- point tracking in wind energy conversion system.” *In: Proceedings of Energy Conversion Congress and Exposition (ECCE)*, Atlanta, GA, 4075-4082.
- Ribeiro, P. F., Johnson, B.K., Crow, M.L., Arsoy, A. and Liu, Y. (2001). “Energy storage systems for advanced power applications.” *Proceedings of the IEEE*, 89(12), 1744-1756.
- Ro, K. S. and Rahman, S. (1998). “Two-loop controller for maximizing performance of a grid connected photovoltaic-fuel cell hybrid power plant.” *IEEE Transactions on Energy Conversion*, 13(3), 276–281, 1998.
- Robert B. Schainker, (2004). “Executive overview: energy storage options for a sustainable energy future.” *IEEE Power Engineering Society General Meeting*, Denver, CO, 2309-2314.
- Robert Lasseter, Abbas Akhil, Chris Marnay, John Stephens, Jeff Dagle, Ross Guttromson, A. Sakis Meliopoulos, Robert Yinger, and Joe Et, (2002). “White paper on integration of distributed energy resources: the CERTS microgrid concept.” Berkeley Lab Report LBNL-50829, Berkeley, CA, 1-27.
- Rodolfo, D., Jose, L. B., Franklin, M. (2009). “Design and economical analysis of hybrid PV–wind systems connected to the grid for the intermittent production of hydrogen.” *Energy Policy* 37, 3082-3095.
- Rodriguez, P., Pou, J., Bergas, J., Candela, J. I., Burgos, R. P., Boroyevich D. (2007). “Decoupled double synchronous reference frame PLL for power converters control.” *IEEE Trans. Power Electronics*, 22(2), 584-592.
- Rym Marouani, Kamel Echaieb and Abdelkader Mami, (2011). “New alternative of design and control for three-phase grid connected photovoltaic system.” *European Journal of Scientific Research*, 55(1), 37-45.
- Salameh, Z. M., Casacca, M. A. and Lynch, W. A. (1992). “A mathematical model for lead-acid batteries.” *IEEE Transactions on Energy Conversion*, 7(1), 93-98.
- Samosir, A. S. and Yatim, A. H. M. (2010). “Implementation of dynamic evolution control of bidirectional DC/DC converter for interfacing ultracapacitor energy storage to fuel cell system.” *IEEE Trans. Ind. Electron.*, 57(10), 3468-3473.

- Scott, W.G. (1998). "Microturbine generators for distribution systems." *IEEE Proc. on Industry Applications Magazine*, 4(3), 57-62.
- Senjyu, T., Tamaki, S., Urasaki, N., Uezato, K., Higa, H., Funabashi, T., Fujita, H. and Sekine, H. (2004). "Wind velocity and rotor position sensor less maximum power point tracking control for wind generation system." *IEEE Power Electronics Specialists Conference*, Aachen, Germany, 3, 2023-2028.
- Seul Ki Kim, Eung-Sang Kim and Jong-Bo Ahn (2006). "Modeling and control of a grid connected wind/PV hybrid generation system." *In: Proceedings of IEEE PES Transmission and Distribution Conference and Exhibition*, Dallas, TX, 1202-1207.
- Shao Zhang, King-Jet Tseng, Mahinda Vilathgamuwa, D., Trong Duy Nguyen and Xiao-Yu Wang (2011). "Design of a robust grid interface system for PMSG based wind turbine generators." *IEEE Transactions on Industrial Electronics*, 58(1), 316-328.
- Slootweg, J. G., Haan, S. W. H., Polinder, H., Kling, W. L. (2003). "General model for representing variable speed wind turbines in power system dynamics simulations." *IEEE Trans. on Power Systems*, 18(1), 144-151.
- Solero, L., Caricchi, F., Crescimbin, F., Honorati, O. and Mezzetti, F. (1996). "Performance of a 10 kW power electronic interface for combined wind/PV isolated generating systems." *In: Proceedings of IEEE Power Systems Conference and Exposition, PESC-96*, Baveno, 1027-1032.
- Strauss, P. and Engler, A. (2003). "AC coupled PV hybrid systems and microgrids-state of the art and future trends." *In: Proceedings of 3rd World Conference on Photovoltaic Energy Conversion*, Osaka, Japan 3, 2129-2134.
- Tao Zhou and Bruno Francois, (2011). "Energy management and power control of a hybrid active wind generator for distributed power generation and grid integration." *IEEE Transactions on Industrial Electronics*, 58(1), 95-104.
- Thomas S. Basso and Richard DeBlasio, (2004). "IEEE 1547 Series of standards interconnection issues." *IEEE Tran, on Power Electronics*, 19(5), 1159-1162.

- Tremblay, O., Dessaint, L. A. and Dekkiche, A. I. (2007). "A generic battery model for the dynamic simulation of hybrid electric vehicles." *In: Proceedings of IEEE-Vehicle Power and Propulsion Conf.*, Arlington, TX, 284-289.
- Tsai, M. S., Lin, C. E., Tsai, W. I. and Huang, C. L. (1995). "Design and implementation of a demand side multifunction battery energy storage system." *IEEE Trans. on Industrial Electronics*, 42(6), 642-652.
- Uzunoglu, M. and Alam, M. S. (2006). "Dynamic modeling, design, and simulation of a combined PEM fuel cell and ultracapacitor system for standalone residential applications." *IEEE Transactions on Energy Conversion*, 21(3), 767-773.
- Vechiu, I., Llarra, A., Curea, O. and Camblong, H. (2009). "Control of power converters for microgrids." *In: Proceedings of Ecologic Vehicles Renewable Energies, (EVRE-09)*, Monaco, 1-6.
- Wakao, S., Ando, R., Minami, H., Shinomiya, F., Suzuki, A., Yahagi, M., Hirota, S., Ohhashi, Y. and Ishii, A. (2003). "Performance analysis of the PV/wind/wave hybrid power generation system." *In: Proceedings of IEEE World Conf. Photovoltaic. Energy Conversion*, Osaka, Japan, 3, 2337-2340.
- Wang, Q. and Chang, L. C. (2004). "An intelligent maximum power extraction algorithm for inverter-based variable speed wind turbine systems." *IEEE Trans. Power Electronics*, 19(5), 1242-1249.
- Xiangjun Li, Dong Hui, and Xiaokang Lai (2013). "Battery energy storage station (BESS) based smoothing control of photovoltaic (PV) and wind power generation fluctuations." *IEEE Transactions on Sustainable Energy*, 4(2), 464-473.
- Xu, G., Xu, L., and Morrow, DJ, (2011). "Wind turbines with energy storage for power smoothing and FRT enhancement." *In: Proceedings of the 2011 IEEE Power and Energy Society General Meeting*, Detroit, MI, USA, 24-29.
- Yanzhu Ye, Ratnesh Sharma and Di Shi (2013). "Adaptive control of hybrid ultracapacitor-battery storage system for PV output smoothing." *In: Proceedings of the ASME 2013 Power Conference Power 2013*, Boston, Massachusetts, USA, 1-7.

- Yaow Ming Chen, Yuan-Chuan Liu, Shih-Chieh Hung, and Chung-Sheng Cheng, (2007). "Multi-input inverter for grid connected hybrid PV/wind power system." *IEEE Transactions on Power Electronics*, 22(3), 1070-1077.
- Yasin, A., Napoli, G., Ferraro M. and Antonucci, V. (2011). "Modeling and control of a residential wind/PV/battery hybrid power system with performance analysis." *Journal of Applied Sciences*, 3663-3676.
- Yoshimoto, K., Nanahara, T. and Koshimizu, G. (2006). "New control method for regulating state-of-charge of a battery in hybrid wind power/battery energy storage system." *In: Proceedings of IEEE Power Syst. Conf. and Exposition, (PSCE'06)*, Atlanta, GA, 1244-1251.
- Youssef, O. E. M., Abdel-Rahim, N. M. B. and Shaltout A. (2010). "Performance of standalone hybrid wind-photovoltaic system with battery storage." *In: Proceedings of the 14th International Middle East Power Systems Conference (MEPCON'10)*, Cairo University, Egypt, 853-859.
- Yuanye Xia, Khaled H. Ahmed, and Barry W. Williams, (2011). "A new maximum power point tracking technique for permanent magnet synchronous generator based wind energy conversion system." *IEEE Transactions on Power Electronics*, 26(12), 3609-3620.
- Zhou, T., Lu, D., Fakham, H. and Francois, B. (2008). "Power flow control in different time scales for a wind/hydrogen/supercapacitors based active hybrid power system." *In: Proceedings of EPE-PEMC*, Poznan, Poland, 2205-2210.

LIST OF PUBLICATIONS:

International Journal Publications:

- [1] Jayalakshmi, N. S. and Gaonkar, D. N. “A New Control Method to Mitigate Power Fluctuations for Grid Integrated PV/Wind Hybrid Power System Using Ultracapacitors” submitted to *International Journal of Emerging Electric Power Systems*, Berkeley Electronic Press (Manuscript ID: IJEEPS.2015.0183 - Under Review)
- [2] Jayalakshmi, N. S. and Gaonkar, D. N. “Battery-Electric Double Layer Capacitor Storage Systems for Power Smoothing of Grid Integrated Hybrid Wind/PV System” submitted to *Journal of Modern Power Systems and Clean Energy*, Springer (Manuscript ID: MPCE-D-15-00037R2-Revised Manuscript Submitted)
- [3] Jayalakshmi, N. S. and Gaonkar, D. N. “Operation of Grid Integrated Wind/PV Hybrid System with Grid Perturbations” *International Journal of Renewable Energy Research*, (In Press)
- [4] Jayalakshmi, N. S. and Gaonkar, D. N. (2015). “An integrated Control Approach and Power Management of Standalone Hybrid Wind/PV/Battery Power Generation System with Maximum Power Extraction Capability.” *Distributed Generation and Alternative Energy Journal*, Taylor and Francis Publishers, U.K., 30(4), 15-36.
- [5] Jayalakshmi, N. S. and Gaonkar, D. N. (2014). “Dynamic Modeling and Performance Study of DC Microgrid in Grid Connected and Isolated Mode of Operation with Maximum Power Extraction Capability.” *International Journal of Distributed Energy Resources and Smart Grids*, Technology and Science Publishers, Germany, 10(4), 281-299.
- [6] Jayalakshmi, N. S. and Gaonkar, D. N. (2014). “Modeling and Performance Analysis of Grid Integrated Hybrid Wind and PV Based DG System with MPPT Controllers.” *International Journal of Distributed Energy Resources*

and Smart Grids, Technology and Science Publishers, Germany, 10(2), 115-131.

- [7] Jayalakshmi, N. S. and Gaonkar, D. N. (2014). “Dynamic Modeling and Performance Study of a Standalone Photovoltaic System with Battery Supplying Dynamic Load” *International Journal of Renewable Energy Research, 4(3), 635-640.*
- [8] Jayalakshmi, N. S. and Gaonkar, D. N. (2014). “Maximum Power Point Tracking for Grid Integrated Variable Speed Wind based Distributed Generation System with Dynamic Load” *International Journal of Renewable Energy Research, 4(2), 464-470.*
- [9] Jayalakshmi, N. S. and Gaonkar, D. N. (2014). “Modeling and control strategy for grid integrated distributed generation systems with maximum power extraction capability.” *International Journal of Engineering, Science and Technology, Multicraft Publishers, 6(2), 101-110.*

International Conference Publications:

- [1] Jayalakshmi, N. S. and Gaonkar, D. N. (2015). “Battery-Ultracapacitor Storage Devices to Mitigate Power Fluctuations for Grid Connected PV System” 12th IEEE India International Conference (*INDICON-2015*) Electronics, Energy, Environment, Communication, Computer, Control (E³-C³), Jamia Millia Islamia, New Delhi, INDIA - Accepted
- [2] Gaonkar, D. N. and Jayalakshmi, N. S. (2014). “Performance Study of Roof Top Wind Solar Microgrid System in Isolated Mode of Operation.” *In: Proceedings of IEEE International Conference on Power Electronics, Drives and Energy Systems 2014 (PEDES-2014), IIT Bombay, Mumbai, India, 1-6*
- [3] Jayalakshmi, N. S. and Gaonkar, D. N. (2012). “Dynamic Modeling and Control of Grid Integrated Wind Generation System Using PMSG with MPPT Algorithm.” *In: Proceedings of IEEE-PES Fifteenth International Middle East Power Systems Conference (MEPCON’12) Alexandria, Egypt, 1-5.*

- [4] Jayalakshmi, N. S. and Gaonkar, D. N. (2012). "Dynamic Modeling and Performance Analysis of Grid Connected PMSG based Variable Speed Wind Turbines with Simple Power Conditioning System." In: Proceedings of IEEE International Conference on Power Electronics, Drives and Energy Systems (PEDES-2012) CPRI, Bangalore, India, 1-5.
- [5] Jayalakshmi, N. S. and Gaonkar, D. N. (2012). "Dynamic Modeling and Analysis of an Isolated Self Excited Induction Generator Driven by a Wind Turbine." In: Proceedings of IEEE PES International Conference on Power signals control and computations (EPSICON-2012), Vidya Academy of Science and Technology, Thrissur, Kerala, India, 1-5.
- [6] Jayalakshmi, N. S. and Gaonkar, D. N. (2011). "Performance Study of Isolated Hybrid Power System with Multiple Generation and Energy Storage Units." In: Proceedings of IEEE International Conference on Power and Energy Systems (ICPS-2011), IIT Madras, Chennai-600 036, Tamil Nadu, India, 1-5.

CURRICULUM VITAE

Permanent address:

Jayalakshmi N. S.
8-1-43B1A, "Sannidhi"
LLR Marg, Near MGM College
Kunjibettu, Udupi-576102
Karnataka
Phone: +91-9481970925
Email: jayalakshmi.ns@manipal.edu

Qualification:

1. M.Tech. in Power Systems from National Institute of Engineering, Mysore University, 1997-1999.
2. B.E. degree in Electrical Engineering from M. S. Ramaiah Institute of Technology, Bangalore University, 1987-1991.